UNIVERSITÀ DELLA CALABRIA
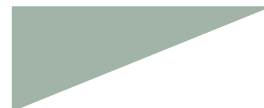
Dipartimento di Elettronica,
Informatica e Sistemistica

Dottorato di Ricerca in
Ingegneria dei Sistemi e Informatica
XXIII ciclo

Tesi di Dottorato

New Engine control functions for CO2 reduction and performance improvement

Iolanda Montalto

UNIVERSITÀ DELLA CALABRIA
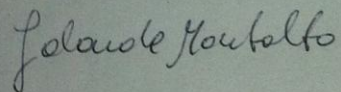
Dipartimento di Elettronica,
Informatica e Sistemistica

Dottorato di Ricerca in
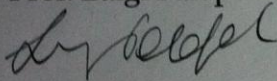Ingegneria dei Sistemi e Informatica
XXIII ciclo

Tesi di Dottorato

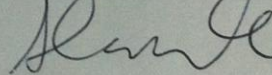# New Engine control functions for CO2 reduction and performance improvement

Iolanda Montalto

Coordinatore
Prof. Luigi Palopoli

Supervisore
Prof. Alessandro Casavola

DEIS

Summary

Today's automotive market is extremely competitive and quickly changing. The customers demand excellent driving performance, new legislations impose increasingly stricter constraints and competition imposes increasingly shorter development cycles because of reduced times-to-market. Environmental awareness and public concerns about CO2 emissions have been for a long time a substantial factor in promoting technological advancements in the automotive industry. In this scenario, the actual high penetration of electronic devices in cars is and will be a key factor for the fulfillment of all the above requirements. In fact, in a recent study it has been estimated that 90% of automotive innovation includes the electrical and electronics parts.

On the other side, next generation of engines will increase in complexity, functionalities and self monitoring capabilities, with true shifts in technology, like e.g. intelligent alternators and variable valve actuation systems. In this respect, the contents of this thesis summarize my last four years of research activity which has been carried out in the field of engine control systems design and validation.

Actually, the problem of the production of polluting substances during the combustion phases depends not only by the engine structure but also on the engine management system. Therefore, the control software plays an important role in the achievement of suitable engine and vehicle performance while maintaining low emission levels. To this end, the complexity of the software functions needs to be increased, both in terms of algorithmic complexity and for the need to handle the additional degrees of freedom available (i.e. model based torque management during take off, valve timing or valve actuation management, different values for battery voltage and so on). In turn, the larger control systems complexity imposes the use of more sophisticated tools and methods for the optimization of the engine control system parameters.

Most of the work underlying this thesis has been carried out in the automotive company where I actually work for and reports the results of the many efforts accomplished in addressing such kind of problems. In particular, the research activities have been undertaken and experimented on a gasoline engine equipped with a Variable Valve Actuation (VVA) module. The potentialities of VVA systems represent the actual frontier of the engine technology and therefore such a kind of engine represents a relevant baseline for experimenting novel approaches. In particular, four main topics have been

investigated: the first one regards the design of smart alternator management algorithms that allow the achievement of lower emission levels than standard alternators and improve the performance during certain manoeuvres.

The second topic regards the development of a new method, named drive off algorithm, for handling the take off phases. This algorithm has been proved so effective in test benches that it has been implemented in all commercial vehicles since the beginning of this year. The third and fourth topics have regarded the way to manage the additional algorithmic complexity due to the availability of the further degrees offered by the new VVA technology. For this reason, a new spark advance algorithm has been developed, being the standard one not so good in adequately taking into account the specificities of the VVA technology. A second more complex aspect being addressed it has been the increased number of engine control parameters to be calibrated for this new kind of engines. The old tuning methodology based on a trial-and-error approach resulted not enough accurate for the novel control requirements and too much time-consuming. A novel tuning methodology has been developed which, on the contrary, is based on an optimization approach and allows one to achieve the desired accuracy in short times. For this reason, it has been adopted in my company since last year and it is actually used for steady state calibration of each motorization of MULTIAIR$^®$ engines.

The thesis is organized in eight chapters.

The first and second ones describe the scenario in which my work has been developed, showing the restrictive emission levels required in the automobile world and some technological enhancements for fuel economy, emission legislation fulfillment and engine performance improvements.

In the third chapter, the control algorithms developed to manage the smart alternator technology are described, showing the achieved benefits. The details of the control algorithms and the obtained results have been described in the paper (SAE2011) [12].

The fourth chapter describes the control functions used to improve the engine performance during the take off maneuver in MULTIAIR$^®$ engines. This work has been published in the paper (EAEC2011) [11].

In the fifth chapter a control function that optimizes the performance of a VVA engine has been detailed. This algorithm calculates the spark ignition timing (one of the necessary engine parameters) in order to obtain the optimal behavior in each engine working mode and in each variable valve mode. This work has been presented at the Fisita 2010 Conference (see [10]). The tools and the methodology developed for the optimization of the engine parameters have been described in another paper presented at the same conference (see [9]).

In the sixth chapter, several tools for engine control systems design and calibration have been described. This chapter contains material published in the book's chapter [16]) and in the conference papers [71], [78], [79], [80], [81].

The seventh chapter concludes the thesis, reporting some results and showing the benefits of the proposed methodologies on a real application.

Table of contents

List of figures

Chapter 1 New automotive requirements and the role of the Engine Control Systems

The automotive industry is facing a very challenging phase. The coming scenario consists of more and more ambitious requirements regarding fuel consumption, fun to drive and also important constraints due to new emissions legislation:

- Euro 5+ for additional diagnostic requirements

- Euro 6 for challenging emission levels

which are going to be mandatory for every new vehicle homologation starting from September 2011 and for every vehicle registration from January 2014.

The most part of these new requirements are principally affecting the powertrain with additional mechanical subsystems and related pieces of electronics to manage them. Consequently, the engine control systems necessarily will become more complex, for the need to manage additional functionalities and govern the cooperation between the new and the old technologies. Also, they will have to maintain back compatibility with the old engines guaranteeing in any case the best possible performance.

1.1 EMISSIONS RESTRICTION

The regulation norms on emissions for the automotive industry were introduced first in the United States in the sixties, when the growing amount of vehicles started to increase the atmospheric pollution, producing effects on people health. For this reason, the USA authorities began to emit specific legislations in order to regulate the vehicle emissions. After that, during the seventies, also the Europe defined first laws on pollution emissions. European Union emission regulations for new light duty vehicles (passenger cars and light commercial vehicles) were once specified in the Directive 70/220/EEC with a number of amendments adopted through 2004. In 2007, this Directive has been repealed and replaced by the Regulation 715/2007 (Euro 5/6). Some of the important regulatory steps implementing emission standard for light-duty vehicles were:

- Euro 1 standards (also known as EC 93): Directives 91/441/EEC (passenger cars only) or 93/59/EEC (passenger cars and light trucks), approved in July of 1992.

- Euro 2 standards (EC 96): Directives 94/12/EC or 96/69/EC, approved in January of 1996.

- Euro 3/4 standards (2000/2005): Directive 98/69/EC, further amendments in 2002/80/EC, Euro 3 was approved in January of 2000, Euro 4 in January of 2005 for the vehicle homologation, in January of 2006 for the vehicle registration.
- Euro 5/6 standards (2009/2014): Regulation 715/2007 ("political" legislation) and Regulation 692/2008 ("implementing" legislation)

The emission standards for light-duty vehicles are applicable to all vehicles of categories M1, M2, N1 and N2, with a reference mass not exceeding 2610 kg (Euro 5/6). EU regulations introduce different emission limits for compression ignition (diesel) and positive ignition (gasoline, NG, LPG, ethanol) vehicles. Diesels have more stringent CO standards but are allowed higher NOx. Positive ignition vehicles were exempted from PM standards through the Euro 4 stage. Euro 5/6 regulations introduce PM mass emission standards, equal to those for diesels, for positive ignition vehicles with DI engines.

The 2000/2005 standards were accompanied by an introduction of more stringent fuel regulations that require minimum diesel cetane number of 51 (year 2000), maximum diesel sulfur content of 350 ppm in 2000 and 50 ppm in 2005, and maximum petrol (gasoline) sulfur content of 150 ppm in 2000 and 50 ppm in 2005. "Sulfur-free" diesel and gasoline fuels ($\leq$ 10 ppm S) must be available from 2005, and became mandatory from 2009.

EU emission standards are summarized in the table 1.1. All dates listed in the table refer to new type approvals. The EC Directives also specify a second date, one year later, unless indicated otherwise, which applies to first registration (entry into service) of existing, previously type-approved vehicle models.

EU Emission Standards for Passenger Cars (Category M_1*), g/km

Tier	Date	CO	HC	HC+NOx	NOx	PM
Diesel						
Euro 1†	1992.07	2.72 (3.16)	–	0.97 (1.13)	–	0.14 (0.18)
Euro 2, IDI	1996.01	1.0	–	0.7	–	0.08
Euro 2, DI	1996.01[a]	1.0	–	0.9	–	0.10
Euro 3	2000.01	0.64	–	0.56	0.50	0.05
Euro 4	2005.01	0.50	–	0.30	0.25	0.025
Euro 5	2009.09[b]	0.50	–	0.23	0.18	0.005[e]
Euro 6	2014.09	0.50	–	0.17	0.08	0.005[e]
Petrol (Gasoline)						
Euro 1†	1992.07	2.72 (3.16)	–	0.97 (1.13)	–	–
Euro 2	1996.01	2.2	–	0.5	–	–
Euro 3	2000.01	2.30	0.20	–	0.15	–
Euro 4	2005.01	1.0	0.10	–	0.08	–
Euro 5	2009.09[b]	1.0	0.10[c]	–	0.06	0.005[d,e]
Euro 6	2014.09	1.0	0.10[c]	–	0.06	0.005[d,e]

* At the Euro 1..4 stages, passenger vehicles > 2,500 kg were type approved as Category N_1 vehicles
† Values in brackets are conformity of production (COP) limits
a - until 1999.09.30 (after that date DI engines must meet the IDI limits)
b - 2011.01 for all models
c - and NMHC = 0.068 g/km
d - applicable only to vehicles using DI engines
e - proposed to be changed to 0.003 g/km using the PMP measurement procedure

Figure 1.1 EU emission standard.

In order to measure the emission index, the vehicle has to cover a real representative driving cycle that covers idle conditions, low and high constant speed, acceleration and deceleration, urban and extra-urban driving cycles. Effective after year 2000 (Euro 3), that test procedure was modified to eliminate the 40 s engine warm-up period before the beginning of emission sampling. This modified cold start test is referred to as the New European Driving Cycle (NEDC) or as the MVEG-B test. All emissions are expressed in g/km.

The Euro 5/6 implementing legislation introduces a new PM mass emission measurement method (similar to the US 2007 procedure) developed by the UN/ECE Particulate Measurement Programme (PMP) and adjusts the PM mass emission limits to account for differences in results using the old and the new method. The Euro 5/6 legislation also introduces a particle number (PN) emission limit in addition to the mass-based limits.

In Figure 1.2 the "New European Driving Cycle" NEDC is reported, composed by the ECE cycle, which represents a typical urban driving cycle and it is considered for four times, and by the EUDC cycle, which represents a typical extra urban driving cycle, where the vehicle runs up to 120 km/h.
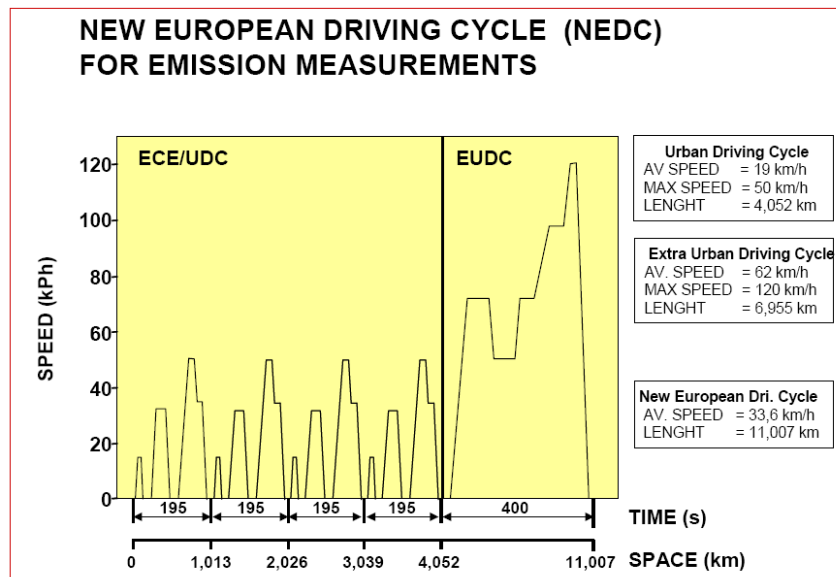
Figure 1.2 ECE/EUDC Driving Cycle, representative for EU norm.

During the cycle, the exhaust gas are sampled, the pollulants species are individuate and compared with the target thresholds.

Starting from the Euro 3 stage, vehicles must be equipped with an onboard diagnostic system for emission control. Driver must be notified in the case which a malfunction or deterioration of the emission system occurs that would

cause emissions to exceed mandatory thresholds. The thresholds are based on the NEDC (cold start ECE+EUDC) test. To distinguish from the US OBD, the European limits are also referred to as the EOBD (European OBD).

1.2 STATE OF ART FOR DIESEL AND GASOLINE ENGINES

Besides their fuel economy advantage, the diesel engines emit extremely low concentrations of unburned hydrocarbons and carbon monoxide emissions [8].

The reason for these extremely low hydrocarbon (HC) and carbon monoxide (CO) emissions is that diesels operate in very lean regimes where λ (relative air/fuel ratio) is greater than 1 [1].Carbon dioxide (CO_2) is the major product generated in the combustion of fossil fuels. This exhaust species is generally referred to as a greenhouse gas and considered responsible for global warming.

In spite of this belief, CO_2 remains an unregulated emission species. However, at recent environmental world meetings where concerns over the global effects of emissions were discussed, new commitments were made to collectively work at reducing CO_2 emissions. Interestingly, CO_2 emissions produced by natural phenomena far exceed those which are manmade. Figure 1.3 shows the apportionment of CO_2 emission from natural sources [8]. The total yearly CO_2 emissions from natural sources is estimated at 770×10^9 tons/annum. By contrast, the total yearly manmade CO_2 emissions is estimated at 26×10^9 tons/annum, less than 4% of the total CO_2 inventory.
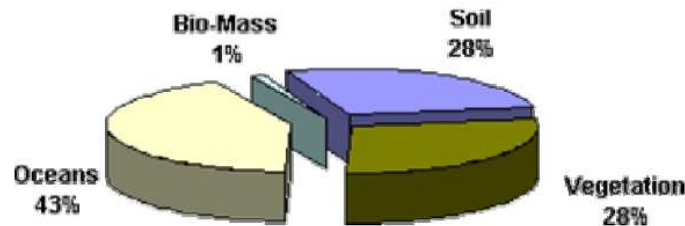
Figure 1.3 Sources of natural CO_2 emissions

Even though manmade CO_2 emissions may represent a small percentage of the global CO_2 problem, it is important that actions are taken to minimize its impact on the environment. Figure 1.4 gives the CO_2 allocation of each manmade source [8]. Power generation, heating, and industrial activities are responsible for about 70% of manmade CO_2, while transportation-related CO_2 represents about 16% of all manmade CO_2.
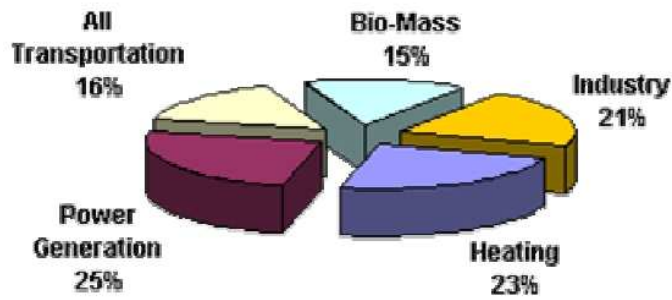
Figure 1.4 Allocation of CO2 emissions for manmade sources.

With the worldwide predominance of gasoline-powered personal transportation, conversion to modern diesel-powered vehicle could reduce transportation-related CO2 by about 25% from current levels. Figure 1.5 represents the results obtained by the German Federal Environmental Agency on 99 gasoline- and 36 diesel-powered vehicles in 1991 [8]. From that study, it was concluded that diesels had an average of 19% advantage over gasoline engines, in CO2 emission. The diesel engines involved in that study were mostly indirect-injected engines that are lower in fuel efficiency than their direct-injected counterparts by about 10 to 15%.

Hence a 25% reduction in transportation-related CO2 emissions by encouraging dieselization of gasoline-powered vehicles is thought to be quite feasible.
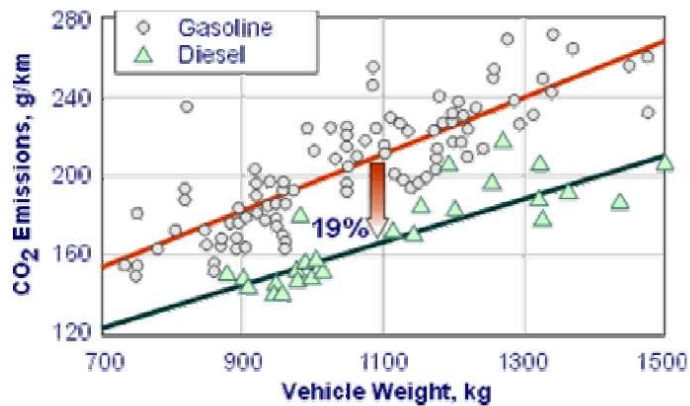
Figure 1.5 Comparison between Gasoline and Diesel-Powered CO2 emissions.

While diesel engines are known for their high engine-out emission of nitrogen oxides, the NOx issue is perhaps worth further examination to put matters in their proper perspective. A sample of about 15 heavy-duty gasoline engines calibrated to meet the 1991 US Federal emission standards were tested according to EPA specifications. The mathematical average of their emissions is given in Table 1, where the corresponding results of a statistically representative sample of diesel engines of the same capacity are included. In addition, a line of emission data obtained by testing the same heavy-duty gasoline engine when equipped with a 3-way catalyst is also provided in Figure 1.6, for comparative purposes.

Test Condition	Emissions, g/bhp-hr			
	HC	CO	NOx	PM
Diesel, engine-out	0.15	1.50	3.40	0.07
Gasoline, engine-out	0.81	30.22	4.30	-
Gasoline with 3-way catalyst	0.07	2.30	0.04	-
Note: Results are composites for EPA heavy-duty transient FTP cycle. Engine-out results are the mathematical average of 15 gasoline engines, 9 diesel engines, and 3 heavy-duty gasoline engines equipped with 3-way catalysts. All engines were about 7.0 L capacity.				

Figure 1.6 Emissions from Heavy-Duty Diesel and Gasoline Engines.

In diesel engines both HC and CO emissions are a small fraction of those found in their gasoline engine-out counterparts. Even diesel engine-out NOx emissions, in the example of Figure 1.6, are almost 1.0 g/bhp-hr less than their corresponding gasoline emissions. However, thanks to the 3-way catalyst conversion efficiency, the same gasoline engines emit extremely low HC, CO, and NOx emissions. Of course, conditions in the exhaust have to be conducive to the optimum operation of the 3-way catalyst. With accurate control of the fuel and air, modern gasoline engines operate at stoichiometric ratio where the catalyst performs at its highest conversion efficiency. Unfortunately, diesel exhaust is extremely lean and reducing NOx in an oxygen-rich environment is a very challenging task. The catalyst industry is developing solutions for the diesel NOx problem, but so far there is a lot of debate regarding the most plausible method of dealing with this problem.

Another problematic pollutant associated with diesel engines is particulate matter. The casual observer is made aware of this pollutant in the form of black smoke or soot emitted from either the tail pipes of many diesel-equipped passenger cars or the stacks of diesel-powered heavy-duty vehicles. Emission of soot is also accompanied with other matter suspended in the exhaust, such as: unburned lube oil, unburned fuel, trace metals, and sulfur byproducts.

Emission of soot in particulate matter results from the nature of the heterogeneous combustion process or diffusion type combustion that is prevalent in diesel engines. Fuel and air mixture preparation in modern diesel engines has greatly reduced this problem. In addition, the development of diesel particulate filters promises to eliminate it altogether. Particulate matter is not yet regulated in gasoline engines.

Due to the wedlock explained before, joining with the overall constraints necessary to optimize a vehicle; as consumption reduction and performance increasing, the old engine management techniques isn't enough to fulfill all these demands.

In Figure 1.7 the complexity of control system has been expressed in terms of new components and number of control parameters (to be calibrated).
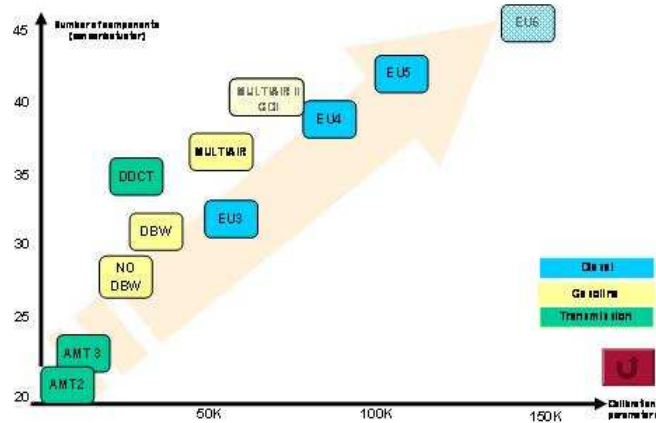
Figure 1.7 Control system complexity

Because of competition, time to market is more and more reducing and consequently the development time is becoming shorter and shorter: for instance only 18 months are allowed for the development of new engine and related control system while that time was of 25 months only few years ago.

The peculiarity of automotive industry, consisting of large scale production, makes it a risky business because a single problem can affect thousands and sometimes millions of models: there is less time to develop the system but no errors are admitted. Several cases regarding recall campaigns have been published also for the most important carmakers. In this situation, being able to meet requirements and guarantee the necessary quality level (Index Per Thousand Vehicles indicators are used to define the expected level of quality: some units are the current targets) is really a challenge if an effective, predictable and fast development process is not available.

1.3 PERFORMANCE AND ROBUSTNESS ENCREASING

The automotive industry is one of the most competitive markets in terms of performance and cost. Obviously clients will have to pay an increased number of mechanical failures and driving feelings from reducing the development and producing costs. These issues lead many journalists to criticize new models by

doing benchmarks and product tests. A negative feedback can create problems in the market, reducing the amount of vehicles sold and therefore the profit.

OEMs are always searching for innovative solutions that can give them market advantages:

- on gasoline engines, the need of responsiveness and fuel consumption reduction brought to the introduction of the MULTI-AIR® technology that manages in a flexible way the air intake valves;
- to reduce noise and vibration harshness (NVH) at the stop light or in traffic queues, Start & Stop technology, that switches off the engine automatically at each vehicle stop, are being deployed;
- to improve fun to drive and once again to reduce fuel consumption, smart management of the alternator has been developed; it manages the battery charge in braking and acceleration phases;
- emission reduction on diesel engines, has been achieved with a flexible fuel injection management on common rail systems, so called MULTI-JET II®, up to 10 injections per engine cycle;
- to improve driving comfort and safety, Hill Holder technology, that brakes the vehicle automatically in a drive off on a slope to prevent vehicle roll-back;
- to improve the drive off maneuver the analogic clutch and the accelerometer sensor are employed.

These complex electronics peculiarities are also necessary for low-segment vehicles. Therefore, the electronic components are increasing, such as the degrees of freedom.

Each new technology introduced cannot be seen as a component that is simply added to the vehicle but must be managed by algorithms in charge to coordinate all present features with the added ones. Because the increase of complexity is exponential, it is very difficult to foresee the complete interaction of each technology with the risk of delivering products with lacks of performance.

Chapter 2 Overview of Engine Control Systems

The recent trend in engines design is the use of low displacement engines (the so called "downsizing") to fulfill the new requirements. The need for torque and power increments is obviously in contrast with fuel consumption reduction. Therefore, new technologies need to be used in order to induce different engine working conditions. On gasoline engine the industrial research is focused on the development of a new way to let the air enter into the engine: the Variable Valve Timing, or Variable Valve Actuation system (and also the use of Turbo Charger) have the objective to minimize the power required for pumping the air in the cylinders and, in turn, maximize the engine efficiency. In this scenario a revolutionary approach has been introduced by Fiat by means of the MultiAir technology, detailed in this chapter, that permits to define the desired inlet valve timing.

2.1 VARIABLE VALVE TIMING SYSTEM

In traditional internal combustion engines (ICE), gas exchange valve timing is mechanically fixed with respect to the crankshaft position. This timing determines when the valves open and close, thereby affecting the air-fuel mixture and exhaust flow.

Variable Valve Timing (VVT) is a generic term for various concepts that allow one to change the advance, overlap, and even (in the case of some overhead-cam engines) the duration and lift of a four-stroke internal-combustion engine's intake and exhaust valves while the engine is operating. This technology has been under development for more than a century (a variation was tried out on some early steam engines), but it is only within the last twenty years or so with the advent of sophisticated electronic sensors and engine management systems that it has become practical and effective. There are a number of different variable valve timing systems, currently available and under development, to control the different valve timing parameters. These systems can be grouped in terms of their operations as:

- Phase Changing Systems
- Profile Switching Systems
- Cam Changing and Cam Phasing Systems
- Valve Duration Systems

Phase Changing Systems

Examples of cam-phasing VVT are:

- Toyota's VVT-i (Variable Valve Timing with Intelligence), which intelligently adjusts the overlap time between the exhaust valve closing and the intake valve opening;

- Lexus's VVT-iE (VVT – intelligent by Electric motor), which consists of the cam phase converter, mounted on the intake camshaft which converts the motor rotational input into the advance and retard of the cam phase, and a brushless electric motor, installed in the engine chain case.
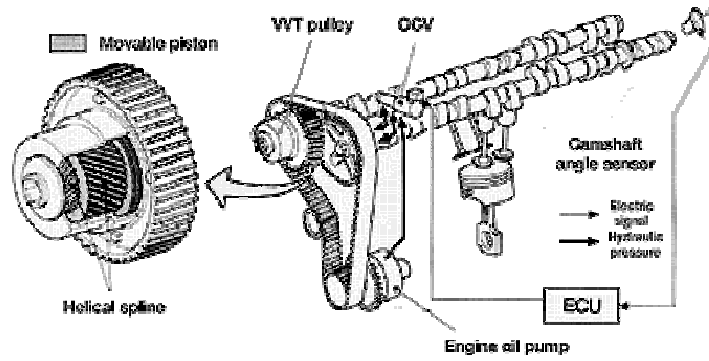
Figure 2.1 Cam- phasing VVT
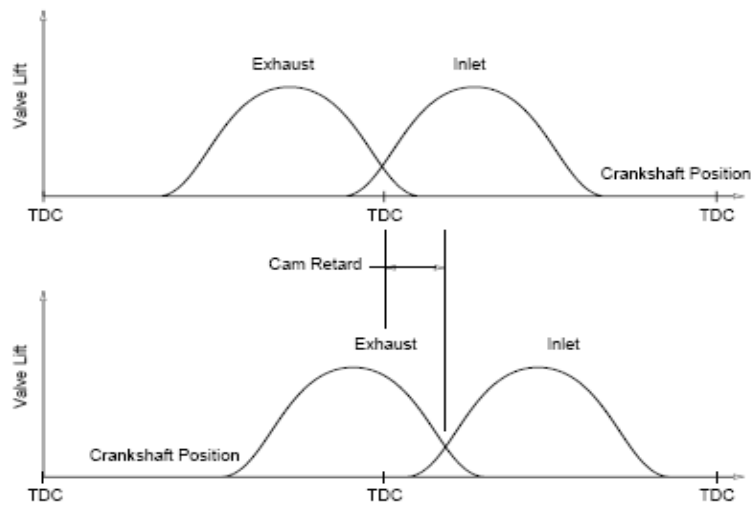
Figure 2.2 Valve Lift for an Engine with Cam Phasing VVT

Phase changing systems have been available on production engines for a number of years but have tended to be applied only to the highest specification engines of a particular range. Phasing the intake camshaft to gain increased performance, with a mechanism that can be moved between two fixed camshaft timings, is the most common application with the change in timing normally

17

occurring at a particular engine speed. More recently, there has been a move towards more flexible control systems that allow the camshaft phasing to be maintained at any point between two fixed limits. This has facilitated camshaft phase optimization for different engine speed and load conditions and has allowed exhaust camshaft phasing to be used for internal EGR control.

Profile Switching Systems

This type of variable valve timing system is capable of independently changing the valve event timing and the valve peak lift. The system switches between two different camshaft profiles on either or both of the camshafts and is normally designed to change at a particular engine speed (Figure 2.3). One profile designed to operate the valves at low engine speeds provides good road manners, low fuel consumption and low emissions output. The second profile is comparable to the profile of a race cam and comes into operation at high engine speeds to provide a large increase of power output. Therefore, cam- changing VVT systems act as if two different cam types at high and low speed were used.
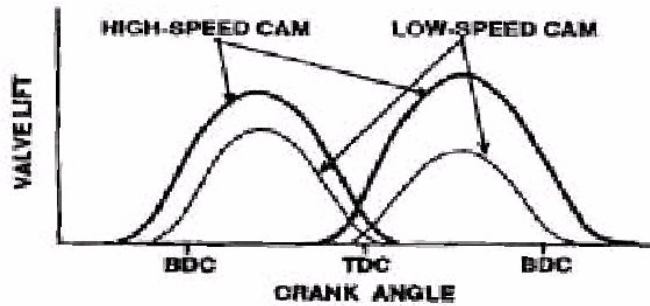
Figure 2.3 Valve Lift for an Engine with Cam Changing VVT

Honda, with the VTEC (Variable Valve Timing and Electronic Lift Control) system started production of a system that gives an engine the ability to operate on two completely different cam profiles, eliminating a major compromise in the engine design. In its simplest form, VTEC allows the valves to remain open for two different durations: a short opening time for low-speed operations to give good torque and acceleration, and a larger opening time at higher speeds to give more power. For accomplishing that, the camshaft has two sets of cam lobes for each valve and a sliding locking pin on the cam follower that determines which lobe is operating the valve. The locking pin is moved by a hydraulic control valve based on the engine speed and power delivery requirements. The two lobe shapes are referred to as fuel economy cams and high power cams, meaning that Honda engines with this technology are really two engines in one - a performance engine and an economical engine.

Because these systems have inherently two-position operations, they are not suitable for being optimized under different load conditions, e.g. EGR control. The ability to change the valve event timing, the lift and duration ensures that

these systems are capable of providing very high power output from a given engine whilst still complying with the emissions legislation.

Cam Changing and Cam Phasing Systems

By combining cam-changing VVT and cam-phasing VVT, one could satisfy the requirement of both top-end power and flexibility throughout the whole rev range, but it is inevitably more complex.

A typical example of this system is the Toyota's VVTL-i (Figure 2.4). The system can be seen as a combination of the existing VVT-i and Honda's VTEC, although the mechanism for the variable lift is different from Honda. Like VVT-i, the variable valve timing is implemented by shifting the phase angle of the whole camshaft forward or in reverse by means of a hydraulic actuator attached to the end of the camshaft. Like VTEC, Toyota's system uses a single rocker arm follower to actuate both intake valves (or exhaust valves). It also has two cam lobes acting on that rocker arm follower, the lobes have a different profile - one with longer valve-opening duration profile (for high speed), another with shorter valve-opening duration profile (for low speed). At low speed, the slow cam actuates the rocker arm follower via a roller bearing (to reduce friction). The high speed cam have not any effect on the rocker follower because there is sufficient spacing underneath its hydraulic tappet. At low speeds, the long duration cam idles while when the speed has increased to the threshold point, the sliding pin is pushed by hydraulic pressure to fill the spacing. The high speed cam becomes effective. Note that the fast cam provides a longer valve-opening duration while the sliding pin adds valve lift (while for Honda VTEC, both the duration and lift are implemented by the cam lobes). VVTL-i offers variable lift, which lifts its high speed power output a lot. Compared to Honda VTEC, Toyota's system has continuously variable valve timing which helps it to better achieve low to medium speed flexibility. Therefore, it is undoubtedly the best commercial VVT system today available. However, it is also more complex and probably more expensive to build.
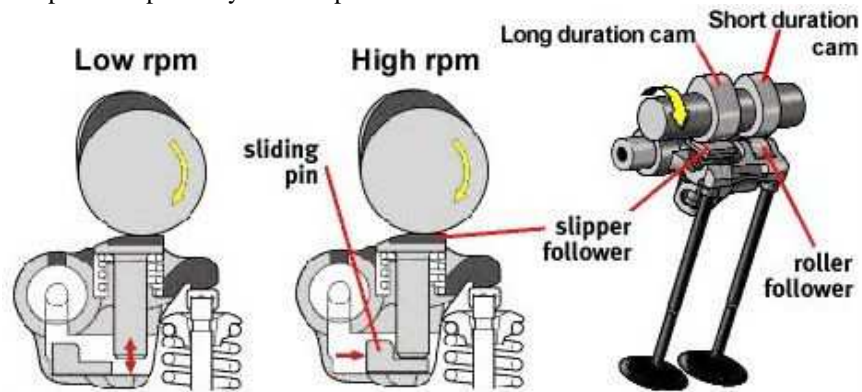
Figure 2.4 Toyota's VVTL-i system

Valve Duration Systems

The basic concept of this system is that of lengthening the duration of the opening of the valves. This system was introduced by Rover who call it Variable Valve Control (VVC). The VVC principle is based on an eccentric rotating disc to drive the inlet valves of every two cylinders. Since the eccentric shape creates nonlinear rotation, the opening period of the valves can be varied by controlling the eccentric position of the disc. With VVC the outlet camshaft is not part of the VVC system and is driven normally by the toothed belt from the crankshaft. Figure 2.5 shows an example of a working VVC system. When the eccentric wheel, which is connected to crankshaft with revolution speed halved, rotates at 180°, the camshaft turns, for example, only 140°. In the following 180° of eccentric wheel, the camshaft turns instead 220° so that it remains totally in phase with the crankshaft. This variable camshaft speed can change the duration of inlet valves opening. Figure 2.6 shows the valve lift for an engine with VCC Rover.
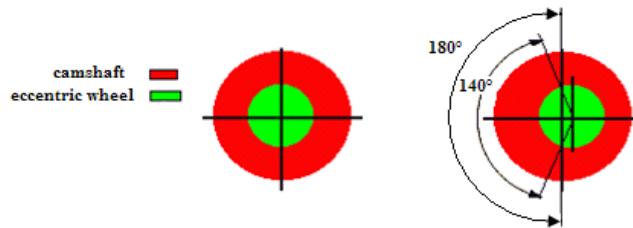
Figure 2.5 VVC system working
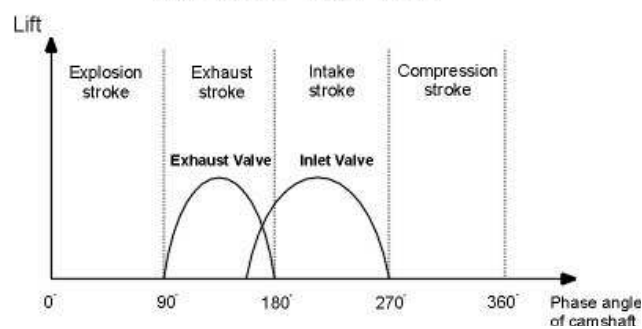
Figure 2.6 Valve Lift for engine with VVC system

2.2 VARIABLE VALVE ACTUATION TECHNOLOGY

The Variable Valve Actuation technology represents the new timing system with variable lift of the intake valves that has been developed in recent years. The VVA has been introduced as a promising technology able to improve the performance of the vehicle in terms of fuel economy, emission reductions and, more generally, the whole efficiency of the system. Contrary to classical engines, where the intake and exhaust valves are commanded mechanically by

the camshaft and so both the timing and the duration of valves opening are fixed by events, the VVA system offers the possibility to vary the valves actuation. Moreover, the innovative VVA system allows one to control the air mass flow rate that is inducted in an internal combustion engine without any use of the throttle plate; this last situation has the benefit of having an air pressure upstream of intake valves always constant because the pump losses near the throttle body are zero.

The adopted VVA system is shown schematically in Figure 2.7. The valve actuator consists of a piston connected through an oil chamber to the intake valve, a solenoid valve to regulate the pressure inside the oil chamber and a hydraulic brake to assure the soft landing. When the electro-valve is open, the oil comes out from the high pressure chamber and it can be consequently possible to obtain any condition included between the two following extreme modalities:

- if the solenoid valve is open the intake valves remain closed;
- if the solenoid valve is always closed, the lift of the valves is the same as that of the cams.
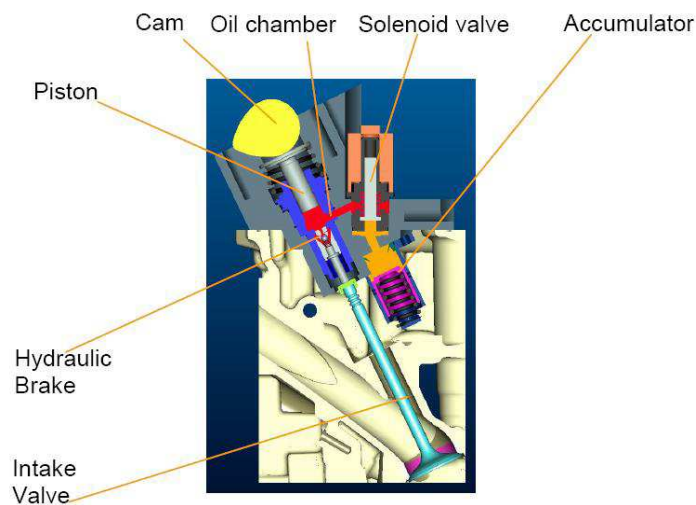
Figure 2.7 VVA system

As reported in Figure 2.8, the valve lift profile can assume different forms depending on the required air mass flow rate and engine speed. In fact, with this particular VVA system many strategies are possible, such as those indicated in the following points:

- Full Lift (FL) actuation mode represents the normal functioning of the valves, i.e. commanded mechanically by the camshaft: the solenoid valve remains closed assuring high pressure into the oil chamber and, consequently, assuring a rigid connection between the intake valve and the camshaft through the piston;

- Early Closure (EC) valve mode is obtained by opening the solenoid valve at a certain cam angle, i.e. the control angle, reducing the pressure inside the oil chamber. The motion of the intake valve is then decoupled from the piston and, forced by the valve springs. It starts to close earlier than in the full-lift mode. Soft landing of the intake valve is controlled by a hydraulic dampening unit (hydraulic brake);
- Late Opening (LO) valve mode can be achieved by regulating the solenoid valve partially opened. In this way, the pressure inside the oil chamber is regulated to a lower pressure than in the full lift mode, obtaining a rigid connection, but with a shorter distance function of the chamber pressure, between the intake valve and the camshaft. Consequently, the valve profile is similar to the full lift mode, but with a smaller time duration;
- Multi Lift (ML) actuation mode is a particular operative actuation mode obtained combining the late opening with the early closure, as is shown in Figure 2.9 This profile is limited by the mechanical cam constrains, in fact the next late opening must be activate before 50% of the full lift cam.

The flexibility of the intake valve control offered by the VVA system leads to enhancing the efficiency of the combustion process. More in general, the following advantages can be addressed by the introduction in the vehicle of the VVA system:

- high charge trapping efficiency over the entire speed range through a wide modulation of valve lift;
- throttle-less engine operation, through direct air control at the valves resulting in a reduction of pumping work and fuel consumption;
- dynamic control, cylinder by cylinder and stroke by stroke, of the inlet charge aimed at an improvement of emissions, drivability and fuel consumption in transient operation.
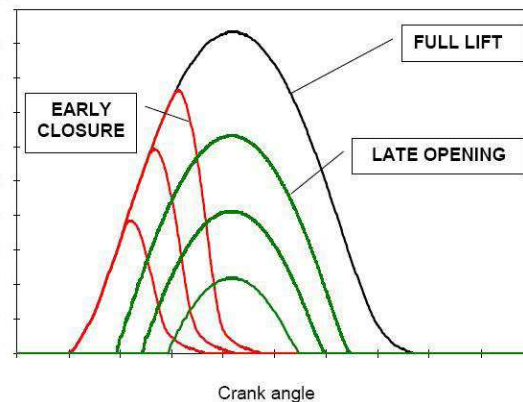
Figure 2.8 Valve lift profiles
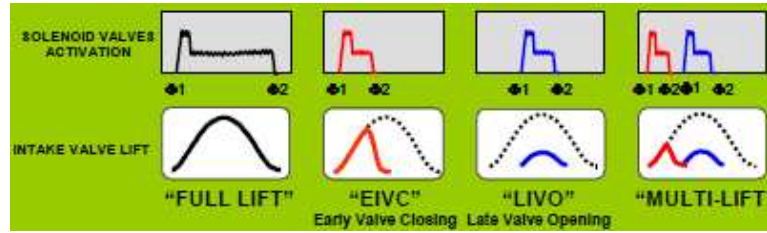
Figure 2.9 Solenoid valves activation and valve lift

The electro-hydraulic actuator that has been developed is relatively simple and behaves high hardiness characteristics and low sensitivity to critical parameters, like variation of the oil viscosity related to temperature.

Finally, the control of this innovative VVA system is achieved by a specific electronic control system that contains model-based strategies allowing the elaboration of the valve actuation signals according to the demands of the driver [5].

The MultiAir technology developed by Fiat is an example of application of Variable Valve Actuation system.

The MultiAir technology

In the last decade, the development of the Common Rail technology for Diesel engines marked a breakthrough in the passenger car market. To be competitive also in the field of gasoline engines, Fiat Group decided to follow the same approach and focus on breakthrough technologies. The aim was to provide customers with substantial benefits in terms of fuel economy and fun-to- drive while maintaining the engine intrinsic comfort characteristics, based on a smooth combustion process and on light structures and components.

The key parameter to control Diesel engine combustion and therefore performance, emissions and fuel consumption is the quantity and characteristics of the fuel injected into cylinders. That is the reason why the Common Rail electronic Diesel fuel injection system was such a fundamental breakthrough in Direct Injection Diesel engine technology. The key parameter to control gasoline engine combustion, and therefore performance, emissions and fuel consumption, is the quantity and characteristics of the fresh air charge in the cylinders. In conventional gasoline engines the air mass trapped in the cylinders is controlled by keeping the intake valves opening constantly and adjusting upstream pressure through a throttle valve. One of the drawbacks of this simple conventional mechanical control is that the engine wastes about 10% of the input energy in pumping the air charge from a lower intake pressure to the atmospheric exhaust pressure.

A fundamental breakthrough in air mass control, and therefore in gasoline engine technology, is based on direct air charge metering at the cylinder inlet ports by means of an advanced electronic actuation and control of the intake valves, while maintaining a constant natural upstream pressure.

Research on this key technology started in the eighties, when engine electronic control technologies reached the stage of mature technologies. At the

beginning world-wide research efforts were focused on the electromagnetic actuation concept, following which valve opening and closing is obtained by alternatively energizing upper and lower magnets with an armature connected to the valve. This actuating principle had the intrinsic appeal of maximum flexibility and dynamic response in valve control, but despite a decade of significant development efforts the main drawbacks of the concept (its being intrinsically not fail-safe and its high energy absorption) could not be fully overcome. At this point most automotive companies fell back on the development of the simpler, robust and well-known electromechanical concepts, based on the valve lift variation through dedicated mechanisms, usually combined with cam phasers to allow control of both valve lift and phase. The main limitation of these systems is low flexibility in valve opening schedules and a much lower dynamic response; for example, all the cylinders of an engine bank are actuated simultaneously, thereby excluding any cylinder selective actions. Many similar electromechanical valve control systems were then introduced over the past decade.

In the mid 90's Fiat Group research efforts switched to electro-hydraulic actuation, leveraging on the know-how gained during the Common Rail development.

The goal was to reach the desired flexibility of valve opening schedule air mass control on a cylinder-by-cylinder and stroke-by-stroke basis. The electro-hydraulic variable valve actuation technology developed by Fiat was selected for its relative simplicity, low power requirements, intrinsic fail safe nature and low cost potential.

The operating principle of the system, applied to intake valves, is the following: a piston, moved by a mechanical intake cam, is connected to the intake valve through a hydraulic chamber, which is controlled by a normally open on/off solenoid valve.

When the solenoid valve is closed, the oil in the hydraulic chamber behaves like a solid body and transmits to the intake valves the lift schedule imposed by the mechanical intake cam. When the solenoid valve is open, the hydraulic chamber and the intake valves are de-coupled; the intake valves do not follow the intake cam anymore and close under the valve spring action. The final part of the valve closing stroke is controlled by a dedicated hydraulic brake, to ensure a soft and regular landing phase in any engine operating conditions.

Through solenoid valve opening and closing time control, a wide range of optimum intake valve opening schedules can be easily obtained.

For maximum power, the solenoid valve is always closed and full valve opening is achieved completely following the mechanical cam (**Full Lift** mode), which was specifically designed to maximize power at high engine speed (long closing time). For low-rpm torque, the solenoid valve is opened near the end of the cam profile, leading to early intake valve closing (**EIVC** mode). This eliminates unwanted backflow into the manifold and maximizes the air mass trapped in the cylinders. In engine part load, the solenoid valve is opened earlier (before finishing of the cam profile) causing partial valve openings to control the trapped air mass as a function of the required torque (**Partial Load** mode). Alternatively the intake valves can be partially opened by closing the solenoid

valve once the mechanical cam action has already started (**LIVO** mode: Late Intake Valve Opening). In this case the air stream into the cylinder is faster and results in higher in-cylinder turbulence. The last two actuation modes can be combined in the same intake stroke, generating a so-called "**Multilift**" mode, which enhances turbulence and combustion rate at very low loads. Figure 2.10 shows possible valve profiles using the multi-air technology.

Figure 2.10 Possible valve profiles using the MultiAir technology

The Multiair Technology potential benefits for gasoline engines exploited so far can be summarized as follows:

- Maximum Power is increased by up to 10% thanks to the adoption of a power-oriented mechanical cam profile;
- Low-rpm Torque is improved by up to 15% through early intake valve closing strategies that maximize the air mass trapped in the cylinders;
- Elimination of pumping losses brings a 10% reduction of fuel consumption and CO_2 emissions, both in naturally aspirated and turbocharged engines with the same displacement;
- MultiAir turbocharged and downsized engines can achieve up to 25% fuel economy improvement over conventional naturally aspirated engines with the same level of performance;
- Optimum valve control strategies during engine warm-up and internal Exhaust Gas Recirculation, realized by reopening the intake valves during the exhaust stroke, result in emissions reduction ranging from 40% for *HC/CO* to 60% for *NO_x*;
- Constant upstream air pressure, atmospheric for naturally aspirated and higher for turbocharged engines, together with the extremely fast air mass control, cylinder-by-cylinder and stroke-by-stroke, result in a superior dynamic engine response.

The MultiAir technology, a Fiat worldwide premiere in 2009, has introduced further technological evolutions for gasoline engines:

- Integration of the MultiAir direct air mass control with direct gasoline injection to further improve transient response and fuel economy;
- Introduction of more advanced multiple valve opening strategies to further reduce emissions;
- Innovative engine-turbocharger matching to control trapped air mass through combination of optimum boost pressure and valve opening strategies.

While electronic gasoline fuel injection developed in the '70s and Common Rail developed in the '90s were fuel specific breakthrough technologies, the MultiAir Electronic Valve Control technology can be applied to all internal combustion engines whatever fuel they burn.

MultiAir, initially developed for spark ignition engines burning light fuel ranging from gasoline to natural gas and hydrogen, has wide potential also for Diesel engine emissions reduction. Intrinsic NO_x reduction of up to 60% can be obtained by internal Exhaust Gas Recirculation (*iEGR*) realized with intake valves reopening during the exhaust stroke, while optimal valve control strategies during cold start and warm-up bring up to 40% *HC* and *CO* reduction of emissions. Further substantial reduction comes from the more efficient management and regeneration of the diesel particulate filter and NO_x storage catalyst, thanks to the highly dynamic air mass flow control during transient engine operation.

Diesel engine performance improvement is similar to that of the gasoline engine and is based on the same physical principles. Instead, fuel consumption benefits are limited to few percentage points because of the low pumping losses of Diesel engines, one of the reasons of their superior fuel economy. In the future, power train technical evolution might benefit from a progressive unification of gasoline and Diesel engines architectures.

A MultiAir engine cylinder head can therefore be conceived and developed, where both combustion systems can be fully optimized without compromises. Moreover the MultiAir electro-hydraulic actuator is physically the same, with minor machining differences, while internal subcomponents are all carry over from the Fire and SGE (small gasoline engine) applications [6], [7].

2.3 INTELLIGENT ALTERNATOR CONTROL SYSTEM

An alternator is an electromechanical device that converts kinetic energy into electrical energy and is used in modern automobiles to charge the battery and to power a car's electric system when its engine is running. It is connected to the engine via a belt that transmits the motion of rotation that within the alternator is used to produce alternating electric current (AC). Automotive alternators use a set of diodes to convert AC to DC (direct current). A voltage regulator makes for the voltage output from the alternator to remain constant.

Intelligent Alternator Control System (IAC) allows some energy to recover, through "intelligent" use of the alternator, which during braking is dissipated as heat in brake discs. The IAC system generates electric power for a car's on board network exclusively in over-run and during braking to transform the

kinetic energy resulting from the inertia of the vehicle into electrical energy that is transferred to the battery becoming an energy surplus, which can return available in the following phases of acceleration when it is used to feed the electrical components of the vehicle, thus decreasing the work required at the alternator at this stage. This results in more torque being produced and delivered to the wheels. Normally, the engine control system determines the power that is used to activate the alternator --through a torque-based model.

The IAC system establishes that:

- in the acceleration phase, the alternator output voltage is set so that it is equal or close to the level of battery voltage, which, in this way, provides alone for the electricity needs of the car;

- in over-run or during breaking, the alternator output voltage is set to a value higher than the battery voltage, so the alternator is not only able to cover the entire electricity demand of the vehicle, but at the same time to charge the battery.

In the latter case, the alternator is actually a load on the crankshaft and thereby exerts a braking effect on the vehicle which represents precisely the recovery of part of the energy dissipated in the brakes. For the IAC system it's necessary to have precise information about the charging status and battery usage which are acquired by using a sensor IBS (Intelligent Battery Sensor). The battery is charged to only about 80% of its capacity as long as the engine is propelling the car, depending on ambient conditions. A reserve charge that is adequate for the consumption of power while the car is at a standstill and enabling the driver to start at any time, is maintained under all circumstances. Battery charge exceeding the 80% threshold is generated only in over-run and while the driver is applying the brakes. Since the number of charge cycles increases as a function of such battery management, IAC uses modern AGM (absorbent glass mat) batteries able to handle greater loads than conventional lead acid batteries.

The IAC system improves the overall efficiency of a vehicle by decreasing ancillary loads on the engine and by recuperating more of the waste heat energy so as to reduce fuel consumption.

Chapter 3 Control functions for CO2 reduction – Intelligent Alternator Management

In modern internal combustion engines a greater reduction of CO_2 emissions is required in order to significantly reduce fuel consumption and minimize the emissions of polluting gases, allowing them to fall within the strict limits set by current regulations. In a conventional engine control system, it is not possible to optimize the efficiency of the alternator in terms of emissions and fuel consumption, due to a constant voltage which is imposed and is not modifiable. On the contrary, in a system capable of controlling the voltage of the alternator, referring to such an alternator as "smart" hereafter, it would be possible to optimize its efficiency as a function of the vehicle/engine working points. This system requires first and foremost a communication protocol between the alternator and engine control unit, and a special sensor that gets data on the charging status of the battery.

In this chapter a management strategy is proposed for regulating the alternator regulation voltage in order to maximize its efficiency on the basis of the engine and vehicle conditions. This is done by using an "Intelligent Alternator Module (IAM)", that communicates using the LIN protocol with the Engine Control Module (ECM), and an "Intelligent Battery Sensor (IBS)", which provides the information about the battery State-Of-Charge (SOC).

The main features of the management strategy are:

- switch off the alternator during tip-in manoeuvres in order to maximize the performance;
- switch off the alternator when the catalyst is cold, so as to reduce the emissions, and in idle conditions if the battery SOC is high enough;
- increase the alternator load during tip-out manoeuvres, braking or cut-offs, and during shut-down in order to recover the kinetic energy otherwise dissipated as heat in the brakes;
- control the alternator voltage regulation in steady-state as a function of battery SOC, loading it only when needed.

These procedures are implemented for both Gasoline and Diesel Engines and several improvements result: the average life of the vehicle battery has been increased and fuel consumption and emission have been reduced. In particular, measurements done have shown that consumption reduction due to the control system described above is about 2-3% on the NEDC homologation cycle.

3.1 ALTERNATOR PRINCIPLES

In Figure 3.1 the mono-phase equivalent circuit of the alternator is reported in order to better shows the voltage and the current under analysis.
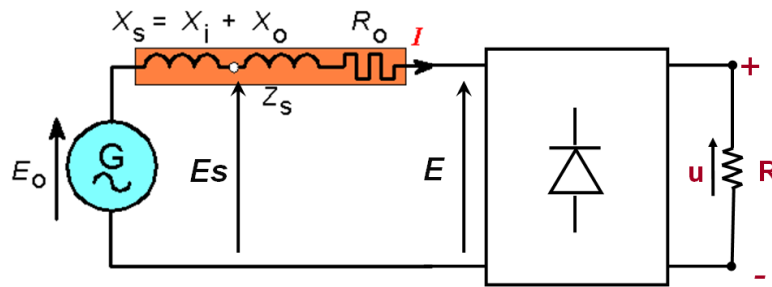
Figure 3.1 Alternator circuit.

The voltage u is the output of the three-phase bridge showed in Figure 3.2. The three-phase bridge has as output voltage (3.1) the signal with a frequency pulse six times higher than the individual voltage signal in input, and having a medium value showed in (3.2).

$$E_i(t) = \sqrt{2} \cdot E.sen(\omega t + \varphi_i) \qquad \textbf{(3.1)}$$

$$U_m = \frac{3\sqrt{6}}{\pi} E \cong 2.34 \cdot E \qquad \textbf{(3.2)}$$

In short, there is a constant of proportionality between the effective value E and the output voltage on the load u.
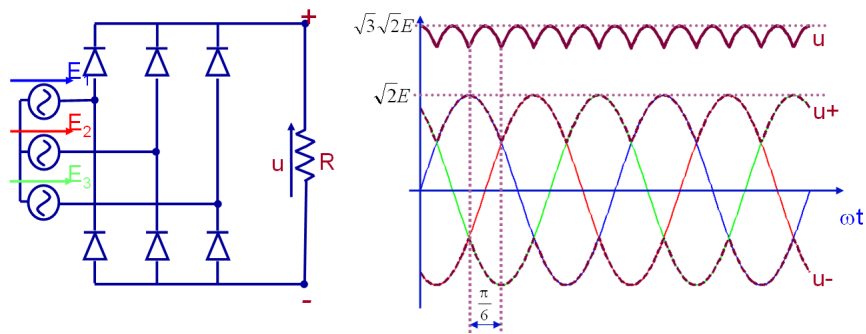
Figure 3.2 . Thee-phase bridge.

By referring to Figure 3.1, the impedance Z_S is the parameter of the equivalent circuit that takes into account the following phenomena:

- Ohmic losses R_0 on the stator wrapping;
- Dispersion X_0 of the main flow (in air or into the wrapping not active);
- Presence of the demagnetizing armature reaction $X_{i,}$.

By analyzing the elements from which this parameters depend, it is possible to evaluate the effect on the current output.

In (3.3), the relationship of the current output I is reported:

$$I = \frac{E_S - E}{Z_0} \propto \frac{N \cdot \omega_{alt} \cdot \varphi\left(I_{ecc}, I_{phase}\right) - E}{N^2 \cdot \sqrt{c_R + c_X \cdot \omega_{alt}^2}} \qquad (3.3)$$

In order to maintain the current I>0, the alternator speed has to be:

$$\omega_{alt} > \frac{E}{\varphi\left(I_{ecc}, I_{phase}\right) \cdot N} \qquad (3.4)$$

With ω_{alt} low, we have:

$$I \propto \frac{\omega_{alt} \cdot \varphi\left(I_{ecc}, I_{phase}\right) - E}{N \cdot \sqrt{c_R}} = -k_1 + k_2 \cdot \omega_{alt} \qquad (3.5)$$

With ω_{alt} high, we have the maximum value for the current given by:

$$I \propto \frac{N \cdot \omega_{alt} \cdot \varphi\left(I_{ecc}, I_{phase}\right) - E}{N^2 \cdot \sqrt{c_X \cdot \omega_{alt}^2}} = I_{max} \qquad (3.6)$$

where

- N is the number of conductors in the stator;
- ω_{alt} is the alternator rotational speed;
- φ is the magnetic flow.

By considering the battery voltage constant and assuming N conductors, in Figure 3.3 it can be seen the plot of the current as a function of the angular velocity.
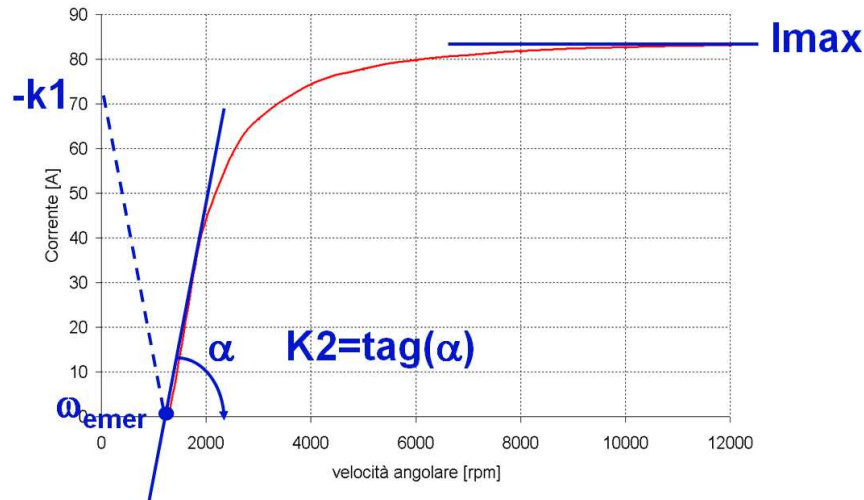
Figure 3.3 . Alternator characteristic at E and N constant.

3.2 GENERAL DESCRIPTION OF SMART ALTERNATOR SYSTEM

The current state of the art of the alternator voltage regulation consists of the regulation of the rotational speed and current of the alternator in relation to an efficiency index related to the actual working point of the engine [1] [2]. This solution has, as a disadvantage, that the current depends on the electrical loads and on the battery voltage. The loads are not controllable while the latter is only slowly controllable. This approach may not take into account in an appropriate way the battery SOC. Therefore, the control action is not aimed at preserving the battery life time for as long as possible.

The proposed solution consists in the regulation of the alternator voltage on the basis of the engine and vehicle conditions so as to maximize its efficiency. This is done by using an "Intelligent Alternator Module (IAM)", that communicates with the Engine Control Module (ECM) using the LIN protocol, and an "Intelligent Battery Sensor (IBS)" which provides the information about the battery SOC.

The main features of the management strategy are:

- switch off the alternator during tip-in manoeuvres in order to maximize the performance;
- switch off the alternator when the catalyst is cold, so as to reduce the emissions, and when it is in idle conditions if the battery SOC is high enough;
- increase the alternator load during tip-out manoeuvres, braking or cut-offs, and during shut-down in order to recover the kinetic energy otherwise dissipated as heat in the brakes;

- control the alternator voltage in steady-state as a function of battery SOC, loading it only when needed.

3.3 LOGIC ARCHITECTURE

The components required to perform the above mentioned algorithm are:

- The Intelligent Alternator Module – IAM
- The Engine Control Module – ECM
- The Body Control Module – BCM
- The Intelligent Battery Sensor – IBS
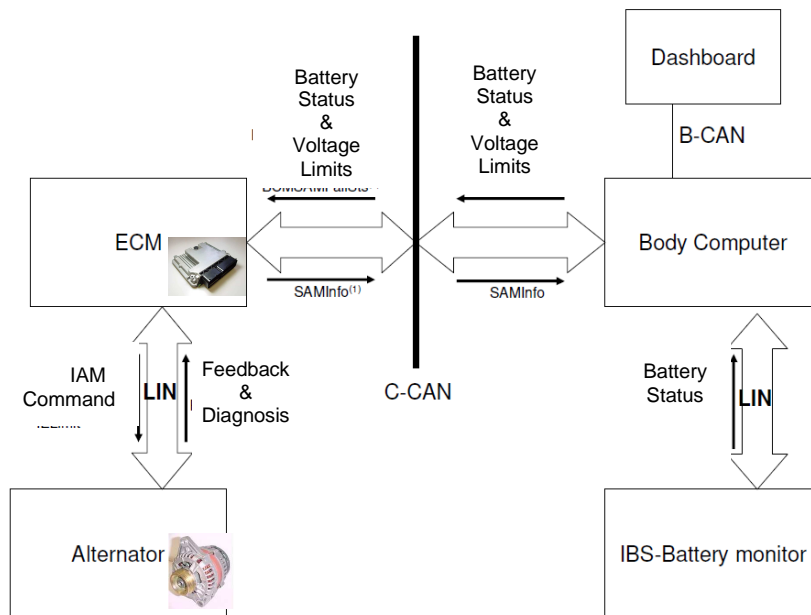
Figure 3.4 Logic Architecture Scheme

The ECM manages:

- The alternator, via the LIN protocol, by sending the command set-points;

- The vehicle/engine conditions to identify the driving conditions;

- The engine conditions to establish the regulation voltage boundaries versus the IAM module;

- The regulation range of voltage coming from the BCM module, comparing it to the ECM boundaries;

- The transmission of diagnostic information coming from the IAM module.

The BCM handles:
- The vehicle electrical loads (e.g. fog lights or headlights, windshield wipers, heated rear window) to establish the voltage control range and forward it to ECM module via the CAN protocol;

- The transmission to the ECM module of the information about the battery status (SOC, voltage, current, temperature) coming from IBS module;

- The alternator warning lamp for announcing fault occurrences.

The IAM manages:

- The voltage regulation, starting from the set-point received via LIN from ECM;

- The delivering of the feedback messages coming from the alternator (e.g. diagnostic information, operating duty cycle).

3.4 ALGORITHM DESCRIPTION

The main states of the Smart Alternator Management (SAM) strategy are:

- **PB** : Passive Boost, in which the alternator is switched off during tip-in manoeuvres. When a fast increase or, alternatively, a high absolute level of torque is required, the ECM controls the alternator with the voltage level as low as possible, according to the voltage limits imposed by the BCM module.

- **RB**: Regenerative Braking, in which the alternator is regenerating in braking manoeuvres. When the vehicle is decelerating (braking or cut-off manoeuvres) the ECM controls the alternator with the voltage level as high as possible, according to the voltage limits imposed by the BCM module.

- **SS**: Steady State, in which the Battery SOC is controlled. Outside the above conditions, the ECM controls the voltage to maintain an optimal SOC, chosen as a trade-off value between fuel consumption and battery life.

- **CE**: Cold Engine Management, in which the alternator is switched on during cold conditions in order to increase the engine load for quickening the catalyst light-off phase.

- **CRK**: Cranking Management, in which the IAM is managed during engine crank or automatic re-start (for Stop & Start feature). During the cranking phase, depending on the engine speed, two starting sub-phases are defined in which the set-point voltage regulation is kept low at first, in order to facilitate the engine speed rising, and then is increased (with ramp law) to a high value, in order to reduce the engine speed overshoot in the post-cranking phase without compromising the FEAD (Front End Accessory Drive) system performance.

- **SHUTOFF**: Shutoff Management, in which the IAM is managed during engine shutdown (either manually from the driver or automatically from a Stop & Start strategy). During an engine shut down the ECM module controls the alternator with the voltage level as high as possible, according to the limits imposed by BCM module, in order to increase engine load for reducing engine bouncing during shutdown and quickening the whole maneuver.

- **QC**: Quick Charge, when the SOC is too low, it's required that the alternator is set to the highest possible voltage level in order to quicken recharges the battery.

- **NP**: Normal Production, in which the IAM is set in the case of recovery. In the case of fault occurrences in the system (either components or communication lines), the ECM controls the alternator with typical voltage set-points of current productions (usually with values between 13.5V and 14.5V).

Figure 3.5 State flow diagram of Smart Alternator Management

In PB, RB, QC states, two controls are applied by ECM: one in open-loop, used to calculate the target voltage set-point and one in closed-loop based on a filtered battery voltage signal, where the instantaneous noise on the IBS measurement is reduced.

Figure 3.6 Voltage Battery Control Scheme in PB, RB, QC IAM status

The first alternator control algorithm, used in Passive Boost state, is in charge to determine the target voltage V_{obj}. through the following steps:

- compute the $V_{ECM_{lim}}$ voltage, that is related to the vehicle electronic equipment rotating with the internal combustion engine, e.g. the engine cooling fan assembly rotating to a preset speed;
- compute the $V_1(I_{bat})$ voltage, which is related to the current generation of the electrical battery.

$V_{ECM_{lim}}$ corresponds to a minimum preset alternator voltage which is enough to supply the active electronic equipment on the vehicle; the voltage $V_1(I_{bat})$ basically corresponds to a minimum predetermined voltage necessary to prevent an excessive battery current draining during the electrical supply. This term has been studied in order to guarantee a safety monitoring of the battery.

The Figure 3.7 shows the Alternator position and feature in the vehicle, and how the electrical loads are represented.
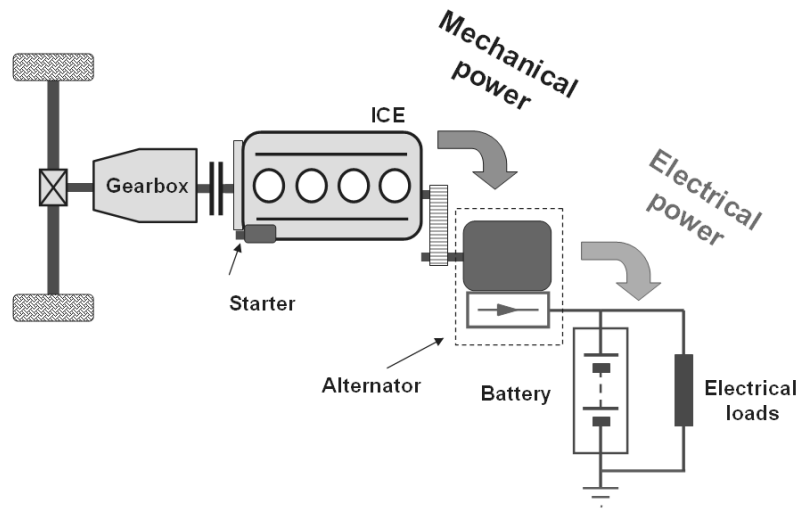
Figure 3.7 Alternator feature scheme.

The first alternator control algorithm, as showed in Figure 3.9, starts to define V_{obj} which establishes the lower voltage limit of the SAM strategy, as defined below:

$$V_{obj} = \max((V_{MIN_P}, V_{ECM_{lim}}, V_1(I_{bat\_meas})))$$

(3.7)

Where:
- o VMINP is the minimum value of the supply voltage range ΔVlimit(VMINP, VMAXP) that takes into account the electrical vehicle load status, and it is determined by the body computer;
- o VECMlim is the minimum alternator voltage which is enough to supply the active equipment on the vehicle;
- o $V_1(I_{bat})$ is the minimum voltage that allows to don't run down the battery.

Next, the regulation voltage V_{reg} is determined through the PI regulation system. In the Figure 3.8 the generic PID scheme is reported:
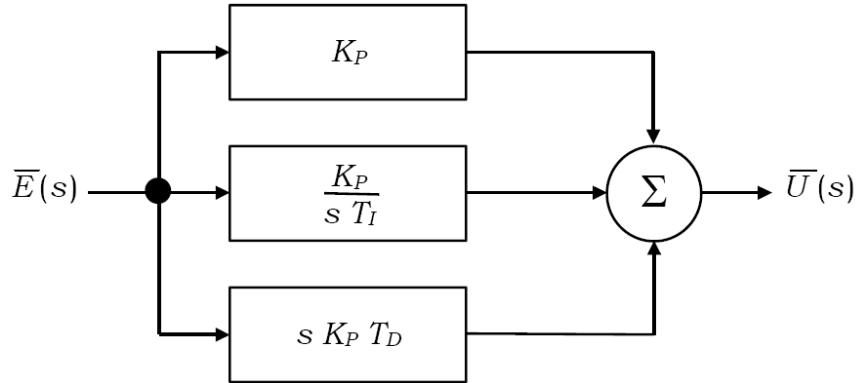
Figure 3.8 Generic PID scheme.

$$\overline{U}(s) = K_P \cdot \left(1 + \frac{1}{sT_I} + sT_D \right) \cdot \overline{E}(s) \tag{3.8}$$

This control has to be discretized in order to be implemented on a ECU algorithm, by using ZOH method. So the discretized PID becomes:

$$U(z^{-1}) = K_P \cdot \left(1 + \frac{T_s}{T_I \cdot (1 - z^{-1})} + T_D \frac{(1 - z^{-1})}{T_s} \right) \cdot E(z^{-1}) \tag{3.9}$$

Once the target voltage V_{obj} has been calculated, the voltage regulation control system consists of the following steps:

1) compute the error signal V_{err} as:

$$V_{err} = V_{obj} - V_{bat\_filt} \tag{3.10}$$

where:
- V_{obj} is the target voltage;
- V_{bat_filt} is the filtered battery voltage.

2) define the regulation voltage V_{reg} as reported in the block scheme of figure 3.3:

$$V_{reg} = V_{obj} + K_P \cdot \left(1 + \frac{T_s}{T_I \cdot \left(1 - z^{-1}\right)}\right) \cdot V_{err} \qquad (3.11)$$

The battery voltage decreasing during Passive Boost phase can lead to an engine friction decrease, causing a fuel consumption and emission reduction.
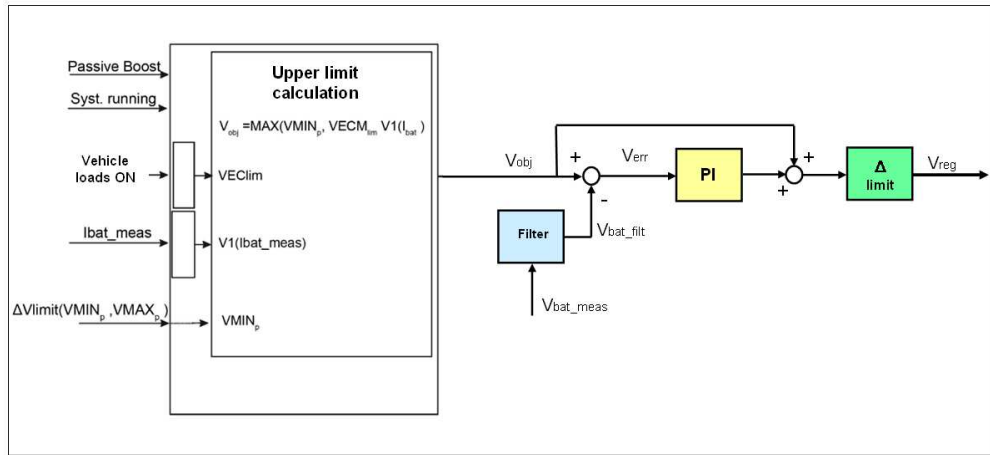
Figure 3.9 First Alternator Control algorithm scheme.

The second alternator control algorithm, used in Regenerative Braking and Quick Charge states, is used to determine the target voltage V_{obj} as a function of the following parameters: the $V_{ECM_{lim}}$ voltage related to the action of vehicular electronic devices; the $V_1(I_{bat\_meas})$ related to battery current I_{bat_meas}, the $V_2(en\_sp)$ voltage related to rotational engine speed *en_sp*.

The $V_2(en\_sp)$ voltage corresponds to the minimum voltage value which limits the braking torque variation caused by the alternator electrical friction in order to guarantee the benefit due to gradual transitions for the engine from the nominal to the idle condition, in which the internal combustion engine has the rotational engine speed fixed to the minimum value, so as to improve the vehicle driveability.

The second control alternator algorithm, as showed in Figure 3.10, computes the target voltage V_{obj} defining the lower limit as showed in (3.12)

$$V_{obj} = \min\left(V_{MAX_P}, V_{ECM_{lim}}, V_1\left(I_{bat\_meas}\right), V_2\left(en\_sp\right)\right) \qquad \textbf{(3.12)}$$

where:

- o V_{MAX_P} is the maximum value of the supply voltage range $\Delta Vlimit(V_{MIN_P}, V_{MAX_P})$ that takes into account the electrical vehicle load status and it is determined by the body computer;
- o $V_{ECM_{lim}}$ is the minimum alternator voltage which is enough to supply the active equipment on the vehicle;
- o $V_1(I_{bat})$ is the minimum voltage that allows the batteries to not run down;
- o $V_2(en\_sp)$ is a minimum value of voltage that allows the limitation of the engine braking torque. It is used in order to improve the vehicle driveability.

The second alternator control algorithm defines the target voltage V_{obj} when the vehicle is in deceleration mode, which is the highest possible value according with the limits coming from the active electrical loads and from the battery state of charge. The battery voltage increasing can lead to an engine friction increase, causing from one side an engine torque reduction during the deceleration phase and, on the other side, the battery life time improvement.

After the target voltage computation V_{obj}, the second alternator control algorithm calculates the alternator regulation voltage V_{reg} through the control system (closed loop and open loop) showed in Figure 3.10.
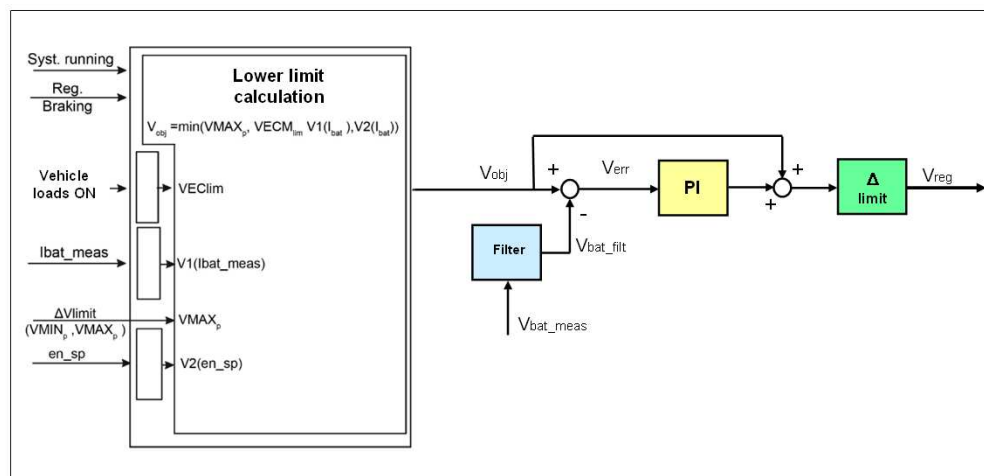
Figure 3.10 Second Alternator Control Algorithm scheme

According to Figures 3.9 and 3.10, the filtering block could be a Moving Average low pass filter, configured in order to receive as an input the battery voltage V_{bat_meas}, and remove from it the high frequency contents introduced by IBS sensor, providing in output the filtered battery voltage V_{bat_filt}. This technique assures the smoothing of the signal oscillations, in a window of 2N+1 size:

$$V_{bat\_filt} = \frac{1}{2N+1}\left(\begin{array}{l}V_{bat\_meas}(i+N)+V_{bat\_meas}(i+N-1)+...\\ ...+V_{bat\_meas}(i-N)\end{array}\right) \quad \textbf{(3.13)}$$

The PI controller is realized as described in (3.9). The open-loop rate assures a more gradual regulation of voltage V_{reg}, together with no over- and under shooting and null errors in steady state. From the other hand, the closed-loop rate assures the recovery of any loss or loads on the electrical system consisting of the electric battery and the alternator.

Afterwards, a gradient limiter has been introduced in order to guarantee a slow variation of the target voltage for the alternator command. The slew rate can be a tuning parameter.

In the third alternator control procedure, used in steady state outside the conditions described above, the engine control module regulates the voltage V_{reg} in order to ensure an optimal State Of Charge. This algorithm includes the step of determining the regulation voltage V_{reg} as a function of the ΔSOC error defined as:

$$\Delta SOC = SOC\_obj - SOC\_meas \quad \textbf{(3.14)}$$

where
   o   SOC_obj is the battery state of charge target
   o   SOC_meas is the state of charge measured by IBS sensor.
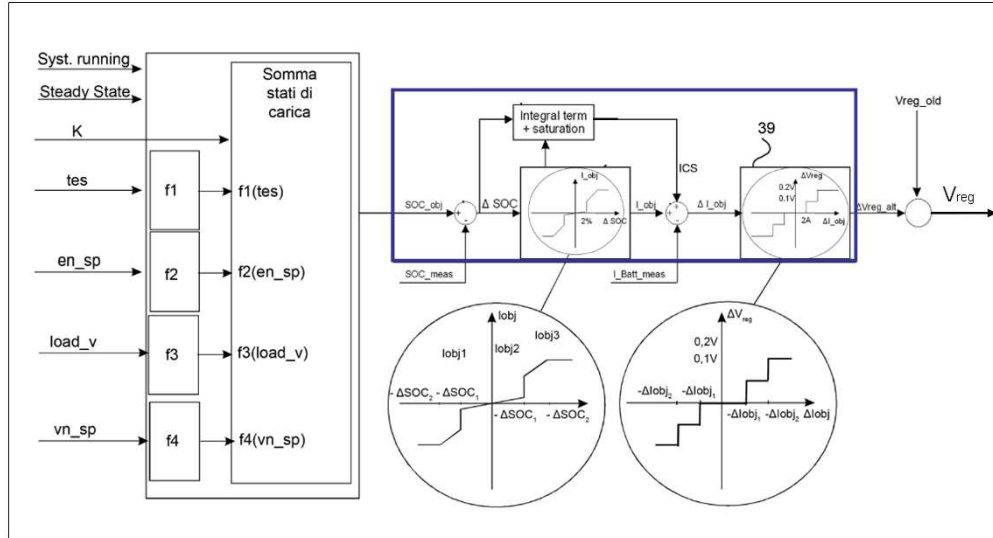
Figure 3.11 Third Alternator Control Algorithm scheme

With reference to Figure 3.11, the engine control unit is configured so as to determine the target battery state of charge SOC_obj according to a set of data: the engine speed *en_sp*, the vehicle speed *vn_sp*, the internal combustion engine torque *load_v* and the ambient temperature *tes* outside the electric battery. For this purpose, the electronic control unit can determine the target battery state of charge SOC_obj through the following function:

$$SOC\_obj = K + f_1(vn\_sp) + f_2(en\_sp) + f_3(load\_v) + f_4(tes) \quad \textbf{(3.15)}$$

where:

- o K is a constant predetermined, which represents the desired SOC value to guarantee an optimal battery efficiency;
- o $f_1(vn\_sp)$ is a function that defines a value indicative of a loading state to variation of vehicle speed, e.g. at high vehicle speed the target SOC could be reduced to storage better the energy in the next regenerative braking;
- o $f_2(en\_sp)$ is a function that defines a value indicative of the alternator charging efficiency depending on the engine speed;
- o $f_3(load\_v)$ is a function that defines a value indicative of the alternator charging efficiency depending on the engine combustion efficiency;
- o $f_4(tes)$ is a function that defines an indicative value of battery SOC when the external temperature of the battery changes.

The purpose of the third control algorithm is that to allow the battery to reach an optimal SOC, along with the minimization of the current crossing the battery.

Once the target battery SOC has been defined, the control algorithm consists in two control loops: the outer loop is based on the battery SOC feedback, used in order to reach the target SOC around a relative small error band. The inner loop is instead based on the battery current feedback so as to limit the battery current draining. The overall control scheme is described in the following picture:
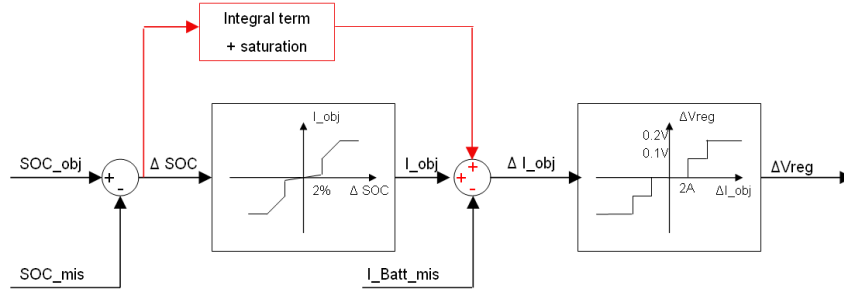
Figure 3.12 Third Alternator Control Algorithm Simulink scheme

According to Figure 3.11, the current target I_obj is determined as a linear function of SOC error ΔSOC, with a 2% dead band with respect to the nominal SOC, limited to a maximum current value equal to a 75% of the maximum alternator capacity. The compensator block is configured so as to receive as input the charge error ΔSOC and the current target I_{obj}, and provides as an output the compensation factor ICS referred to the current target.

The compensator block is active when the following condition is satisfied:
1. the absolute value of current target $|I_{obj}|$ is lower than a predetermined threshold max_drift correlated with possible current losses into the measurement chain;
2. the absolute value of charge error $|\Delta SOC|$ is greater than a given minimum error.

Then, the compensator block is configured so as to guarantee that the current losses on the measurement chain are compensated by the command ICS, avoiding the steady error in the charge error ΔSOC.

The additional block provides the current target error ΔI_{obj} computed as follows:

$$\Delta I_{obj} = I_{obj} + ICS - I_{bat\_meas} \tag{3.16}$$

The computation block, receives the current target error ΔI_{obj} and generates a voltage variation ΔV_{reg} through the function:

$$\Delta V_{reg} = fg\left(\Delta I_{obj}\right) \qquad\qquad \textbf{(3.17)}$$

In the example shown in Figure 3.11, the function fg(ΔI_{obj}) is stepwise and defined as:
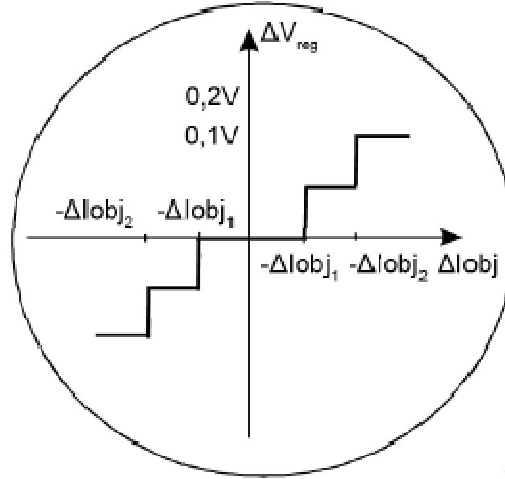
Figure 3.13 Voltage Variation function

In this example, |VR1| is equal to 0.1V, |VR2| equal to 0.2V, | ΔI_{obj1}|=2A, |ΔI_{obj2}|=4A.

In the fourth alternator control algorithm, that is used when the SOC is too low (Quick Charge Status), the engine control unit requires a relatively high regulation voltage V_{reg} to the alternator, e.g. as high as 105% of the nominal battery voltage.

During the cranking phases, depending on the engine speed *en_sp*, the engine control unit defines two cranking sub-phases. The regulation voltage V_{reg} is low in the first sub-phase, in order to favourite the engine speed increment. Then is set to a high value (in the second sub-phase) in order to reduce the engine speed overshoot during post-cranking phase. By means of an opportune calibration process it is possible to achieve different alternator behaviours, such as "hard attacks" (step turn on) or "soft attacks" (ramp turn on).

The engine control unit could be also configured to execute the third algorithm for a predetermined time interval (typically each two months), named "Battery Regeneration" cycle, in such a way the alternator is forced to provide a target voltage sufficient to recharge the battery up to 95% of its maximal charge, reducing the so-called "memory effect" and assuring a longer life to the electric battery. The battery regeneration cycle is configured to recharge completely the battery for a calibratable time (usually about 10 hours).

3.5 EXPERIMENTAL RESULTS AND CONCLUSIONS

The main goal of the smart alternator control algorithms is to reduce the emissions level when such a smart unit equips a standard car. To characterize and objectivise this feature, statistic measurements have been undertaken, with and without this new strategy enabled. Two different types of test cycles have been considered.

Client-oriented cycle

This driving cycle follows a pre-defined test profile or uses the standard NEDC (New European Driving Cycle) profile. It starts by using a battery state of charge equal to the target SOC value. This test represents approximately a typical driving behaviour in urban and extra-urban road and it is useful to test the effects of different calibrations and/or the presence of new components on driveability and fuel consumption.

In order to validate the CO_2 emissions, the following criteria have been assured:

- the electrical vehicle loads (such as high beams, fog lights, infotainment systems, etc.) must be the same on each cycle;
- the SOC value at the end of the test must be sufficiently close to the initial SOC value (maximum error: 1%). In the case of too high SOC reduction, in fact, a further consumption/emission reduction could be measured because part of the energy needed for performing the cycle should already be drained by the battery.

Homologation cycle

This test starts with a completely charged battery (SOC $\geq$ 98%). CO_2 emission measurements was done during a standard NEDC cycle for homologation purposes. During the test, the SOC decreases of some percentage points, assuring the correct control strategy operation.

At the end of the test, it has to be checked that the alternator command average duty-cycle has been sufficiently low (less than 10%), except during gas pedal cut-off and braking phases.

In Figure 3.14 and Figure 3.15, two examples of use of the SAM strategy have been reported, both referring to client-oriented cycles performed on a NEDC cycle. The used prototype car was a Lancia New Ypsilon vehicle equipped with 0.9l TwinAir 85hp turbocharged gasoline engine.

A brief description of the plotted variables is reported below:
- The red line represents the engine speed
- The yellow line represents the battery SOC
- The red line represents the vehicle speed
- The white line represents the SAM state machine status
- The highlighted yellow line represents the target alternator voltage
- The blue line represents the measured battery voltage

- The purple lines represents the min/max battery voltage limits
- The orange line represents the measured battery current
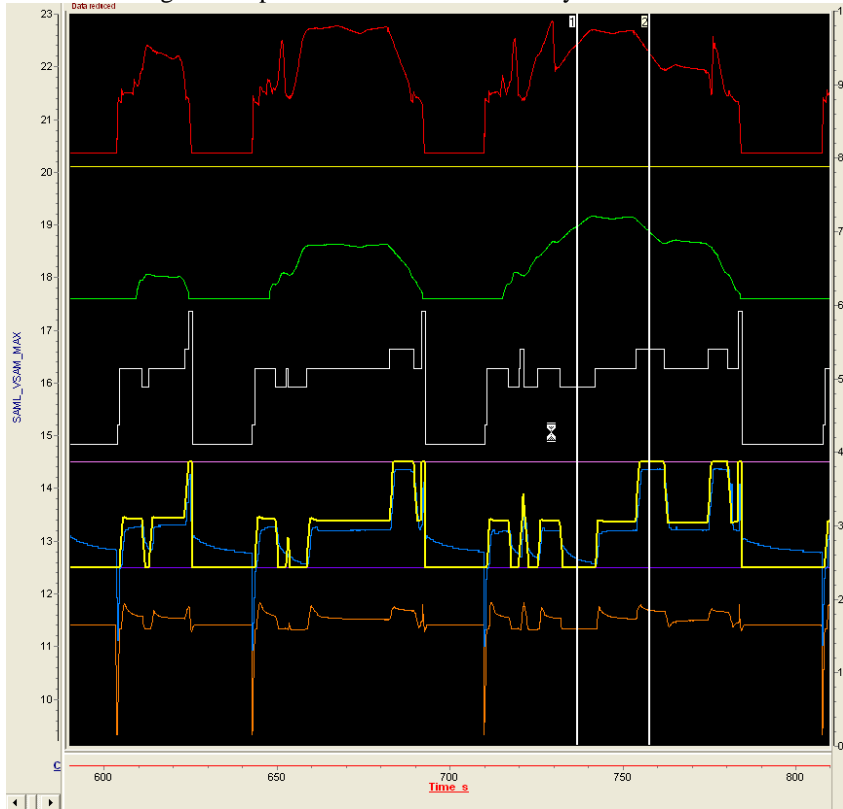
Figure 3.14 Urban cycle example on TwinAir gasoline engine
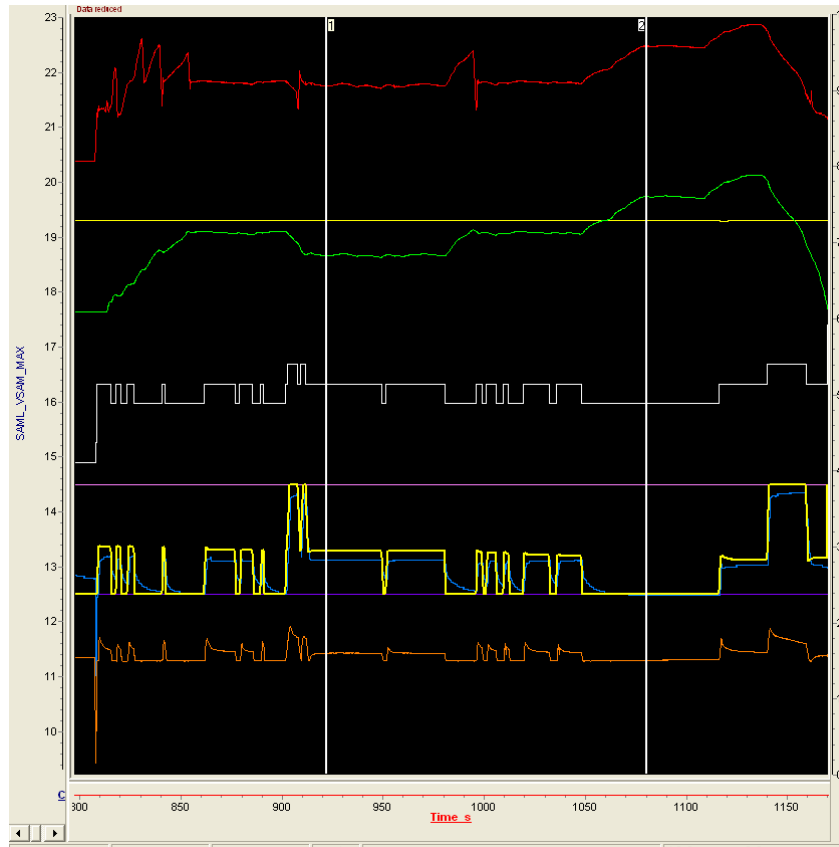
Figure 3.15 Extra-urban cycle example on TwinAir gasoline engine

The performed tests have shown a correct operation of the SAM strategy operation and the achievement of the target performance, expressed in terms of:

- target alternator voltage smoothness, which guarantees an optimal FEAD performance together with "fun to drive" feeling;
- target tracking of the battery voltage;
- battery life time improvement;
- engine friction torque reduction, which guarantees a further improvement on the engine driving performance;
- fuel consumption reduction, assured by a 2% reduction in CO_2 emission.

Chapter 4 Control functions for performance improvement – Drive Off Algorithm

One of the most critical operations in powertrains is the drive off manouver, consisting of connecting the engine shaft to the driveline through the clutch. For this reason, a dedicated control algorithm exists in the engine control unit to deal with this manouver which should be executed with the highest efficiency possible, i.e. without requiring high fuel consumption.

In this chapter a novel algorithm that improves the drive off performance without increasing fuel consumption is presented.

4.1 INTRODUCTION

The *drive off* is defined as the maneuver in which the engine and the driveline are mechanically coupled, through the operation of the clutch, in order to transmit the torque to the wheels.

When an internal combustion engine (ICE) is used, the intrinsic inability to generate torque at low speeds could create bad drivability feelings to the driver, due to engine stalls, engagement of shock phenomena or engine speed falls.

Moreover, in the last years the carmakers have moved toward the use of downsized engines to improve the fuel economy, reduce the emission and the production costs. Despite the use of over-boost technology, if an engine is downsized the power that it can produce at low engine speeds is still reduced worsening the *drive off* manoeuvre, that is one of the most important for the customer satisfaction.

In manual transmission automobiles, the *drive off* is much more critical due to the inability of the engine control unit (ECU) to control the actuation of the clutch.

Other aspects that negatively affects the *drive off* maneuver are:
- unavoidable dispersion between the pedal position and the actual position of the clutch plates
- backlash of the accelerator pedal
- increase of vehicle weight and of the road load; i.e. uphill road
- clutch wear

The aim of this algorithm is to address customers' complaints in situations of uncomfortable *drive off* manoeuvres. The number of these complaints is rising on manual transmission vehicles equipped with downsized engines.

This innovative control algorithm, termed DOMA (Drive off Management Algorithm, DoMA), will be shown to be able to cope with all the difficulties presented above. The main goal of DoMA is to reduce the occurrences of engine

stalls and avoid the engagement shock phenomena during the *drive off* manoeuvres.

To achieve its goals, DoMA recognizes the start of a drive off maneuver, it raises the engine speed in order to increase the available engine torque before the coupling phase, increases the authority of idle speed controller to manage the growing total inertia during coupling phase and, at the end, it smoothly reduces its action to avoid the engagement of shocks.

DoMA has been firstly tested in simulation environment (MATLAB/Simulink) on a simplified powertrain model. Then, it has then been tested on a vehicle using a Rapid Control Prototyping environment (RCP). In both cases DoMA has shown a good performance, confirmed by objective measurements and drivers evaluations.

4.2 DRIVE OFF IMPROVEMENT REASONS

The *drive off* manoeuvre is generally critical due to the engine intrinsic inability to generate torque at low operating speeds. This aspect is more amplified if combined with low-size vehicles, clutch disk and gas pedal aging: it means that the drivability is not comfortable in urban cycles and unfriendly engine stall events occur very frequently.

Especially in manual transmission vehicles, the goodness of the drive off is strictly linked the way the driver releases the clutch pedal. In any cases, the coupling clutch is a disturbance effect for the engine, difficult to manage.

The actually implemented control strategies are not able to correctly manage the vehicle drive off in all kind of driving scenario and this is the cause of the rising number of customers' complaints.

In the following Figure 4.1, an example of the drive off maneuver performed on a FIAT Lancia Musa normal production is shown.
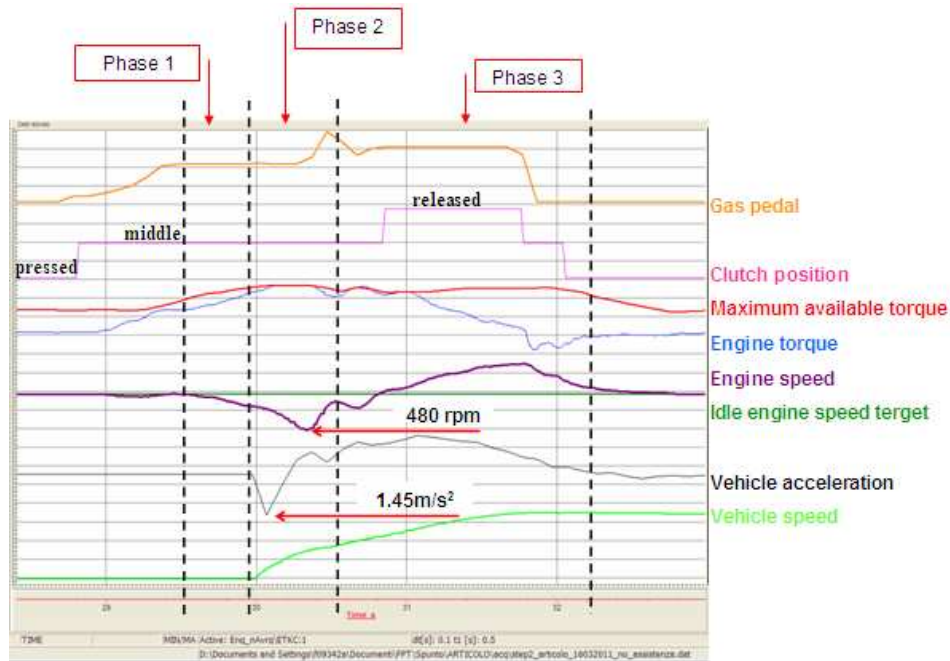
Figure 4.1 Example of drive off manoeuvre.

Analyzing Fig. 4.1 it is possible to identify three different phases:

1. The clutch plates are creeping, the amount of the engine torque transmitted to the clutch is lower then the static friction and is dissipated as heat. During this phase, the vehicle is stationary and the clutch plates are worn. The static friction affects the engine behavior. So the engine speed decreases.

2. The engine torque is greater than the static friction. So the passive torque imposed on the engine decreases. As a result the vehicle starts to move and the engine speed increases. The clutch plates are not completely coupled during phase 2. The engine speed trend depends on the clutch slip rate and on the way the pedal clutch is moved.

3. The clutch is completely coupled, the clutch plates speeds are equal. As soon as the clutch plates are coupled completely, all the vehicle inertia is instantaneously applied to the engine, causing the second engine fall. This phenomenon is called the *engagement shock*.

At the end of the phase 3 the drive off maneuver can be considered finished, the engine shaft and the transmission shaft are completely coupled and the engine has reached the target speed corresponding to the vehicle speed, depending on the driveline transmission ratio.

Looking at the engine torque depicted in Figure 4.1 it is also possible to notice that the control logic attempts to prevent the engine speed falls during

phase 1 and phase 3, using all the available torque. At these engine speeds, the maximum torque available is not enough to avoid the engine speed falls. Moreover, the greater the engine speed fall, the lower the torque available and so an engine stall can occur.

4.3 VEHICLE EQUIPPEMENT

The aim of this section is to describe the vehicle sensors and the related information needed for implementing the DoMA control strategy.

The vehicle configuration described below could be called "*full optional configuration*" : DoMA can reach the maximum performance with it.

DoMA is also able to work with a different vehicle configuration: "*low cost configuration*", with reduced performance.

In Figure 4.2 the position of the sensors is depicted
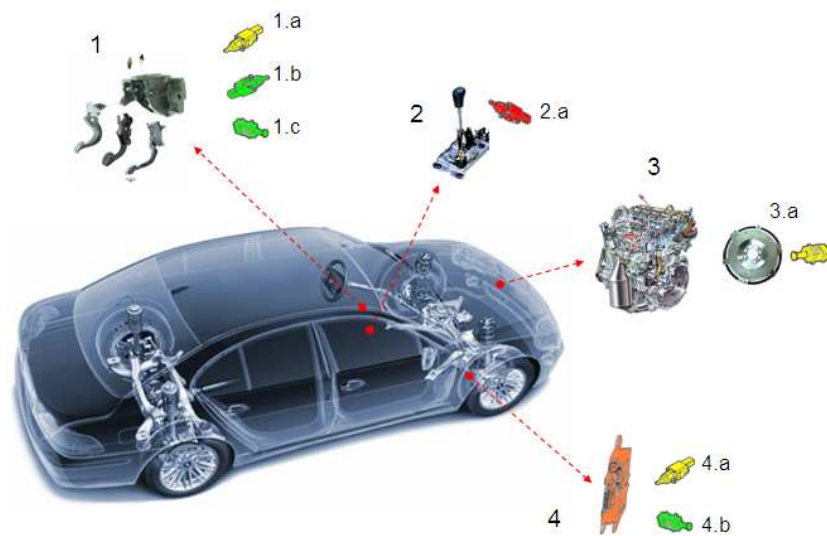
Figure 4.2 Vehicle interface configuration.

1. *pedals*
    a. double clutch switch sensor. The engine control module (ECM) receives the internal signals *ClutchSwitch* and *ExtendedClutch* and generates the internal variable CLUTCH_POSITION following the table below

ClutchSwitch (Top Travel)	ExtendedClutch	CLUTCH_POSITION

50

Not Active	Not Active	HIGH
Active	Not Active	MIDDLE
Active	Active	LOW

The following Figure 4.3 represents the configuration of double switches in the case of pedal clutch completely pressed.
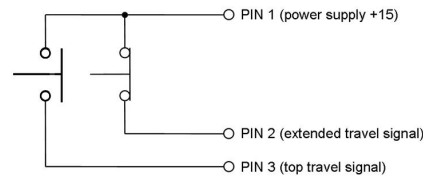
Figure 4.3 Completely pressed pedal clutch configuration

Only one switch is present in the case of "*low cost configuration*" .
   b.   brake sensor
   c.   accelerator pedal potentiometer sensor
2.   *gear shift*
   a.   neutral sensor. It gives the information of the neutral gear. It is not present in a "*low cost configuration*".
3.   *engine*
   a.   engine speed sensor
4.   *brake control module*
   a.   vehicle speed sensor
   b.   accelerometer. It gives the information about the longitudinal and transversal vehicle acceleration. It is not present in a "*low cost configuration*".

DoMA does not require any particular sensors or actuators. All the devices shown in Figure 4.2 are available on most of the FIAT standard vehicles.

4.4 THE DRIVE OFF MANAGEMENT ALGORITHM

The Drive off management algorithm is presented in details. In the first paragraph the general principles of DoMA are outlined. In the second part, a more deep analysis of the architectural details of DoMA is undertaken in order to show how it combines with the existing engine control unit software.

4.4.1 DOMA GENERAL PRINCIPLES

In the drive off manoeuvre the clutch plates of the transmission line are coupled in order to transmit the engine torque to the transmission shaft and, as a consequence, to the wheels.

When the clutch plates are not coupled, the driveline is open, and no engine torque is transmitted to the transmission. It means that no external load would affect the engine when the clutch plates are open.

The drive off maneuver can be expressed by the following torque balance:

$$
\begin{cases}
T_{engine}=(RPM_{idle})=T_{\substack{internal \\ losses}}(RPM_{idle})+T_{\substack{engine \\ inertial}}(I_{engine},\dot{\omega}_{engine})+T_{vehicle}(\zeta) \\
\dfrac{dRPM}{d\vartheta}>0 \\
\dfrac{dS_{svehicle}}{d\vartheta}>0
\end{cases}
$$

(4.1)

where,

- T_{engine} (RPM_{idle}) is the engine torque at idle;

- $T_{internal\_losses}$ (RPM_{idle}) are the engine thermodynamic and mechanical losses;

- $T_{engine\_inertial}$ (I_{engine}, $\dot{\omega}_{engine}$) is the torque related to the engine inertial mass I_{engine} and to the engine acceleration $\dot{\omega}_{engine}$;

- $S_{svehicle}$ is the vehicle speed;

- RPM is the engine speed;

- θ is crankshaft angle;

- $T_{vehicle}(\zeta)$ is the torque absorbed by the clutch. It depends on the clutch slip rate ζ;

➤ $\zeta = 0 \rightarrow$ the clutch plates are not coupled; no torque is absorbed by the clutch $T_{vehicle}(\zeta=0)=0$

➤ $0 < \zeta < 1 \rightarrow$ the clutch plates are slipping; part of the engine torque is transmitted to the clutch. Its value depends only on ζ

➤ $\zeta = 1 \rightarrow$ the clutch plates are completely closed:

$$T^{vehicle}_{inertia}(\varsigma = 1) = I_{vehicle} \cdot \frac{d\,S_{svehicle}}{d\vartheta} + T_{slope} \tag{4.2}$$

where T_{slope} is the torque that depends on the road gradient.

In manual transmission vehicles, the amount of clutch slip rate ζ depends on the position of the clutch pedal moved by the driver and so it is not controllable electronically. If the drive off maneuver is completely performed, the slip rate value goes progressively from 0 to 1.

Manipulating equations (4.1) and (4.2) and neglecting the road gradient, it is found that:

$$\underbrace{T_{engine}(RPM_{idle}) - T^{int\,ernal}_{losses}(RPM_{idle})}_{T^{engine}_{effective}} = I_{engine} \cdot \dot{\omega}_{engine} + I_{vehicle}(\zeta) \cdot \dot{\omega}_{vehicle} \tag{4.3}$$

Where
• $T_{engine\_effective}$ is the mechanical engine torque without friction;
• $\dot{\omega}_{vehicle}$ is the vehicle acceleration reduced as rotational speed on the transmission shaft;
• $I_{vehicle}(\zeta)$ is the part of the vehicle inertia imposed on the engine during the drive off maneuver depending on the slip rate.

At the end of the drive off maneuver when the clutch plates are completely coupled:

• $\zeta=1$

• $\omega_{engine} = \omega_{vehicle} \rightarrow \dot{\omega}_{engine} = \dot{\omega}_{vehicle} = \dot{\omega}$

• $I_{vehicle}(\zeta=1)=I_{vehicle} \rightarrow$ all the vehicle inertia is imposed to the engine

For this reason equation (4.3) becomes:

$$T_{effective}^{engine} = \dot{\omega} \cdot (\underbrace{I_{engine} + I_{vehicle}}_{I_{equivalent}})$$

(4.4)

where $I_{equivalent}$ is the inertia of the system engine and vehicle.

From equation (4.3) and (4.4) it is clear that during the drive off maneuver the inertia imposed on the engine grows from the only engine inertia to the sum of the engine and the vehicle inertia depending on the clutch slip rate value.

4.4.2 RECOGNITION OF DRIVE OFF MANEUVRE

The first task that DoMA has to perform is to recognize the desire of the driver to drive off the vehicle. DoMA will process different signals coming from vehicle sensors, see paragraph 4.3.

A drive off manoeuvre is recognized if:
1. the vehicle runs below a tuneable speed threshold, AND
2. the neutral sensor logic response is "*gear shift not in neutral*". It means that a gear is selected, AND
3. the extended clutch pedal switch is closed, see Figure 4.3. It means that the clutch pedal is moving from bottom to top, AND
4. the brake pedal is not pressed

When all of the above *enable conditions* are verified by a tuneable time the driver desire in driving off the vehicle is recognized by DoMA.

Once DoMA recognizes a drive off manoeuvre, all the *drive off support strategies* are armed, as described in the next paragraph.

DoMA will disarm the *drive off support strategies* if:
- the vehicle runs over the creeping speed in first gear (drive off completed)
- the clutch pedal is pressed again (change of mind)

4.4.3 DRIVE OFF SUPPORT STRATEGIES

When the driver desire in driving off the vehicle is recognized, DoMA will take different actions:
- calculating a particular engine speed target shape
- increasing the engine reserve torque by properly changing the spark advance angle (only in the case of gasoline engines)
- increasing the engine speed controller gain depending on the growing equivalent system inertia

Engine Speed Target Calculation

As outlined in paragraph 4.4.1, during the drive off manoeuvre, the engine torque has to grow in order to cope with the growing total inertia to maintain the engine speed above the stall limit.

At low operating speed the amount of torque the engine is able to produce is not always sufficient to correctly support the vehicle drive off manoeuvre. The only way to increase the ability of the engine to produce torque is that of increasing the engine speed. It means to move the engine operating point towards the right side of the engine torque shape, see Figure 4.4.
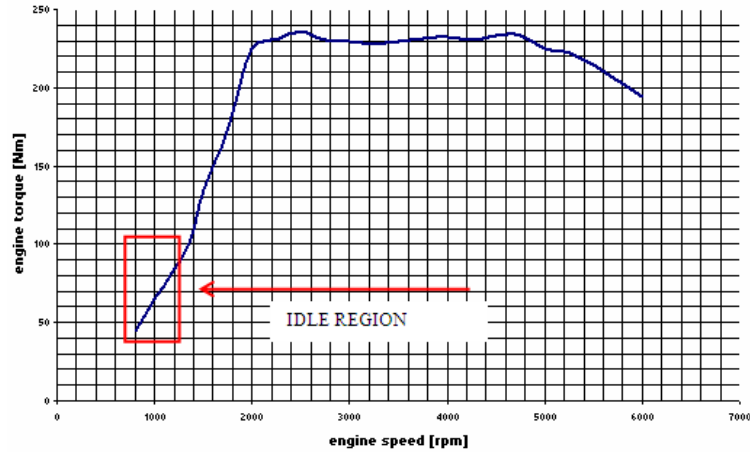
Figure 4.4 Example of engine maximum performance curve

An ideal engine speed target is calculated by DoMA. It comes from a balance of momentum between the engine and the vehicle.

The results is an ideal engine speed target that would always avoid engine stall even in the case of instantaneous clutch coupling.

In the following steps, the calculus of momentum balance is described:

$$vehic\_eq\_speed = \frac{des\_vehic\_speed \cdot tau}{wheel\_rad} \cdot conv\_fact \qquad \textbf{(4.5)}$$

$$vehic\_eq\_inertia = \frac{vehic\_mass \cdot wheel\_rad^2}{tau^2} \qquad \textbf{(4.6)}$$

$$momentum\_obj = vehic\_eq\_speed \cdot (vehic\_eq\_inertia + eng\_inertia) \quad \textbf{(4.7)}$$

$$vehic\_momentum = \frac{vehic\_speed \cdot tau}{wheel\_rad^2} \cdot vehic\_eq\_inertia \cdot conv\_fact\_1 \quad \textbf{(4.8)}$$

$$rpm\_obj = \frac{momentum\_obj - vehic\_momentum}{eng\_inertia} \quad \textbf{(4.9)}$$

where,

- *des_vehic_speed* = desired vehicle speed at the end of the drive off maneuver (dependent on gas pedal pressed percentages) [km/h]
- *vehic_speed* = measured vehicle speed [km/h]
- *vehic_eq_inertia* = equivalent vehicle inertia at the transmission shaft [kg*m^2]
- *vehic_eq_speed* = desired angular vehicle speed at the end of the drive off [rpm]
- *vehic_mass* = vehicle mass [kg]
- *vehic_momentum* = instantaneous vehicle momentum [kg*m/s]
- *wheel_rad* = wheel radius [m]
- *tau* = transmission ratio
- *eng_inertia* = engine inertia [kg*m^2]
- *momentum_obj* = target engine momentum needed to achieve the desired vehicle speed at the end of the drive off [kg*m/s]
- *conv_fact* = conversion factor rad/s → rpm
- *conv_fact_1* = conversion factor km/h→m/s
- *rpm_obj* = drive off target engine speed [rpm]

On the other hand, a significant increase in engine speed could give bad feeling to the driver in terms of safety and noise vibrations harshness (NVH) of the vehicle. The engine speed target during the drive off manoeuvre has to be a trade-off between performance, safety, noisy and vibration.

For this reason, DoMA is able to split the total engine speed increments and hide them following drive actions, supporting the driver in the same way as assistance is provided by an automatic gearbox. In particular, when a drive off manoeuvre is recognized, the engine speed target is calculated in 4 stages:

1. drive off manoeuvre recognized → first idle engine speed target increases;
2. accelerator pedal slightly pressed → second idle engine speed target increases: it is useful to reduce the electrical dead zone of the gas pedal sensor, because, due to the electric characteristic of the accelerator pedal, this action can cause a steep step as input to the ECU and consequently a bad feeling to the driver;

3. when the vehicle longitudinal acceleration is greater then a threshold → third idle engine speed target increases
4. at the end of the drive off manoeuvre the engine speed target becomes the ideal engine speed coming from balance of momentum.

The target engine speed elaborated by DoMA is active only during drive off. Also saturation of the engine speed value is used for safety reasons.

Spark Advance Regulation

Only for the gasoline engines, the total amount of engine torque generally depends on the aspired air quantity (slow dynamic) and on the spark advance (fast dynamic). It means that an increment of the engine torque can be achieved by introducing more air in the cylinders or moving the spark advance toward its optimum value (MBT).

In order to better manage sudden demands of increased engine torques during drive off manoeuvres, as soon as the drive off is recognized, DoMA is instructed to reduce the ignition timing efficiency. So the potential ability of the engine to produce fast torques grows and a sudden torque request can be satisfied, moving again the spark advance toward the MBT point, see Figure 4.5
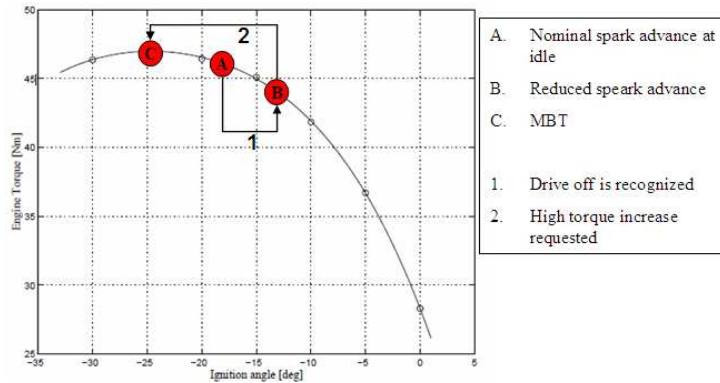
Figure 4.5 DoMA ignition timing management

Engine Speed Controller Authority Improving

During the drive off manoeuvre, the target engine speed calculated by DoMA is the input to the idle speed controller (ISC). ISC calculates the engine torque needed to maintain the engine speed equal to the drive off target. In current engine control strategies, the gains of the ISC controller are kept constant during the overall drive off manoeuvre, without taking into account the increment of the engine torque absorbed by the clutch. DoMA has improved this weakness by calculating the ISC proportional parameter as a function of the vehicle acceleration. The vehicle acceleration is a consequence of the engine torque transmitted through the clutch and so a good estimator of it.
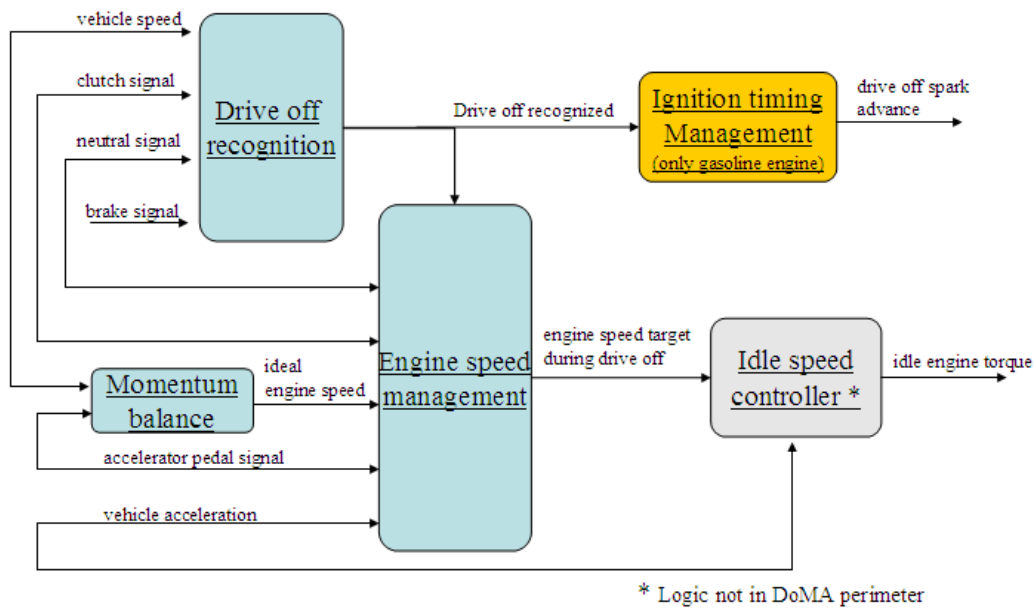
Figure 4.6 DoMA working scheme

4.5 EXPERIMEENTAL RESULTS

DoMA has been firstly tested in a simulation environment (MATLAB/Simulink) on a simplified powertrain model; it has then been tested on a vehicle using a Rapid Control Prototyping environment (RCP).

Rapid Control Prototype (RCP) development process is useful to reduce and assure control algorithm robustness, because RCP allows one to test novel control concepts and strategies directly on a real system (i.e. vehicle, engine) in advance to the SW release time.

The introduction of DoMA functionalities as support for the drive off manoeuvres, increases automatically the engine speed and the delivered torque. It has an impact on the drive off drivers' feelings in that they experienced an increased torque availability and a reduced engagement of shocks. In particular, slightly skilled drivers experience an effective support in the drive off manoeuvre while skilled drivers experience an increased driveability and fun to drive.

Different manoeuvres performed in a rapid control prototyping framework on a FIAT Lancia Musa normal production are shown below, in Figure 4.7.

Figure 4.7 shows four manoeuvres: on the left two drive off manoeuvres performed with DoMA; on the right two drive off manoeuvres performed

without DoMA. Both manoeuvres were performed without pressing the accelerator pedal.
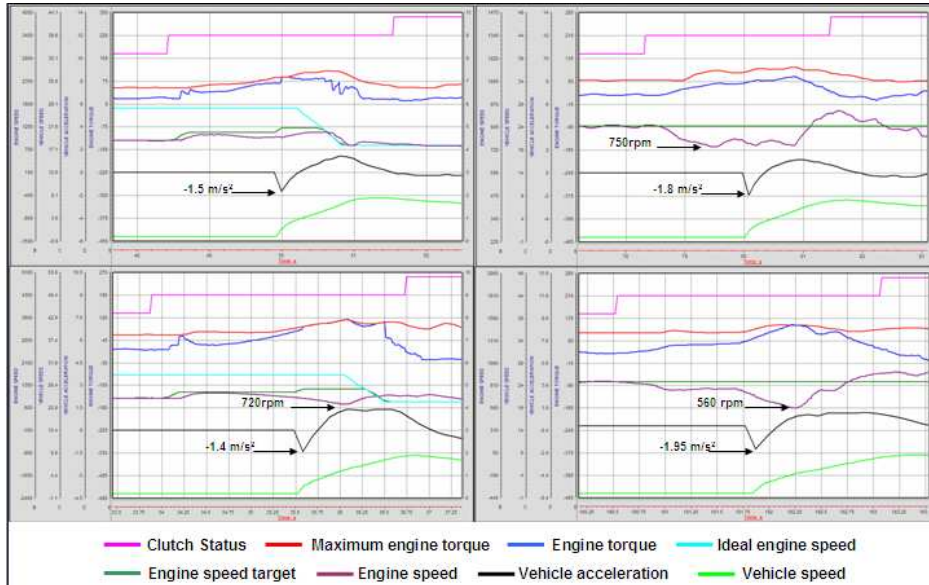
Figure 4.7 Comparison of manoeuvres with and without the DoMa algorithm.

In Figure 4.7 an assessment of the performance obtained can be valuated:
- o In the manoeuvres on the left, the engine torque (the blue signal) required during the take off increases until to the maximum possible engine torque (the red signal), on the right the torque is smoother;
- o The undershoots of the engine speed (the burgundy signal) in the manoeuvres with DoMa are lower than the undershoots in the same manoeuvres without it;
- o The longitudinal acceleration (the black signal) in the manoeuvres with DoMa is lower than the acceleration in the same manoeuvres without it. This means that a more driving comfort is assured under DoMa;

This showed performance improvement has been confirmed by a good SAE evaluation (grade 7 out of 10 for the take off performed with DoMa, in stead off grade 6 out of 10 without this).

4.6 CONCLUSIONS

A novel control algorithm that manages the drive off manoeuvre on manual transmission vehicles has been presented. The original concept has been tested

and validated using Software In the Loop and Rapid Control Prototyping environments. DoMA has shown good performance in all manoeuvres.

The drive off performed with DoMA have shown a reduction of maximum vehicle acceleration value, a smaller engine speed falls and a lower number of engine stall occurrences. This algorithm has been patented and will equip all new FIAT passenger vehicles starting fall 2011.

Chapter 5 Control function for performance improvement – Spark Advance Algorithm

In this chapter a new algorithm for the calculation of the spark advance in engines equipped with Variable Valve Actuation technology will be described.

A general purpose, model based, software development methodology has been used in order to assist control engineers in the development of the algorithm and in performing parameters calibration that best fit the experimental data. The use of this calibration methodology, fully described in next chapter 6, has been integrated here with the control algorithm development process, in order to accelerate, simplify and improve the whole calibration process.

High performance and fun-to-drive are then assured, due to an optimum spark advance strategy attuated according to a precomputed map giving the best spark advance angle for each engine working point.

5.1 SPARK ADVANCE ALGORITHM

The torque supplied by the engine is estimated by using mainly engine speed, air inlet efficiency, valve lift profiles and spark advance. In an engine without the VVA, the algorithm uses only two maps and one vector (see Figure 5.1):
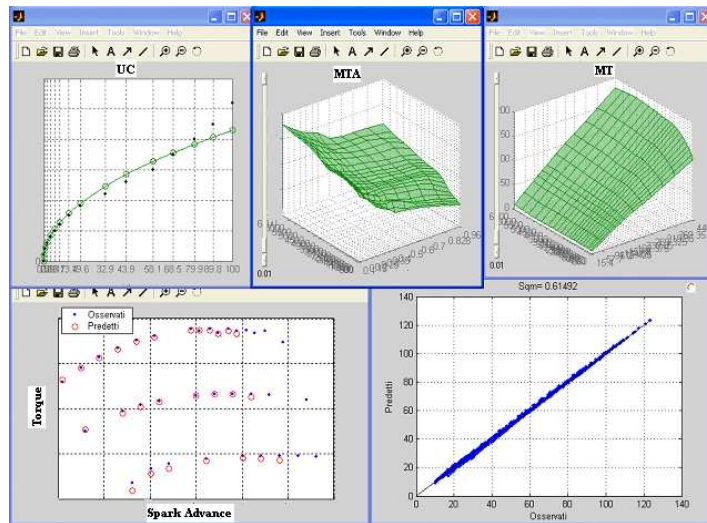
Figure 5.1 Spark Advance algorithm maps.

1.   MTA(speed, eta), called the maximum torque advance map: it describes, for each engine speed - air inlet efficiency point, the spark advance that maximizes the torque. If the detonation occurs before reaching the real maximum, an extrapolated value is used to best fit data. In Figure 5.2 the red triangles x-coordinate represent the maximum torque.

2.   MT(speed, eta), called the maximum torque map: it describes the indicated torque measured at the maximum torque advance. In Figure 5.2 it is the red triangles y-coordinate.

3.   UC(advance - MTA(speed, eta)), called the unique curve: it describes how the distance between the spark advance and the maximum torque spark advance reduces the torque. Its output is 1 if the input is 0. The output decreases while the input difference increases. It is very similar to a parabolic curve and it has the property to fit well the experimental data in the equation

$$TORQUE = MT(speed, eta) \cdot UC(advance - MTA(speed, eta))$$ **(5.1)**

where:
speed is the engine speed
eta is the air inlet efficiency
advance is the actuated spark advance
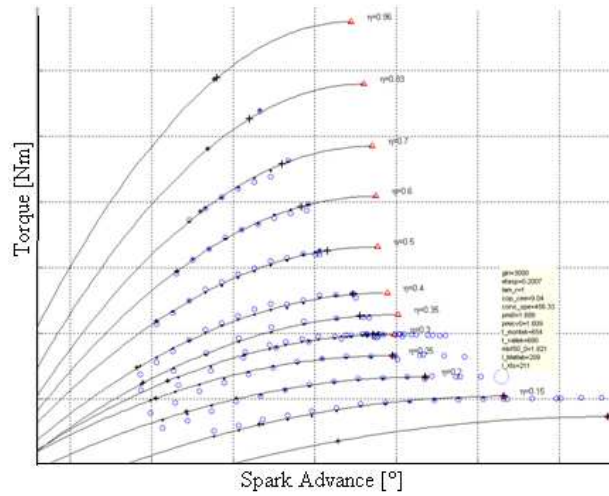
Figure 5.2 Torque interface.

In engines equipped with the VVA technology, this algorithm implies one map and four vectors in Full Lift mode. Generally, a spark advance map is a two-dimensional map dataset consisting of two variables such as engine speed and load.
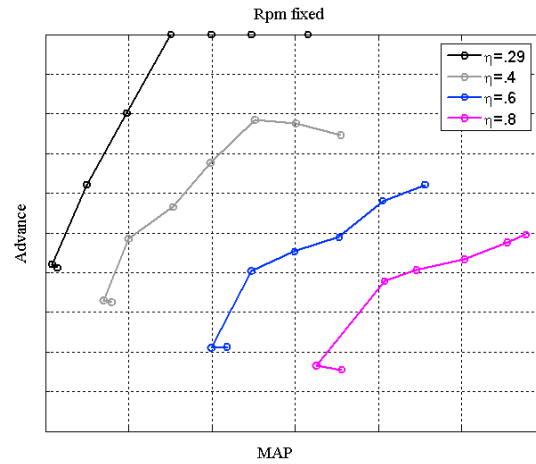
Figure 5.3 Advance vs Manifold Pressure at Rpm fixed for different air inlet load.

In EIVC or LIVO mode, at fixed speed and load, the spark advance depends also on the manifold pressure (Figure 5.3). A higher pressure implies a lower Early Closing angle, reducing the effective compression ratio and the end of compression temperature. This reduces the knock phenomenon, increasing the maximum allowed spark advance.

Figure 5.3 shows, in the EIVC mode, the spark advance trend versus the manifold pressure at fixed speeds, for some values of the air inlet efficiency (the values have been omitted for confidentiality reasons). Therefore, while in Full Lift mode, is yet valid that Advance = f(Speed, Load), in VVA mode it has to be considered the dependency from pressure:

$$Advance = f\left(Speed, Load, Manifold \operatorname{Pr} essure\right) \qquad \textbf{(5.2)}$$

The multi map optimization tool has allowed one to manage the phenomenon, and different proposed algorithms have been automatically calibrated and compared in a short time.

Fig.5.4 shows the algorithm with the best performance.
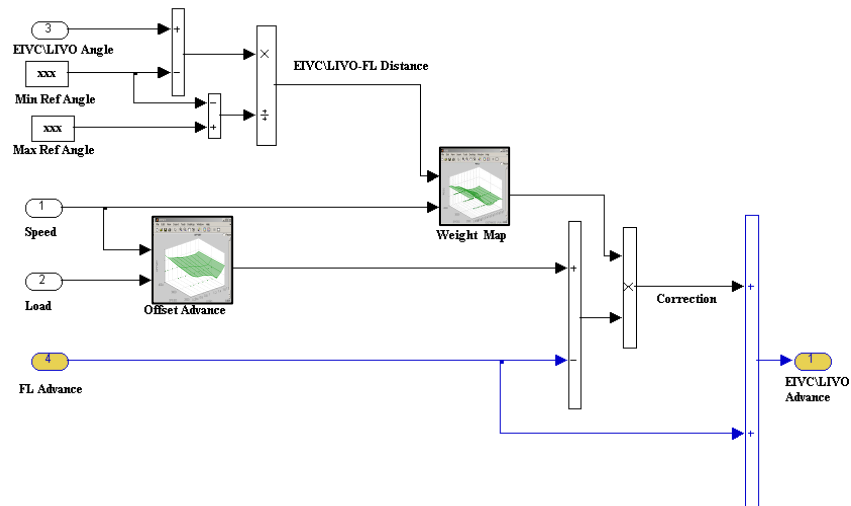
Figure 5.4 Spark advance algorithm.

In EIVC or LIVO mode, the spark advance is calculated as the sum of the spark advance in FL mode and the correction for VVA systems. This correction is the weighted average between the FL spark advance and the reference angle spark advance. The weight factor map is function of the speed and the *EIVC\LIVO-FL Distance*, calculated as follow:

$$EIVC \backslash LIVO - FLDistance = \frac{Current\ EIVC \backslash LIVO\ Angle - MinAngleRef}{MaxAngleRef - MinAngleRef} \quad (5.3)$$

MinAngleRef is the minimum realizable cam angle for each mode, while *MaxAngleRef* is the maximum early closure angle for EIVC and the maximum late opening angle for LIVO on the cam profile (Figure 5.5).
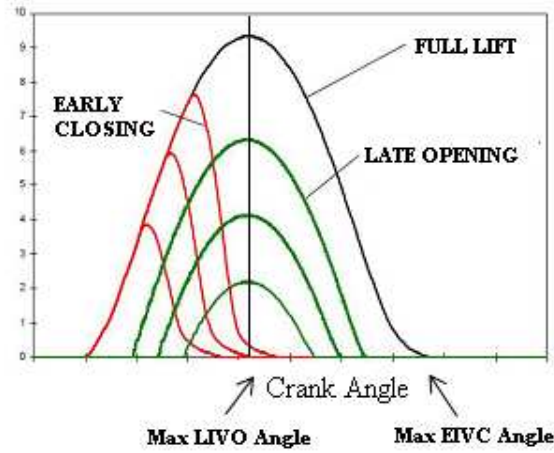
Figure 5.5 Max Angle Ref for EIVC and LIVO mode.

5.2 RESULTS AND CONCLUSIONS

Using the Multi Map Optimization Tool (Figure 5.6), the resulting optimized maps are smooth and the mean square error meets the precision target (see also the error distribution on Figure 5.8) and the predicted versus observed graph shows the validity of the chosen model. The experiments have been conducted on tests bench for a gasoline engine Fiat SI Turbo 1.4l 135 Hp with VVA.
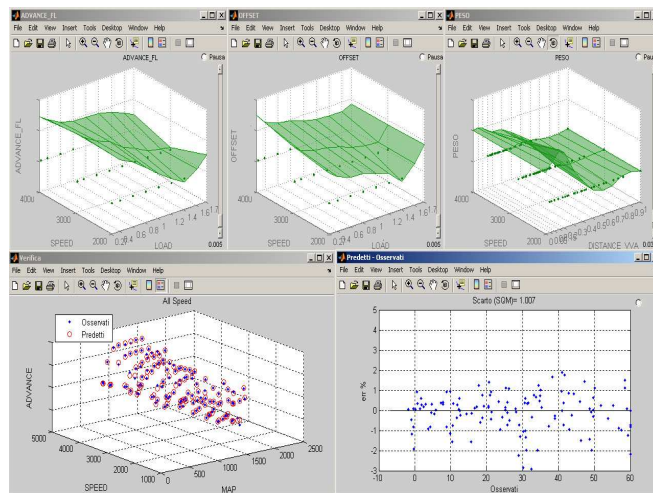
Figure 5.6 The spark advance algorithm tuning.
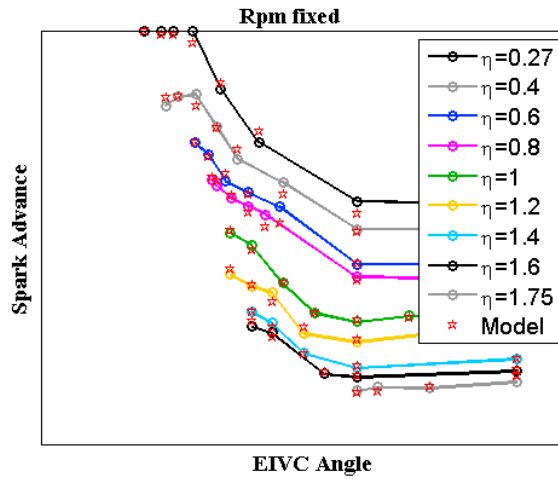
Figure 5.7 Graphic of predicted vs observed.

The Figure 5.7 shows the spark advance trend versus the early closing angle for different values of air inlet efficiency at fixed speed. The circle points are experimental, while the star points are the points predicted by the model.
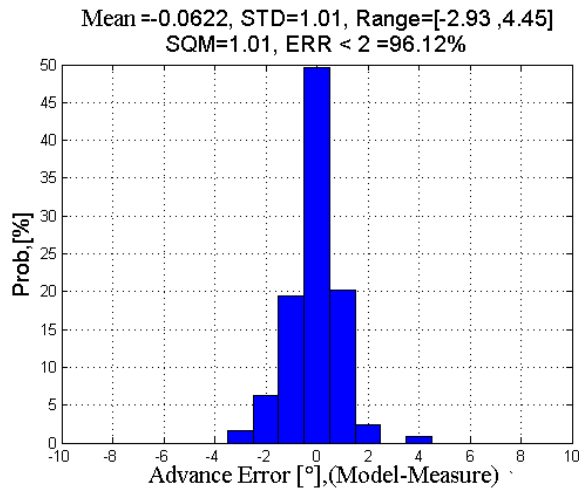
Figure 5.8 Spark Advance algorithm error distribution.

The described algorithm is now equipping FIAT Group automobiles. The good accuracy of the described algorithm has permitted to improve the dynamic response of the engine, taking full advantage of the VVA technology.

66

Chapter 6 Interactive Optimization Methodology and Calibration Tools

As showed before motor vehicles are equipped with a set of embedded control systems with an increasing number of software implemented features. The design of such systems is a challenging problem because of the complexity of the functions to be implemented and for the constraints which exist due to the tight interaction between mechanical and electrical components, also dictated by safety reasons.

Current software development is aided by simulation tools which allow block diagrams generation providing the customers with a graphical environment that supports the design and the simulation activities and can be run on PCs.

However, much more is required for the complete development of embedded control systems. The current lack of automated tools (see [17] and [18]), methods and models make the whole process tedious, time-consuming and potentially affected by errors and omissions because most steps are handmade, especially in the earlier stages.

The main goal of this chapter is to present some ideas for automating the whole embedded control system design process. As a result, many of the above ideas have been implemented in the F.I.R.E. tool which supports the embedded control systems modelling, design and simulation at a high abstraction level, allowing control engineers and software developers to focus on the control system aspects of the problem instead of the platform[1] ones.

Another relevant aspect when dealing with modern internal combustion engine control systems is the availability of new robust and multi-objective engine calibration methods and tools, which potentially allow substantial new flexibility and performance with respect to the traditional calibration practice. In this work, a novel general purpose model-based calibration methodology will also be described which merges statistical concepts, like the robust design theory of experiments, numerical optimization techniques and Engine Control Unit (ECU) algorithm modelling. This approach exploits software tools in order to support the calibration of estimation algorithms used in the ECU. The proposed tools are:

- non-linear multivariate regression;
- discrete regression;
- multi-map optimization;
- graphical user interface for calibration, validation and change;

---

[1] The specific hardware and the operating system on which the control system should be executed.

-    calibration performance meters.

An application of these tools to the "basic engine" calibration process of an actual real thermal engine is presented. With the term "basic-engine" calibration we mean the calibration activity dealing with the ECU algorithms involved in the engine operations which do not depend on a particular vehicle application like charge estimation, injector model, spark advance computation, torque estimation, catalyst protection and so on.

The use of this methodology has been integrated in the control algorithm design process thus speeding up, simplifying and improving the whole process. This tool suite for control algorithms design and calibration is one of the most important results of my research [16].

The application of this approach, compared with the best techniques used in industry, has produced really interesting results:

-    reduction of experimental test bench design effort (more than 50% of reduction);

-    more accurate estimation (almost doubled);

-    more robust behaviour, with respect to engine to engine variability and environmental conditions.

These tools have been developed by using MathWorks' MATLAB$^{®}$ /Simulink$^{®}$ software, which is a de-facto standard in the embedded system industry.

6.1 F.I.R.E. TOOL CONTEXT USE

The development of embedded control systems is usually a complex process, because of the system size and the shared resources amount ([19],[20] and [20]). The modelling of these systems has to include the knowledge of the top level structure, the distribution of the functionalities amongst the system resources, the links and the data transmission amongst the components and the system response to asynchronous or synchronous events [19].

Such different information cannot be expressed by a single graphical notation. As an example, a single graphical view can show some abstract functional aspects, and another one shows the control software organization or the physical structure. An actual design methodology is based on the idea that every control system can be observed by using three different views: the *functional*, the *implementation* and the *re-usability* views.

Functional View

Following a model-based approach for embedded system design, during the functional design phase, where the customer requirements are analyzed, the control engineer plans a logical-functional view (Figure 6.1) of the control system, in which the functions of the different parts of the project, e.g. signal acquisition, error value computation or command signal actuation, are highlighted ([19] and [20]). Such a view focuses on the data flow, that is the process of identifying, modelling and reporting how data flows around the system. In this graphical notation, each activity is data-driven, i.e. every block

undertakes its elaborations as soon as input data are available on its input ports, without waiting for any timing, priority or CPU availability.
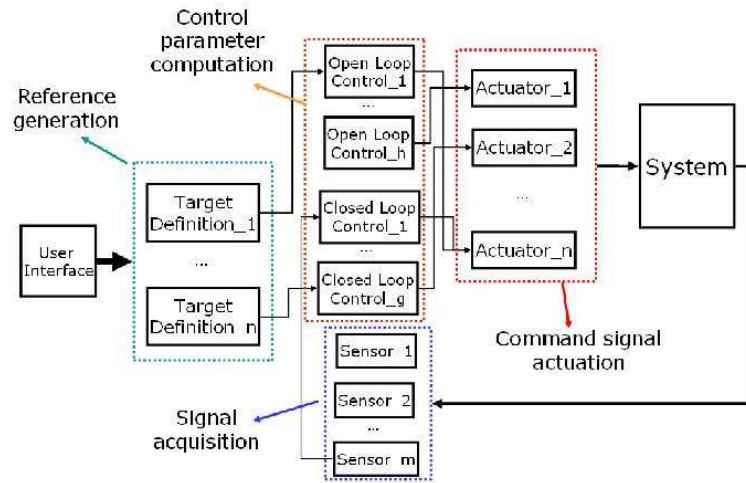
Figure 6.1 Functional view

Implementation View

The next step in system planning is the ANSI-C code implementation of the functional models onto the specific target to be installed into the vehicle Electronic Control Unit, which is usually accomplished by means of some automated production code generator ([24] and [25]).

A functional view is not suitable for dealing with the implementation aspects deriving by the use of a real-time operating system in the ECU, such as task timing and scheduling, or asynchronous events handling ([26] and [27]). Such aspects can be better analyzed in an *implementation* view (Figure 6.2) of the same model where the control flow[2] is also highlighted. In this view, the customer considers the effect of introducing prescribed timing requirements in the execution of each Simulink[®] block. This is accomplished by introducing an additional scheduler block which simulates the real behaviour of the control system when implemented on a RTOS (Real-Time Operating System) for embedded systems.

---

[2] The timing control of the activities that have being processed by the control unit.
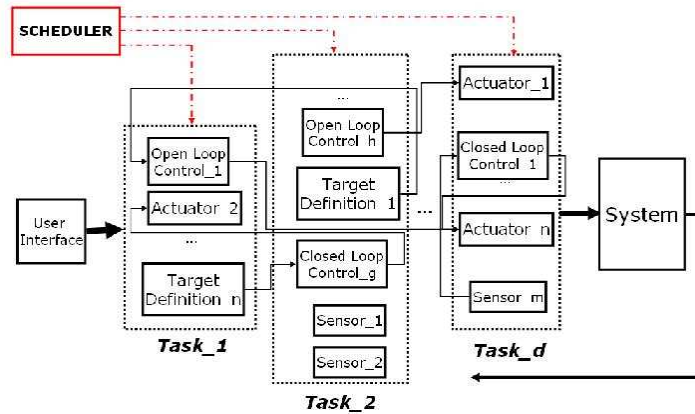
Figure 6.2 Implementation view

Re-usability View

After generating the code, it can be helpful, for taking care of possible future changes, to characterize the subsystems by their hardware dependence in a so-called *re-usability* view (Figure 6.3), in order to identify the HLSW (High-Level SoftWare) and the LLSW (Low-Level SoftWare) part of the generated code.

This view improves the re-usability of a control algorithm, because it provides a physical representation of the control system in which the process resources physical location is illustrated.
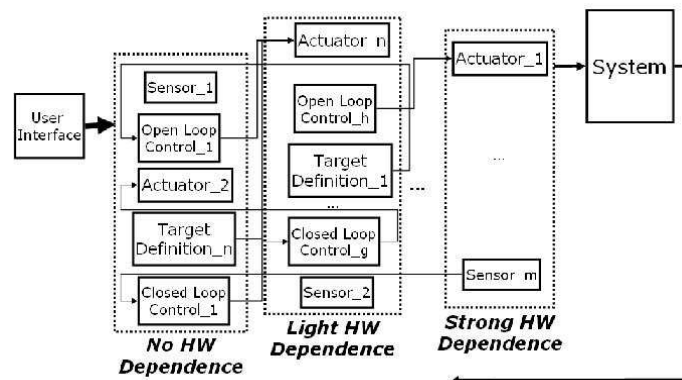
Figure 6.3 Re-usability view

6.2 F.I.R.E. TOOL OBJECTIVES AND MAIN FUNCTIONALITIES

The development of an embedded system involves the cooperation of different planning activities. In particular, the interaction between the design

and algorithm implementation phases requires a (breakable) information sharing between control and software engineering groups. On the other hand, the control and software engineers have different points of view, design approaches, terminology and development tools.

Up to now, the system designer is the person in charge of choosing the most suitable view to model a control system, and all transformations of the Simulink® models, realized in collaboration with the software engineer, are manually accomplished. Such an activity is slow and affected by possible unavoidable errors and omissions.

F.I.R.E[3] has been created to automate these transformations, ensuring data consistency in each view of the same system. F.I.R.E. is a software tool which allows the designer to develop, to analyze and to simulate embedded control systems at a high abstraction level. It helps to realize more correct and efficient implementations of the functional graphical models, it supports the early steps of the *V-cycle* design methodology [20], assures more flexibility and re-usability of the Simulink® models and improves the development cost and time. Morevoer, F.I.R.E. assures that the implementation view is realized according to the Auto-Code Generators (ACG) requirements [24].

The Simulink® library has been extended to support the design of the F.I.R.E. models thus providing a user-friendly graphical interface. From these models, the control engineer can carry out an early investigation of the timing problems potentially affecting the control system, such as delays in the data flow, jitters, potential data-loss in buffers, and priority task handling ([27] and [28]). A simulation with different sampling times on the same system is also possible. In this way the results of such an analysis can be used by the software engineers to produce more correct ECU codes.

It is important to notice that the transformation from a functional view to a re-usability one consists in a graphical blocks rearrangement, which is useful during the reverse engineering phase, when focusing on some particular hardware dependencies of the control system is of interest. Moreover, transit from a functional view to an implementation one offers a logical tasks reorganization based on their timing requirements. On the other hand, the implementation view makes it possible to analyze different multi-rate simulations by acting on the scheduler block.

6.3 F.I.R.E. BLOCKSET

In order to have a user friendly tool, a customized block library is supplied and integrated with the other Simulink® built-in libraries. The F.I.R.E. block set containing all the components required to create new F.I.R.E. models (Figure 6.4). The customer can also introduce new templates of asynchronous event generators and update a MAT-file containing the hardware dependencies of the subsystems inside the functional view.

---

[3] Functional Implementation Re-usability Environment.
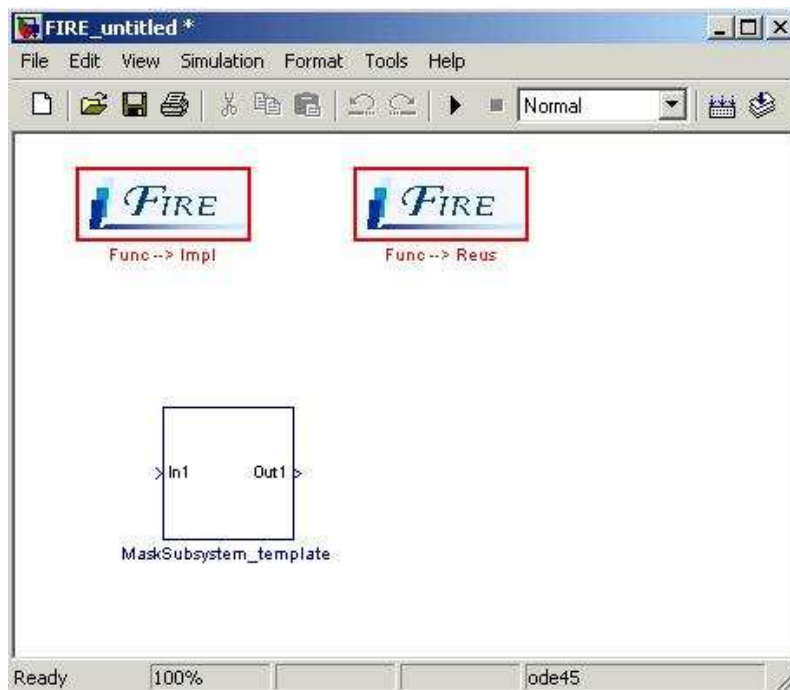
Figure 6.4 Building a new F.I.R.E. model

In order to carry out the transformations, the user must introduce some information into the model about the task timings or hardware dependencies. In order to introduce these properties in a standard and easy way, F.I.R.E. supplies a *MaskSubsystem_template* block (Figure 6.5), in which the customer can set the required information, like the sampling time or the declaration of an asynchronous events, and the hardware dependency.
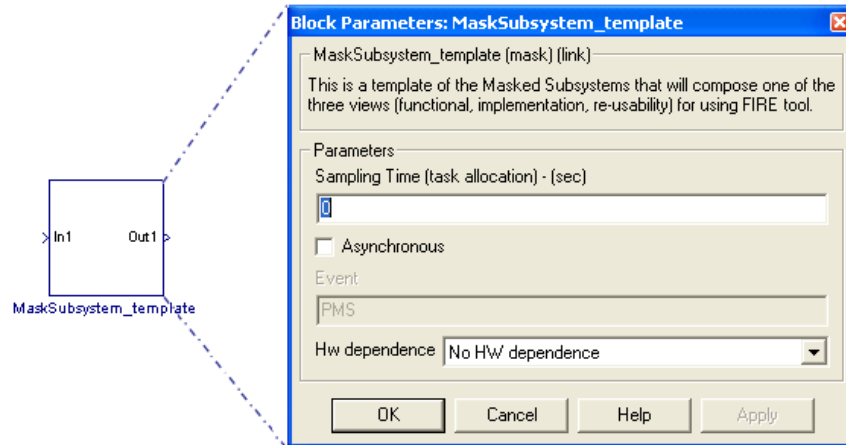
Figure 6.5 MaskSubsystem_template block**.**

Implementation Aspects

The operation provided by the F.I.R.E. tool is accomplished via a text low-level parsing procedure acting on the Simulink files related to the functional view. The parsing is undertaken by means of some MATLAB® scripts which analyze and re-write these files on the basis of the desired transformation chosen by the user.

Each F.I.R.E. transformation is composed by two different sections: a low-level one where the parameters characterizing the new view to build up are extracted from the functional view masked subsystems, and a high-level one, in which the new file is completed with the aid of MATLAB® *Simulink Model Construction* commands, using the information extracted during the low-level phase. The customer has to set task priorities, used by the scheduler block in the implementation view to solve task activation conflicts, by means of a Graphical User Interface.

6.4 EXAMPLES OF F.I.R.E. APPLICATIONS

This software has been tested and validated on two different real control system design problems; a simplified Drive-by-Wire (DBW) [29] and Variable Valve Timing (VVT) [1] units and a real engine management system [30]. Specifically, the F.I.R.E. tool has been used to analyze the timing problems of the control system and to find a correct tasks allocation.

The goal of the first case study is to get a controlled step response in terms of settling time and overshoot, both for first and second order models, which respectively represent their simplified behaviours. In the functional view, the control engineer designs the control algorithm by tuning the controller parameters, like a proportional or an integral gain, but he/she cannot estimate easily the impact of a scheduling choice on the overall control system

behaviour. With the help of the F.I.R.E. tool, the tasks allocation can be more easily analyzed. The control engineer decides the timing of the tasks in the functional view, quickly transforms this view in the implementation one and then analyzes the results of different tasks allocation and scheduling choices on the control system responses. Next Figure 6.6 highlights how different task allocations of the same control system can change the control performance. In particular, see how changing the VVT control task activation from a constant 100 ms sampling time (too slow) to an asynchronous TDC synchronized (Top Dead Center)[4] policy reduces both the settling time and the overshoot, and the same happens for the DBW control module.
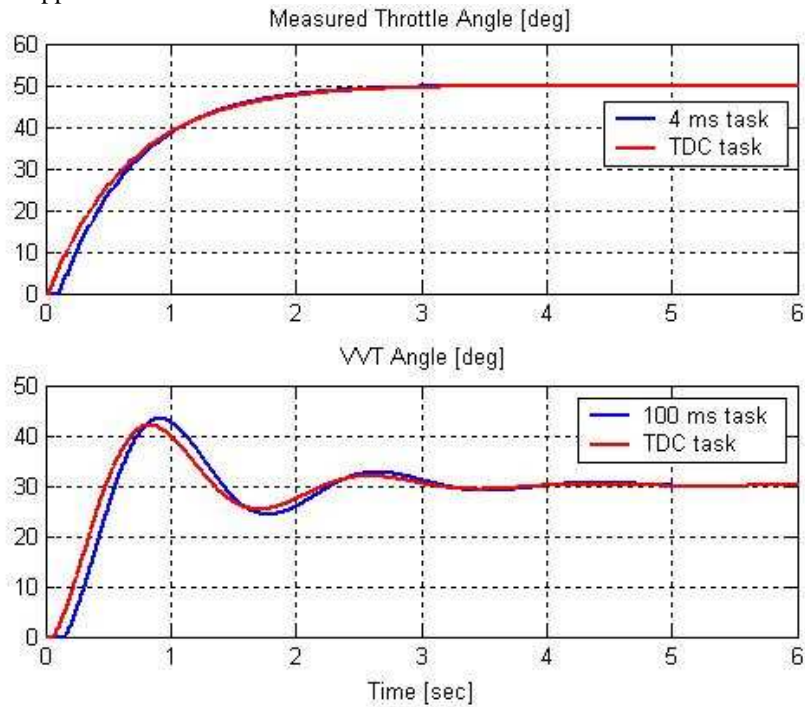
Figure 6.6 Different time slicing on a control system.

From this example is also easy to understand the advantage offered by this tool in autocode generation, because the implementation view provided by F.I.R.E. is ready to be transformed in a TargetLink block diagram.

In the second case study, the F.I.R.E. tool was used for studying the timing behaviour of the overall engine control system before an autocode generation.

In order to carry out such an analysis, four software simulation tests were undertaken in a loop virtual environment, which integrates an engine/vehicle Simulink® model with an Engine Management System model for performing

---

[4] At an engine speed of 2000 rpm TDC event occurs each 15 ms.

both MIL (Model In the Loop) and HIL (Hardware In the Loop) simulation studies. In particular, the following tests have been carried out:

- Air Conditioner Test
- Misfire Test
- Tip In/Tip Out Test
- Efficient Catalyst Test

The relevance of the F.I.R.E. tool in allowing multi-rate simulations to be easily performed before generating the code and performing HIL simulations, can be judged by comparing the simulation results achieved by the Air Conditioner Test, when the same EMS model is described either by the functional (Figure 6.7) or by the implementation (Figures 5.8 and 5.9) views.
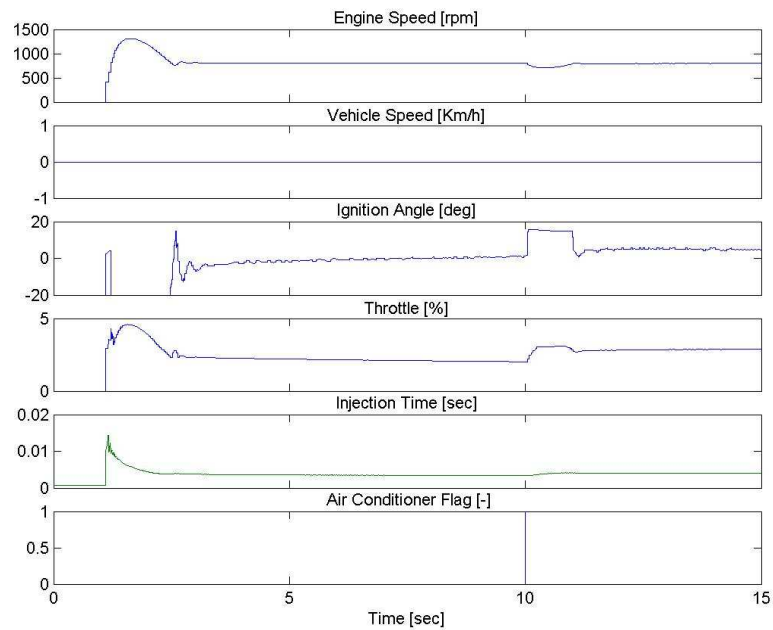
Figure 6.7 Air Conditioner Test with ECU's functional view

In fact, although the idle speed control in Figure 6.7 seems to perform well, the system is not stable and in fact there are oscillations in the engine speed (Figure 6.8) because the erroneous task allocation chosen results in a huge number of scheduling constraints and task execution significant delays.
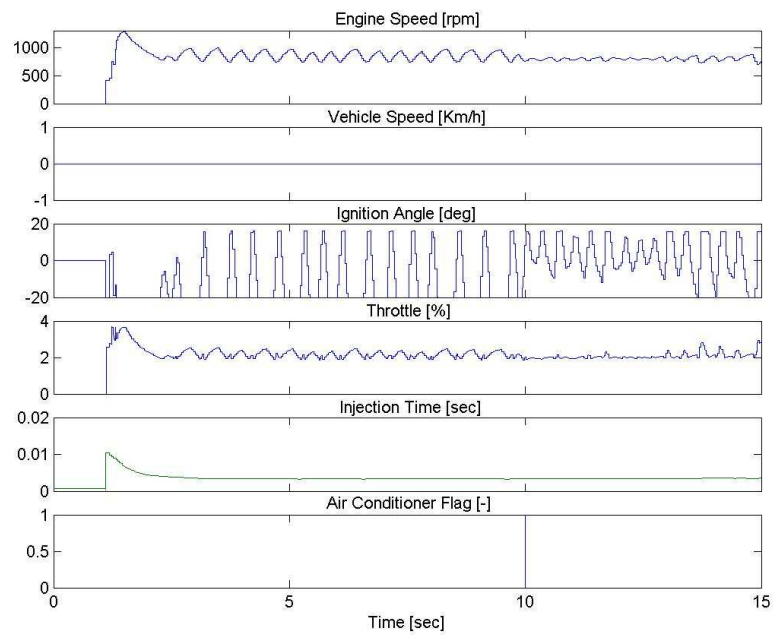
Figure 6.8 Air Conditioner Test with ECU's implementation view

However, repeating the simulation with a new allocation tasks (Figure 6.9), in which the idle speed control task allocation is changed from 100 ms to TDC[5], the control responses become indistinguishable from the prescribed nominal ones reported in Figure 6.7. The repeated simulations have been made possible, before the final production code generation, by executing another *Functional to Implementation* transformation by means of the F.I.R.E. tool. The simulation results obtained with the ECU's re-usability view do not differ significantly from the ones achieved with the ECU's functional one, because that view consists only in a graphical reorganization of the blocks, without any semantic change in the overall model.

---

[5] **At an engine speed of 800 rpm TDC event occurs each about 40 ms.**
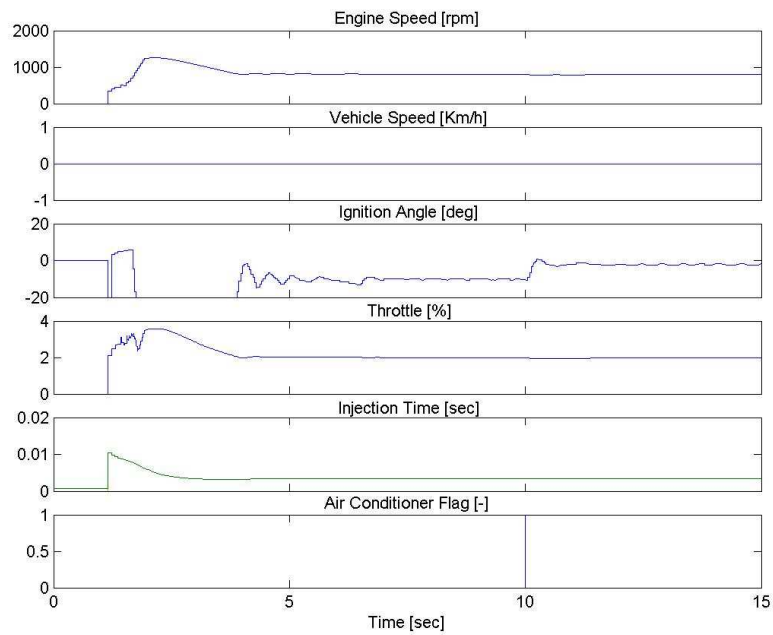
Figure 6.9 Air Conditioner Test with ECU's implementation view with a new task allocation

6.5 BASIC ENGINE CALIBRATION OBJECTIVES

Once the algorithm has been implemented and tested, it is possible to perform an accurate model calibration by using advanced calibration tools integrated in the F.I.R.E. environment. The parameters calibration of the basic-engine control algorithms consists of the identification of the parameter values which, codified in maps and vectors, best describe the engine behaviour in a defined working range.

- The calibration process of a single algorithm (process) can be divided in:
- Bench experimental test design and execution
- Data analysis and algorithm calibration
- Bench test verification

These phases are usually repeated until the target precision is reached. Data analysis consists in the transformation of the experimental results in maps and vectors which will be used to describe the behaviour of the engine in the ECU software.

The entire process can be speeded up by using statistical techniques which reduce the number of experiments to undertake and maximize the informative contents of each test. Using the proposed advanced calibration techniques, again implemented in the MATLAB® environment, it is possible to automatically

77

transform test information in calibration maps directly usable by the ECU. The higher precision achievable, especially when dealing with multidimensional actuation (throttle body, cam phaser for intake or exhaust camshaft, fuel injectors…), correspondingly reflects on better control performance (lower fuel consumption, larger maximum power and so on) and on a more robust characterization of the phenomena for the whole engine family, not only for the "tested engine". This is also important for reducing the influence of noise factors on the engine performance and the generation of diagnostic false alarms. Moreover, the availability of automatic calibration tools speeds up the development process of new engine control algorithms ([1]).

6.6 GENERAL PURPOSE CALIBRATION TOOLS

In a model-based software development process, the simulation models of the processes are often available. A complete collection of general purpose calibration tools has been developed in the MATLAB$^®$/Simulink$^®$ environment. These tools are described below.

Continuous multivariable non-linear regression models

In order to describe a relationship of the type z=f(x,y), it is possible to use a regression model which relates the experimental points having x, y and z coordinates. The model is imposed by the ECU algorithms and/or by the physics underlying the process.

In Figure 6.10, the coloured surface represents the volumetric efficiency of the engine, at a defined speed, which depends by the manifold pressure and cam phaser position. This surface minimizes the mean percentage square error from the experimental points represented by blue circles.

The regression model is quadratic in the cam phaser variable and linear in the manifold pressure until the breaking pressure, usually at a value of 950 mbar, is reached whereas it has a quadratic relationship over that pressure value.

This switching regressor describes the natural supercharge effect ([2]and [32]), which is particularly evident at 2700-3300 rpm in this real engine application. The traditional linear regressor produce an error up to 8% in the air charge estimation at full load, worsening other actuations like spark advance and mixture title.
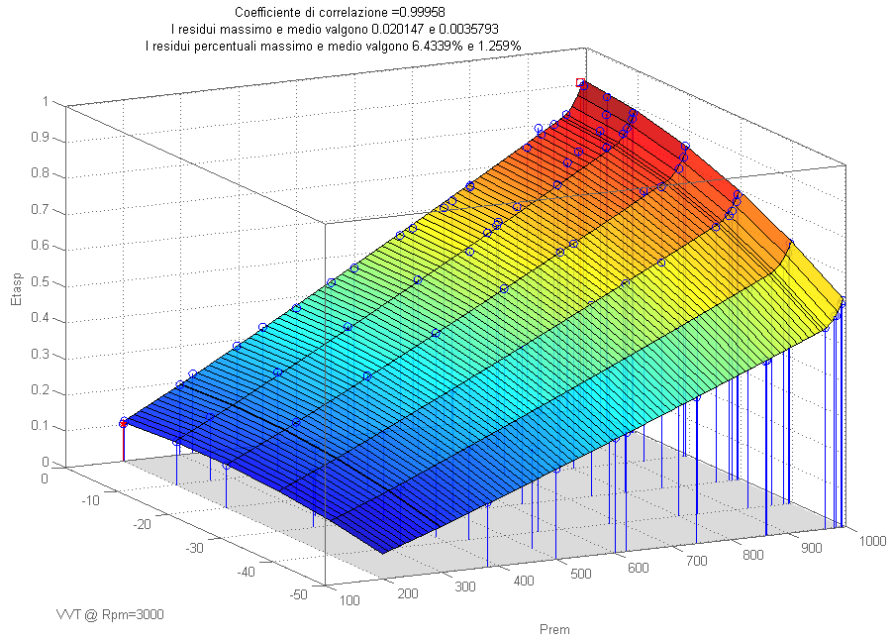
Figure 6.10 Multivariable switching regression model example

Discrete regression model

To describe the relationship of the type z=f(x,y), is possible to use a map which represents the z value for every point on a discrete x-y grid, defined by two breakpoint vectors. The output value of the map in the points that do not belong to this grid, is calculated using a bilinear interpolation method, like in the Engine Control Unit.

The *Discrete Regression* tool has been developed to meet this need. It computes the values of the map that minimize the mean square error between the experimental data and the surface, described as the bilinear interpolation of the map. In Figure 6.10, an example is reported. The experimental points are plotted as red dots, while the map is represented in transparent blue.

The mean quadratic error is: 0.0052127
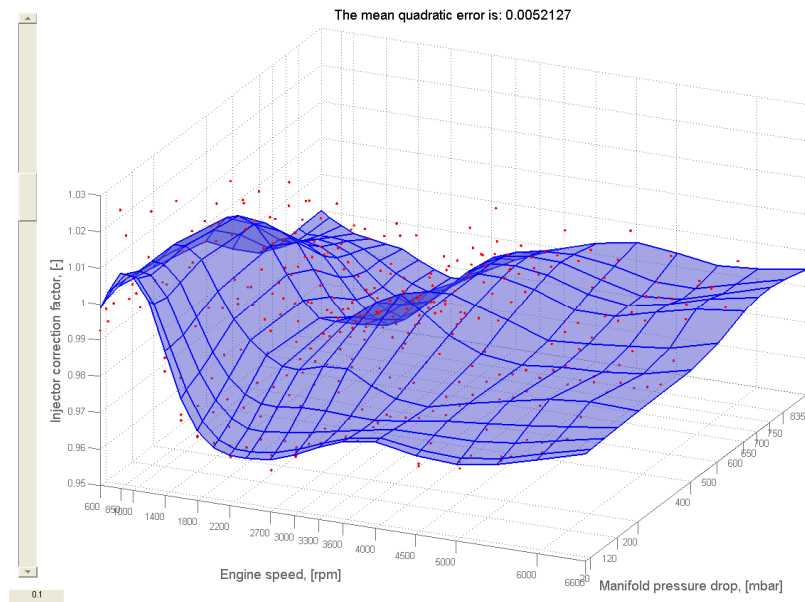
Figure 6.11 Discrete Regression tool example

On the left side of the Figure 6.11, there is a slider that increases the surface stiffness. It works like a spring which stretches the surface edges. A high stiffness generates a plain surface, increasing the mean square error. The map continuity is one of the requirements in the calibration phase. The discontinuities can be caused by a large measurement error in some points. A discontinuous map can generate different output values for very similar input values. This is dangerous in the use of the map, because an error in the input variable or its estimation can generate a big variation on its output, causing instability in the control loop. The stiffness can also be used to impose a rule for the extrapolation of the map in not experimented x and y coordinates.

The discrete regression allows one to be free in the acquisition dataset choice, because it is not any longer necessary, for example, to acquire data exactly in the breakpoint intersection points. It doesn't need to split the problem into sub problems as with the traditional calibration tools.

The advantages are essentially the same of the continuous regression model with the addition of the following ones:

- The model implemented in the ECU is often the output of a map. By acquiring data not only in breakpoint intersections, it is possible to obtain a map which minimizes also the model error, not only the measurement one. This aspect is fully explained below.
- The possibility to interactively stiff the map produces more physically realistic input/output relationships thus avoiding the over fitting problem.

Discrete regression algorithm

The aim of the discrete regression algorithm is to minimize the sum of the squares of the distances amongst the map and the experimental points. In order to achieve this goal, an analogy with a mechanical phenomenon can be done: every experimental point is fixed in the space while the map can slide along z-axis like shown in Figure 6.12. Every experimental point, which is red coloured in the figure, is linked by a spring, in blue, whose stiffness is the same for each point. A damper is also present. The damping value may be critical. The map segments, surfaces in a three dimensional space, have a mass and react to the spring and damper forces according to the second dynamic principle. The forces move the map toward the points. The equilibrium will be reached in the map along a configuration that minimizes the energy of the spring system. The expression of this energy is:

$$E = \sum_i^N K * \Delta z_i^2 \qquad (1)$$

Where: K is the stiffness of the spring

Δz_i is the z-axis distance between the ith experimental point and the map

N is the number of experimental points

Such a formula represents the sum of the square errors between the experimental points and the map.
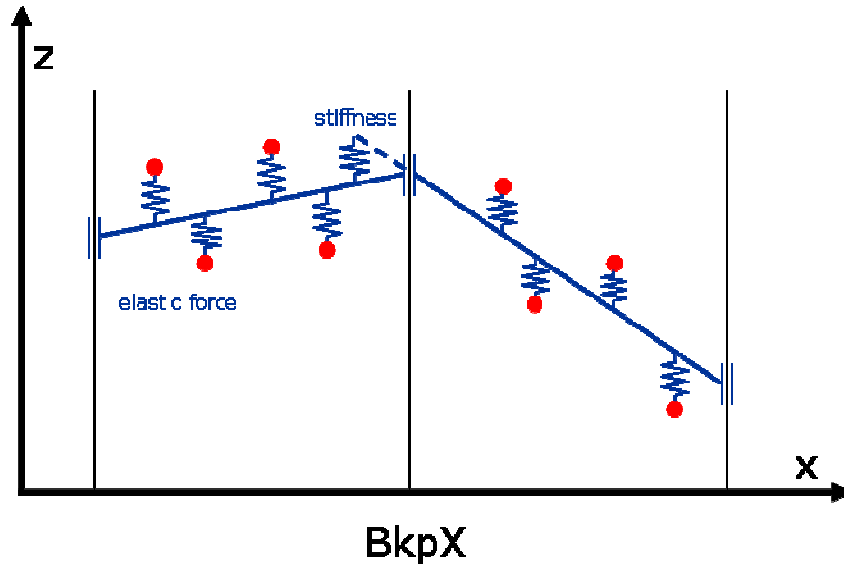
Figure 6.12 DiscreteRegression explanation

The mechanical system dynamic has been discretized and MATLAB® coded with a discrete difference equation. Some programming technicalities have been used to avoid possible instabilities and to enhance the simulation speed. As a result, over 200.000 points can be handled in a few minutes.. Moreover, the

outgoing maps are smoother, more coherent with the description of the physical phenomenon and can be interactively judged and modified by the calibration engineer.

Multi Map Optimization

A MATLAB® / Simulink® model of the algorithm has been implemented. This model, fed by experimental acquisitions, produces an output that depends on the calibration requirements. The multi-map optimization changes the calibration results in several aspects. It changes the values of the vectors and scalars, elements of the maps, until the minimum mean square error or mean percentage square error between measured output and estimated ones is reached.

The implemented optimization method is based on a steepest descent algorithm (see [38], [39] and [40]). The algorithm is a local optimization procedure, but some tricks are used to reduce the probability of getting stuck in a local minimum. The multi-map optimization is extremely fast and can optimize, on a 1.6 GHz Intel Centrino processor, for example, three 12x21 maps, in almost ten minutes.

During the elaboration, the optimized maps are shown, see Figure 6.14, together with predicted vs observed graphs and some statistics, e.g. the mean square error.
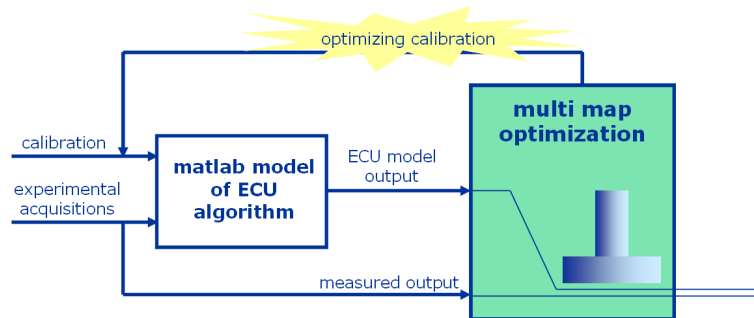
Figure 6.13 Multi map optimization working scheme

The accuracy of the result is up to 4 times better than the traditional techniques. The maps are also smoother because the optimization algorithm is instructed to pick, amongst many solutions with the same error, the smoothest.
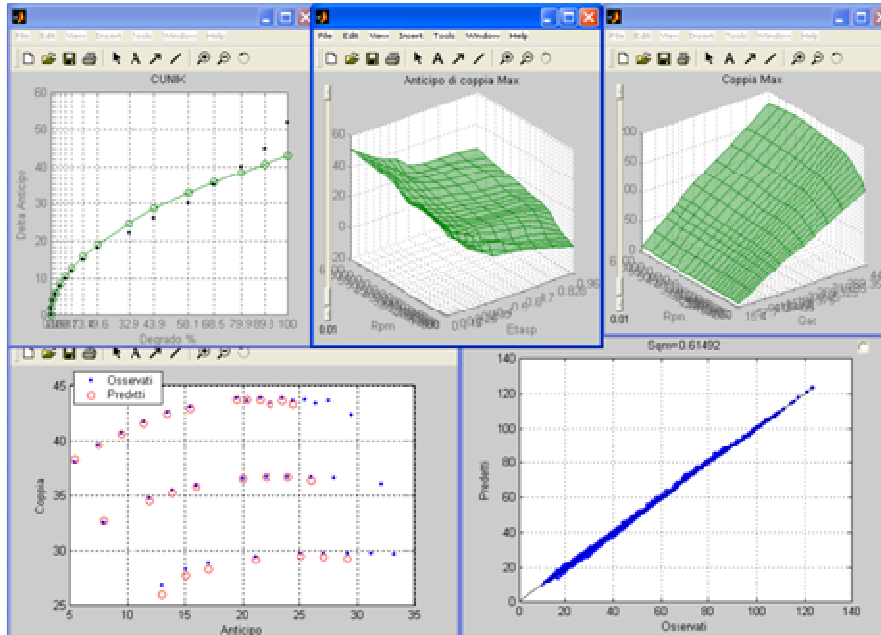
Figure 6.14 Multimap optimization example

In the past, once a first calibration result was achieved over a map, if the breakpoints changed for some reasons no automatic ways to reuse the old calibration were available and only a time-consuming manual retuning, usually undertaken by using Excel sheets, was possible. On the contrary, the proposed multi-map optimization approach frees one from this limitation.

Other advantages include:

- Many maps can be simultaneously optimized. The solution minimizes the total error, not the error of a single map so the results are usually better.
- The accuracy and the continuity of the maps are better than those resulting from traditional methods.
-

Tunable algorithms

The described optimization techniques can be used mainly to calibrate automotive estimation algorithms. These algorithms are, as a first step, validated through specific sensor measurement by means of test bench instrumentation, usually not present in commercial automotive engines.

The algorithms have to be memory-less, like e.g. the torque estimation algorithm. It is difficult to use the above mentioned optimization techniques for dynamic algorithms, like gas temperature estimation; for these dynamic algorithms, only the stationary part is calibrated using multi map optimization, while the dynamic part has to be calibrated in a different way.

It is furthermore impossible to calibrate algorithms which require the control of a non simulated variable, e.g. the mixture title for the calibration of wall wetting compensation strategy, where the wall wetting is the fuel quantity lying into manifold walls next to the injector that will contribute to combustion process in runtime. In this case, the verification tools presented below can anyway help the calibration process.

Performance measurement

The optimized maps are usually evaluated by computing the mean square error, denoted hereafter with σ, of the predicted values related to the experimental ones: the lower the error, the better the representation of the experimental points given by the maps. The σ statistic, multiplied by 3, is a good estimation of the experimental data variation range around the surface described by the map. To be more precise, the experimental data fall in the described range with a probability of 99.97% in the hypothesis of normal error distribution.

For similar applications, the percentage mean square error is more interesting. It is obtained by dividing the square error with the experimental one and by multiplying it by 100. In this way the statistic is more correlated with the final performance; e.g. in the air charge estimation, the percentage mean square error is correlated with the error on the mixture title actuation.

The error of an estimation algorithm can be divided in two parts: model error and measurement error. The model error is caused by the utilization of a model which is not enough complex to describe the examined phenomenon. It can be reduced by using a different model equation, increasing the number or changing the breakpoints of a map.

The measurement error is due to the limited precision of the data acquisition and elaboration instruments. An experimental data measured with a value which is far from the regression model, generally denoted as an outlier, has to be found, eliminated and, if possible, measured again, to enhance the model precision. As a result, the optimized maps are then more robust against measurement errors than the ones manually optimized, where the values are exactly the ones measured at each specific breakpoint. This statement, based on the Chebyshev inequality [38], justifies the improvement in the calibration quality achieved by using multivariable regression models, which are more robust against measurement errors than those based on a single variable. By forcing the continuity on the dependant variables in more dimensions, the resulting model depends on more experimental points, reducing the probability of interpreting a measurement error as a phenomenon.

6.7 CALIBRATION PERFORMANCE VERIFICATION TOOL

For each calibration problem, a specific tool has been developed which graphically and numerically shows the effects of a calibration variation on the engine control algorithm accuracy. This tool is useful to rapidly verify that the calibration agrees with the imposed criteria and to make a final fine tuning,

following the calibration engineer experience. The result of an automatic calibration process has to be verified by an expert for two reasons:

The calibration tool, if there are missing data, extrapolates the behaviour of nearest points. An expert calibrator can do this task better, using his/her knowledge of the phenomenon.

The calibration tool optimizes with respect to a variable that is usually the most important, but in some operating conditions, it may not be the only variable of interest. The calibration engineer can correct the optimization process in such cases; with a user-friendly graphical interface this task is speeded up and the use of bench tests diminished.

In Figure 6.15, it is shown the main screen of the spark advance and torque estimation tool, used for the calibration of a real engine. The main graph shows the so called "umbrella" curves, which show the mean torque depending on the spark advance at a predefined engine speeds and cam phaser positions.

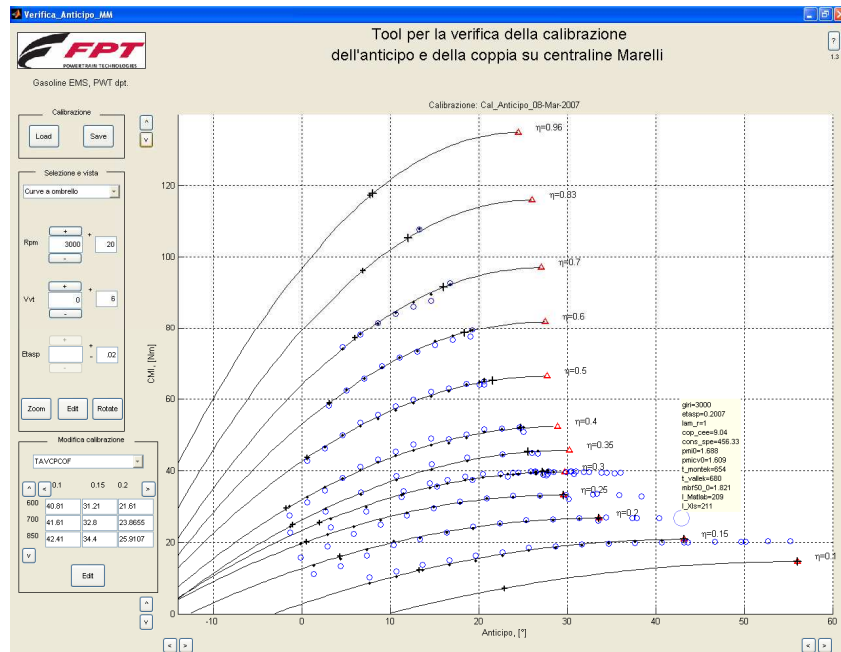Figure 6.15 Torque interface verification tool

Standard files

To make easy the information exchange, some standard file formats and contents have been defined.

Engine bench data

The engine bench data file is generated at the bench test. It is an Excel sheet that contains, in the first row, the names of the acquired variables while in the second row there are the measurement units, and, from the third row, the

acquired data values. Every row represents an operating stationary point, characterized by the measure of input-output values after a stabilizing time. The measure lasts for a predetermined amount of time. All the acquisition process can be automated.

Usually the data are acquired in a first phase for calibration purposes and in a second phase for calibration verification.

Calibration

The calibration file has to contain information about the ECU parameters related to the calibrating algorithm.

6.8 DEVELOPED TOOLS: APPLICATION TO A REAL ENGINE CALIBRATION

The following tools have been developed in the MATLAB®7 / Simulink environment. They are currently used by the calibration engineers for real engine applications.

Air charge estimation

Before the introduction of the above described tools, the experimental plan took 15 days (24 hours per day). This time effort had to be multiplied by the number of significant changes in the hardware during the calibration phase, which are usually up to four. The data analysis requires almost 5 days for each plan. The resulting maps present a significant number of discontinuities and the estimation error is not satisfactory.

The calibration tools were introduced in the development process at the start of one real calibration phase. The experimental plan time has been halved, now taking 8 days, 24 hours a day. The data analysis requires now a few hours. The estimation error is almost halved and it is now fully satisfactory.

Automatic calibration -The criteria exploited by the calibration engineers have been implemented in this tool. The synergies between the calibration department and the engine test department produce the continuous enhancement of the automatic calibration tools.

The inputs are:
- A calibration file, to gather information about the dimensions and the breakpoints to be used in the maps calibration.
- One or more engine bench test files containing the necessary channels.

For each engine speed breakpoint, a multivariable switching regression model is calculated (Figure 6.16) to best describe the manifold pressure - cam phaser position - volumetric efficiency relationship. The used model has been developed by taking in account the ECU reproducibility of the relationship and the physical behaviour of the phenomenon. The volumetric efficiency depends squarely by the cam phaser position, linearly by manifold pressure. Over the breaking pressure, which is a regression parameter, the linear dependency becomes quadratic without first order derivative discontinuity, while, under 300 mbar the slope can change to best fit the data.

The regression model has been then made discrete and transformed, without information loss, in the ECU algorithm model, made by 4 maps, for a total of 1092 parameters

Calibration verification -This software allows one to graphically and numerically visualize the relationship between experimental points and corresponding ECU estimated points. The working algorithm can be explored with the following points of view:

- Iso intake manifold pressure efficiency curves
- Iso cam phaser position efficiency curves
- 3D surface of volumetric efficiency depending on pressure and cam phaser
- Iso volumetric efficiency curves depending on intake manifold pressure and cam phaser
- Percentage error of the total air charge estimation

It is possible to modify the maps, graphically or numerically, interactively for verifying the effect in one of the possible views.

A left mouse click on an experimental point shows additional information, while a right mouse click opens a contextual menu which permits to eliminate the point or open the source data file, highlighting the corresponding row.

By opening multiple instances of the tool, it is possible to compare different calibrations or different bench test data, speeding up the verification and refinement of the calibration.
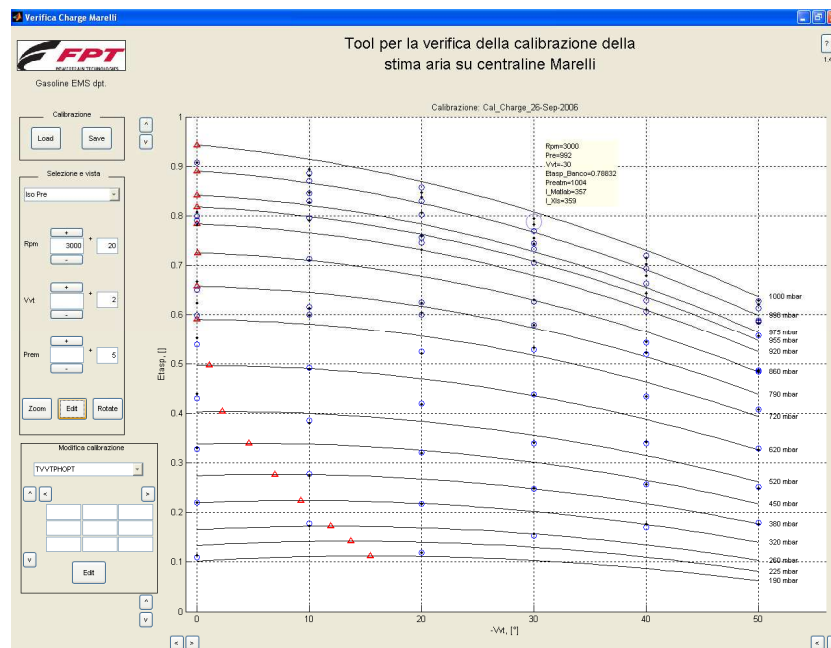
Figure 6.16 Charge estimation calibration verification tool. Inlet efficiency curves depending on cam phaser position, at defined intake manifold pressures
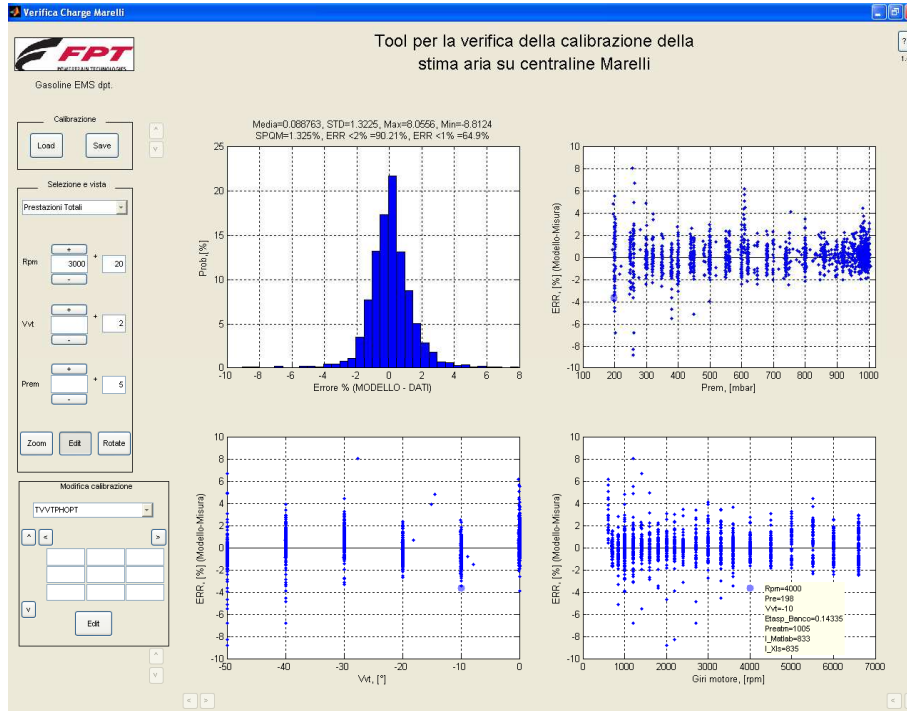
Figure 6.17 Air charge estimation calibration verification tool. Total performance, statistics.

 Performance measurement - This tool measures the total performance, in estimation accuracy sense, of the pair [Calibration – Engine bench test data]. It is possible to compare calibrations from different sources, to rapidly find critical points, and to evaluate different versions of the algorithm. This function is integrated also in the air charge calibration verification tool.

Gasoline injector model

 Automatic calibration - This tool automatically calibrates the gasoline injector model. It uses the same engine bench test data used for charge estimation. The discrete regression tool easily calculates the map which minimizes the error between the injected gasoline estimation, done by the ECU, and the measured one.

Spark advance calculation and torque estimation

 Automatic calibration - The torque supplied by the engine is estimated using mainly the engine speed, air inlet efficiency, cam phaser position and spark advance ([13] and [14]). In an engine without the cam phaser, the algorithm uses only two maps and one vector:

- MTA(speed, eta), called the maximum torque advance map: it describes, for each engine speed - air inlet efficiency point, the spark advance that maximizes the torque. If the detonation occurs before reaching the real maximum, an extrapolated value is used to best fit the data. In Figure 6.15, the x-coordinate of the red triangles represents the maximum torque.
- MT(speed, eta), called the maximum torque map: it describes the indicated torque measured at the maximum torque advance. In it is represented by the y-coordinate of the red triangles.
- UC(advance - MTA(speed, eta)), called the unique curve: it describes how the distance between the spark advance and the maximum torque spark advance reduces the torque. Its output is 1 if the input is 0. The output decreases while the input difference increases. It is very similar to a parabolic curve and it has the property to fit well the experimental data in the equation

TORQUE = MT(*speed*, *eta*) * UC(*advance* – MTA(*speed*, *eta*))   (2)

Where:

- *speed* is the engine speed
- *eta* is the air inlet efficiency
- *advance* is the actuated spark advance

The hyper surface that describes the torque delivery has to be continuous, because it describes a physical phenomenon. The multi-map optimization automatically finds the values of the maps which best fit the experimental data. The result is very continuous. The error on the torque estimation, 0.61 Nm, is almost a quarter of the error obtained with traditional calibration methods, that calculated the maximum torque spark advance by analyzing only the points at the same engine speed and air inlet efficiency, thus resulting extremely sensitive to experimental errors.

By using different implementations of the multi-map optimization and discrete regression, 10 maps can be calibrated, taking into account the cam phaser position dependencies, for a total of 2284 parameters.

Calibration verification - This tool assists the calibration engineer in the verification of the correctness of the calibration of the spark advance calculation and torque estimation. The inputs are:

- A calibration file, in Excel format, generated by the calibration tool
- The engine bench test data

The main graph shows the trend of the "umbrella" curves, CMI(advance), at a fixed engine speed and cam phaser position. Acquired data are represented by blue circles, while calibration estimated corresponding points are the black dots. The red triangle represents the maximum torque point for each load breakpoint, while the big black plus symbol is the working spark advance. Clicking over an experimental point, additional information are shown, like fuel consumption,

temperatures and so on. Clicking over an ECU calculated point, instead, the relative formula adopted will be shown, with input maps values.
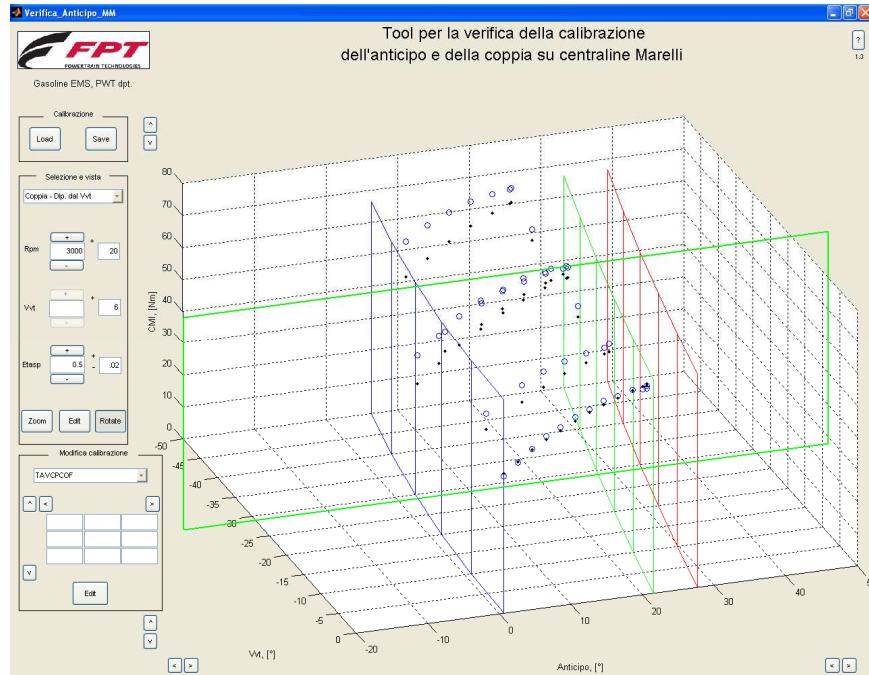
Figure 6.18 Torque verification tool, cam phaser position dependency

On the left panel it is possible to choose the engine speed, the cam phaser position and the load. The cam phaser can be specified with the *obj* string, to select only the points at objective cam phaser position, characterizing the steady state operating points. On the bottom left side it is possible to interactively modify the maps, numerically or graphically and to control the effect in the main graph.

In Figure 6.18, the CMI (advance, cam phaser position) graph is shown, which is of use to verify the phenomena from another point of view.

Other three views are available, to verify that the working advance actuation is correct for every cam phaser position. The modified calibration can be exported in Excel format, ready to be copied in ECU software.

6.9 TCA ENVIRONMENT

The main ECU algorithms are coded in Matlab scripts, which simulate the behaviour of the embedded software. The modeled algorithm are:
- charge estimation for each valve actuation mode;
- injection model;

- exhaust backpressure estimation;
- exhaust temperature estimation;
- delivered torque estimation;
- spark advance calculation;
- engine friction and pumping losses estimation.

Almost sixty maps and vectors are necessary to calibrate these algorithms for each application; it means thousands of scalar parameters. In order to satisfy this target, 33 automatic calibration tools have been developed, integrated in TCA environment.

In Figure 5.19. the main TCA interface is shown.
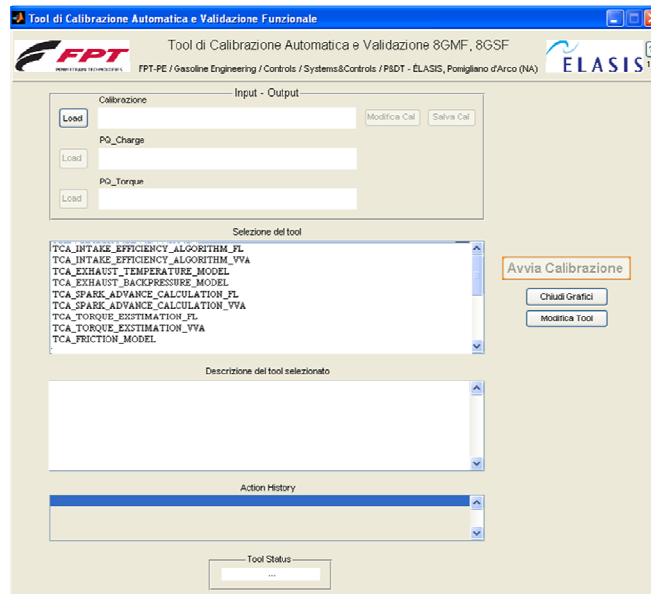
Figure 6.19 TCA tool, user interface.

The inputs are:
- A calibration file, to gather information about the dimensions and the breakpoints to be used in the maps calibration;
- One or more engine bench test data files, specific for charge estimation;
- One or more engine bench test data files, specific for torque estimation, containing also the spark advance sweeps.

After the data loading, the user have to select a tool: all the necessary information to correctly execute the tool are displayed, like which maps have to be calibrated before running the tool and so on. Useful hints are also displayed that take into account the best practices to use the tool, suggested by the application team.

If only one map has to be calibrated the Discrete Regression Tool is used. The mentioned tool has been developed to calculate the values of the map that

minimize the average square error between the experimental data and the surface, described as the bilinear interpolation of the map, using the same algorithm embedded in the ECU.

When the algorithm's output depends on more maps or vectors that interacts each other, it's better used the Multi Map Optimization Tool.

The Multi Map Optimization modifies the calibration, varying the values of the maps, vectors and scalars that compose it, until the minimum average square error, or average percentage square error, between measured output and estimated ones is reached. This tool solves a multidimensional optimization problem, having as optimizing function the absolute error or the percentage square error.

The advantages are the same of the discrete regression, plus the following:

•   Many maps can be optimized simultaneously, the solution minimizes the total error, not the single map one, so the result better fits the data.

•   The precision and the continuity of the maps are better than using other methods.

6.10 CONCLUSIONS

In this chapter an analysis and simulation powerful tool for embedded control system design has been presented. A discussion regarding the related automotive industry demands and the relevance of software support tools for control system design has been provided. From these considerations, F.I.R.E. has been built up to provide multiple views of a Simulink® model, because control system developers have to consider different aspects, not all visible with a single graphical notation. It mainly allows a graphical reorganization and an early timing analysis of the control system, according to the Auto-Code Generator requirements, with the objective of automatically generating the production code for the ECU directly from these models.

This software has been tested and validated on real applications and the relevance of this tool has been illustrated by investigating different closed-loop system behaviours which result from bad scheduling choices and by the tool assistance in finding the most correct time slicing for each task. Future developments include:

•   automatic discretization of continuous-time blocks in the Functional to Implementation transformation;

•   joint comparison of simulation results between functional and implementation views;

•   inverse transformations and overall consistency checks amongst the views;

•   explicit specification of the execution order of subtasks within each task in the Functional to Implementation transformation.

Another important feature which can be added is the possibility to undertake more detailed investigations and comparisons between different dynamic

scheduling policies[6] (e.g. priority-based pre-emptive scheduling and Earliest Deadline First (EDF) scheduling) and a deeper analysis about the synchronization amongst tasks that use shared data for their computation. It could be also interesting to investigate the delay due to common data access and the transmission rate into the network by integrating the F.I.R.E. tool with handmade scripts or other blocks representing different schedulers, networks and monitors for synchronization, as in the TrueTime platform.

On the other hand, the integration of this environment with accurate calibration instruments guarantees the Engine Management System product quality, that is more and more influencing the costs and it has to be accurately managed since the first phases of development. In order to take under control many strictly, even conflicting, requirements the development environment has to allow a strong integration between every single phase. This satisfaction has a big impact on the characteristics of the tools to be used and on the necessary skills of people involved in development. An important goal achieved is that of being able to merge the skills coming from different engineering departments (i.e. engine application, engine control system development) and experiences from different projects to guarantee in a predictable way the required product requirements in future projects.

---

[6] Simulink® simulation engine uses a fixed-priority Rate Monotonic (RM) schedule

ng to simulate multitasking models.

Conclusions

My research activity has been focused on the developing of three new control and management algorithms for the engine control unit and on the developing of more accurate control development and calibration software tools. The developed novel control concepts were required for the integration of new technologies in the existing powertrains, in particular the VVA technology for gasoline engines and intelligent alternators. The MultiAir® engine (with variable intake valve actuation technology) is now a benchmark in the automotive world for its high performance and the achievable fuel/emission reductions. The intelligent alternator is a technology widely used by several OEMs for energy management.

In order to satisfy the more restrictive CO2 requirements, and therefore fuel consumption, Intelligent Alternators give the opportunity to regulate the energy efficiency in recharging the battery according to the driving conditions. The conventional engine control system is not able to optimize the efficiency of the alternator in terms of emissions and fuel consumption, due to a constant voltage which is imposed and is not modifiable. Therefore a management strategy has been proposed for regulating the alternator voltage. This is done by using an "Intelligent Alternator Module (IAM)", that communicates using the LIN protocol with the Engine Control Module (ECM), and an "Intelligent Battery Sensor (IBS)", which provides the information about the battery State-Of-Charge (SOC). Target SOC and battery voltage are set by the control algorithm based on vehicle driving conditions and engine operating mode. This strategy has been tested on a Lancia New Ypsilon vehicle equipped with 0.9l TwinAir 85hp turbocharged gasoline engine. The performed tests showed the correct Smart Alternator Management (SAM) strategy operation and the target performance improvements with respect to the standard alternator management , in terms of:

- target alternator voltage smoothness, which guarantees an optimal Front End Accessory Drive (FEAD) performance together with "fun to drive" feeling;
- target tracking of battery voltage;
- battery life time improvement;
- engine friction torque reduction, which guarantees a further improvement on engine driving performance;
- fuel consumption reduction, assured by a nominal 2% reduction in CO_2 emissions on a NEDC cycle.

The second algorithm has been developed to improve the dynamic response at one of the most critical manoeuvres: the drive off one. The state of the art for drive off algorithms are already present on automatic transmission vehicles

(mainly in the transmission control unit). A study and adaptation of these algorithms were performed and applied directly in the engine control unit for those vehicles that have a manual transmission. The strategy recognizes when a driver is taking off and it manages the engine speed in order to achieve the final vehicle momentum at the end of the manoeuvre. The original concept has been tested and validated using a Software In the Loop environment and Rapid Control Prototyping. The algorithm has shown good performance in all the manoeuvres tested by using the SAE evaluation index (different manoeuvres are evaluated by a commission using subjective considerations and AVL drive instrumentations for objective evaluations with respect to best in class vehicles):

- o   a reduction of maximum vehicle longitudinal acceleration;
- o   a lower engine speed undershoot;
- o   and a less number of engine stall occurrences.

The drive off algorithm will equip all new FIAT Panda Twin Air® passenger vehicles starting from fall 2011.

The third algorithm developed is a strategy to manage the spark advance in VVA equipped vehicles. It has been shown that mapping the spark advance independently from specific MultiAir® Valve and engine working modes, improves fun to drive without losing any advantages in terms of misfiring. The experiments on this algorithm have been conducted on test bench for a gasoline engine Fiat Turbo 1.4l 135 Hp equipped with VVA. Actually is implemented into each vehicle application having MAIR and TWIN AIR gasoline engines.

In order to quickly design all three of these new algorithms, a powerful tool for simulation and embedded control system design has been presented: F.I.R.E (Functional, Implementation, and Re-usability Environment). This tool has been built up to provide multiple views of a Simulink® model:

- o   Full model functional view
- o   Model filtering by task scheduler and Target Link® compatibility
- o   Physical allocation selection

It mainly allows a graphical reorganization and an early timing analysis of the control system, according to the Auto-Code Generator requirements, with the objective of automatically generating the production code for the ECU directly from these models. This software has been tested and validated on real applications. The relevance of this tool has been illustrated by investigating different closed-loop system behaviours which result from bad scheduling choices. With the tool assistance, the developer is able to find the most correct time slicing for each task.

To easily calibrate the models developed for MultiAir® engine, an automatic tool for calibration (TCA, Tool Calibration Automatic) was developed. The tool is a Multimap optimizer, which turns the maps to be optimized (with its interpolation rule) into a physical model and optimizes its equilibrium and the continuity based on the minimum error to be achieved.

All the algorithms developed during my research activity have been tested for long time and reputed as good as to be employed in all future production vehicles. In the next future, EURO6 challenges will impose a re-visitation of the developed control algorithms and the development of new functions.

Bibliography

[1] J. Heywood, "*Internal combustion engine fundamentals*", McGraw Hill, 1988.

[2] R. Della volpe, M. Migliaccio, "*Motori a combustione interna per autotrazione*, Liguori Editori, 2000.

[3] C. F. Taylor, "*The internal combustion engine in theory and practice*", The M.I.T Press, 1966.

[4] P. Scalori, "*L'autoveicolo e la sua evoluzione*", Politecnico di Torino, 2000

[5] A. Palladino, G. Fiengo, F. Cristofaro, A. Casavola, and L. Glielmo, "In cylinder air charge prediction for VVA system: Experimental validation", *Multi-conference on Systems and Control*, 2008.

[6] www.fptpowertrain.com

[7] www.fiatgroupautomobilexpress.com

[8] Schindler, K-P., 1997. "*Why Do We Need The Diesel?*", SAE Technical Paper 972684.

[9] S. Bova, A. Casavola , F. De Cristofaro, A. Guzzo, I. Montalto, A. Riegel "Variable Valve Actuation: performance evaluation and optimization tools", *FISITA* 2010

[10] S. Bova, A. Casavola , F. De Cristofaro, A. Guzzo, I. Montalto, A. Riegel "Development of new algorithm for spark advance calculation for gasoline engine with variable valve actuation", *FISITA* 2010

[11] I.Montalto, M.Santamarina, C.Masiero, A.Riegel, A.Casavola, F.Decristofaro, N.Vennettilli, "A new algorithm for vehicle drive off management in manual transmission vehicles", EAEC11

[12] I.Montalto, D.Tavella, A.Casavola, F.Decristofaro, "Intelligent Alternator Employment To Reduce Co2 Emission And To Improve Engine Performance", SAE2011

[13] A. Palma, A. Palladino, G. Fiengo, F. De Cristofaro, F. Garofalo and L. Glielmo, "A modeling approach for engine dynamics based on electrical analogy", *IFAC* 2008

[14] F. De Cristofaro, G. Fiengo, A. Palladino, A. Palma "Inner phenomena modeling occurring into SI-ICE combustion chamber: Knock, EGR and Scavenging", *International Journal of Modeling, Identification and Control* 2009

[15] B. J. Allison and A.J. Isaksson, "Design and performance of midranging controllers", *Journal of Process Control*, Volume 8, Issue 5, pp. 469474, 2009

[16] A. Casavola, F. De Cristofaro, I. Montalto "A new Development Environment for Embedded Control Systems Design and Interactive Optimization Methodologies for Robust Calibration of Automotive Engines" *Large scale Computation, Embedded Systems and Computer Security*, ISBN: 9781607413073, Nova Science Publisher, NY, 2010

[17] Henriksson, D., Cervin, A. and Årzén, K.E. "TrueTime: Real-time Control System Simulation with MATLAB/Simulink", *Proceedings of the Nordic MATLAB Conference*, Copenhagen, Denmark, 2003.

[18] Ohlin, M., Henriksson, D. and Cervin, A. "*TrueTime 1.4 – Reference Manual*", Department of Automatic Control, Lund Institute of Technology, Sweden, 2006.

[19] Calvez, J.P. "*Embedded real-time systems – A specification and design methodology*", 1st Edition, John Wiley & Sons, Chichester, England, 1993.

[20] Gaviani, G., Gentile, G., Stara, G., Romagnoli, L., Thomsen, T. and Ferrari, A. "From conception to implementation: a model based design approach", *Proceedings of 1st IFAC Symposium on Advances in Automotive Control*, Salerno, Italy, 2004.

[21] Oshana, R. "Introduction to embedded and real-time systems", *Proceedings of Embedded Systems Conference*, Boston, USA, 2003.

[22] Kiencke, U. and Nielsen, L. "*Automotive Control System – For Engine, Driveline and Vehicle*", Springer, Berlin, Germany, 2000.

[23] Törngren, M., Elkhoury, J., Sanfridson, M. and Redell, O. "*Modelling and Simulation of Embedded Computer Control Systems: Problem Formulation*", Technical report, Mechatronics Lab, Department of Machine Design, Royal Institute of Technology, Stockholm, Sweden, 2001.

[24] Köster, L., Thomsen, T. and Stracke, R. "Connecting Simulink to OSEK: Automatic Code Generation for Real-Time Operating Systems with TargetLink", *Embedded Intelligence*, Nuremberg, Germany, 2001.

[25] *TargetLink – Production Code Generation Guide*, for TargetLink 2.0, dSPACE GmbH, Paderborn, Germany, 2004.

[26] Buttazzo, G. "Sistemi Real-Time per il controllo automatico: problemi e nuove soluzioni", *Automazione e Strumentazione*, Anno XLVIII, N. 5, pp. 107-116, 2000.

[27] Redell, O. "*Global Scheduling in Distributed Real-Time Computer Systems – An Automatic Control Perspective*", Technical Report, Mechatronics Lab, Department of Machine Design, Royal Institute of Technology, Stockholm, Sweden, 1998.

[28] Liu, C.L. and Layland, J.W. "Scheduling algorithms for multiprogramming in a hard real-time environment", *Journal of ACM*, Vol. 20, N. 1, pp. 46-61, 1973.

[29] "*Automotive Electrics Automotive Electronics*", Fourth Edition, Robert Bosch GmbH, Plochingen, Germany, 2004.

[30] Annunziata, M., De Cristofaro, F., Flauti, G. and Scala, S. "Development of a Virtual Test Environment for Engine Control Systems: ESILE, Elasis Software In the Loop Environment", *FISITA* 2004.

[31] De Cristofaro F., Riegel A., Di Martino U., De Sisto G., "Estimation of drawn air mass on a ICE: implementation of a new algorithm to better estimate the atmospheric pressure influence", *Proceedings of SAE International* 2007-01-1344, Detroit, 2007

[32] Box, G.E.P., Draper, N.R. "*Empirical Model-Building and Response Surfaces*", Wiley & Sons, New York, 1987

[33] Montgomery, D.C., "*Il Controllo Statistico della Qualità*", McGraw-Hill, New York, 2000

[34] Erto, P., "*Probabilità e statistica per le scienze e l'ingegneria*", McGraw-Hill, Italia, 2004

[35] Box, G.E.P.; Hunter, J.S. ; Hunter, W.G., "*Statistics for Experimenters*", Wiley & Sons, 2005

[36] Peter W.M.J. , "*Statistical Design and Analysis of Experiments*", Classics in Applied Mathematics, Vol. 22, 1998

[37] Taguchi. G., "*System of Experimental Design*", Kraus International Pub., New York, USA, 1987

[38] Wu, C.F.J., Hamada, M., "*Experiments. Planning, Analysis, and Parameter Design Optimization*", Wiley & Sons, 2000

[39] Rao S.,"*Engineering Optimisation Theory and Practice*", Wiley & Sons, 1996

[40] Miettinen K., "*Nonlinear Multiobjective Optimisation*", Kuwler Academic Publishers, 1999

[41] Caraceni A, De Cristofaro F, Ferrara F, Philipp O, Scala S "Benefits of using a real-time engine model during engine ECU development" *Proceeding of SAE* 2003

[42] S.Raman, N. Sivashankar, W. Milam, W. Stuart, S. Nabi, "Design and implementation of HIL simulators for powertrain control system software development", *Proceding of the American Control Conference*.

[43] W. Lee, M. Yoon, M. Sunwoo, "A cost- and time-effective hardware-in-the-loop simulation platform for automotive engine control systems", *Proceedings of the Institution of Mechanical Engineers*, Part D: Journal of Automobile Engineering 217 (1), pp. 41-52

[44] Z. Jiang, R. Dougal, R. Leonard, H. Figueroa, A. Monti, "Hardware-in-the-loop testing of digital power controllers", *IEEE Applied Power Electronics Conference and Exposition* - APEC, 2006, art. no. 1620645, pp. 901-906

[45] B. Lu, X. Wu, H. Figueroa, A. Monti, "A low-cost real-time hardware-in-the-loop testing approach of power electronics controls", *IEEE Transactions on Industrial Electronics*, 54 (2), pp. 919-931

[46] H. Li, M. Steurer, K. Shi, S. Woodru , D. Zhang, "Development of a unified design, test, and research platform for wind energy systems

based on hardware-in-the-loop real-time simulation", *IEEE Transactions on Industrial Electronics* 55 (4), pp. 1144-1151.

[47] S. Karimi, A. Gaillard, P. Poure, S. Saadate, "FPGA-based real-time power converter failure diagnosis for wind energy conversion systems", *IEEE Transactions on Industrial Electronics* 55 (12), pp. 4299-4308.

[48] O. Lpez, J. lvarez, J. Doval-Gandoy, F. Freijedo, A. Nogueiras, A. Lago, C. Pealver, "Comparison of the FPGA implementation of two multilevel space vector pwm algorithms", *IEEE Transactions on Industrial Electronics* 55 (4), pp. 1537-1547.

[49] S. C. Oh, "Evaluation of motor characteristics for hybrid electric vehicles using the hardware-in-the-loop concept", *IEEE Transactions on Vehicular Technology* 54 (3), pp. 817-824.

[50] W. Ren, M. Steurer, T. Baldwin, "Improve the stability and the accuracy of power hardware-in-the-loop simulation by selecting appropriate interface algorithms", *IEEE Transactions on Industry Applications* 44 (4), pp. 1286-1294.

[51] A. Bouscayrol, "Different types of hardware-in-the-loop simulation for electric drives", *IEEE International Symposium on Industrial Electronics*, art. no. 4677304, pp. 2146-2151.

[52] P. Gawthrop, D. Virden, S. Neild, D. Wagg, "Emulator-based control for actuator-based hardware-in-the-loop testing", *Control Engineering Practice* 16 (8), pp. 897-908.

[53] S. Ayasun, R. Fischl, S. Vallieu, J. Braun, D. Cadirli, "Modeling and stability analysis of a simulation-stimulation interface for hardware-in-the-loop applications", Simulation *Modelling Practice and Theory* 15 (6), pp. 734-746.

[54] M. Yoon, W. Lee, M. Sunwoo, "Development and implementation of distributed hardware-in-the-loop simulator for auto-motive engine control systems", *International Journal of Automotive Technology* 6 (2), pp. 107-117.

[55] W. Zhu, S. Pekarek, J. Jatskevich, O. Wasynczuk, D. Delisle, "A model-in-the-loop interface to emulate source dynamics in a zonal dc distribution system", *IEEE Transactions on Power Electronics*, 20 (2), pp. 438-445.

[56] A.Palladino, G.Fiengo, F. Giovagnini, D. Lanzo, "A micro hardware-in-the-loop test system", *IEEE European Control Conference*.

[57] F. Costanzo, M. D. Manes, G. D. Mare, F. Ferrara, A. Montieri, "Testing networked ECUs in a virtual car environment", *Proceeding of SAE* 2004-01-1724.

[58] H. Schuette, P. Waeltermann, "Hardware-in-the-loop testing of vehicle dynamics controllers a technical survey", *Proceeding of SAE* 2005

[59] F. Baronti, F. Lenzi, R. Roncella, R. Saletti, O. D. Tanna, "Electronic control of a motorcycle suspension for preload self-adjustment", *IEEE Transactions on Industrial Electronics* 55 (7), pp. 2832-2837.

[60] J. Du, Y. Wang, C. Yang, H. Wang, "Hardware-in-the-loop simulation approach to testing controller of sequential tur-bocharging system",

Proceedings of the IEEE International Conference on Automation and Logistics.

[61] A. Cebi, L. Guvenc, M. Demirci, C. Karadeniz, K. Kanar, E. Guraslan, "A low cost, portable engine electronic control unit hardware-in-the-loop test system", *Proceedings of the IEEE International Symposium on Industrial Electronics.*

[62] T. Hwang, J. Rohl, K. Park, J.Hwang, K. Lee, L. K, K. Y.-J., "Development of hils systems for active brake control systems", *SICE-ICASE International Joint Conference.*

[63] A. Ali, A. Nadeem, M. Z. Z. Iqbal, M. Usman, "Regression testing based on uml design models", *IEEE International Symposium on Paci c Rim Dependable Computing.*

[64] B. Korel, G. Koutsogiannakis, L. Tahat, "Application of system models in regression test suite prioritization", *IEEE Inter-national Conference on Software Maintenance*, ICSM, art. no. 4658073, pp. 247-256.

[65] Y. Wu, M.-H. C. H. Kao, "Regression testing on object-oriented programs", *Symposium on Software Reliability Engineering*.

[66] S. Elbaum, H. Chin, M. Dwyer, M. Jorde, "Carving and replaying di erential unit test cases from system test cases", *IEEE Transactions on Software Engineering* 35 (1), pp. 29-45.

[67] M. Harrold, A. Orso, "Retesting software during development and maintenance", *Proceedings of the 2008 Frontiers of Software Maintenance, FoSM* 2008, art. no. 4659253, pp. 99-108.

[68] G. Rizzoni, P. Min, "Detection of sensor failures in automotive engines", *IEEE Transactions on Vehicular Technology*, Issue 2, Page(s):487 - 50.

[69] R. Conatsera, J. Wagner, S. Gantab, I. Walkerb, "Diagnosis of automotive electronic throttle control systems", *Control Engineering Practice*, Volume 12, Issue 1, Pages 23-30.

[70] Q. Butt, A. Bhatti, "Estimation of gasoline-engine parameters using higher order sliding mode", *IEEE Transactions on Industrial Electronics*, Volume 55, Issue 11, Page(s):3891 - 3898.

[71] A. Riegel, F. D. Cristofaro, I. Montalto, "Interactive optimization methodology for robust base engine calibration", *EAC* 2007.

[72] A. Casavola, F. De Cristofaro, G. Fiengo, F. Garofalo, A. Palladino, "A Simulation Analysis for VVA and Idle Control Strategies", *18th Mediterranean Conference on Control and Automation* 2010

[73] F. De Cristofaro, G. Fiengo, A. Guzzo, A. Palladino, A. Palma "A Simulation based Investigation of Interaction between VVA and Idle Control for SI Engines", *Virtual Conference Control* 2010

[74] Bosch, "*Gasoline- Engine Management*", Bosch GmbH, Technology, 2004

[75] Amann, C.A., 1989. "*The Automotive Engine - A Future Perspective*", SAE Technical Paper 891666

[76] Amann, C.A., 1990. "*The Passenger Car and the Greenhouse Effect*", SAE Technical Paper 902099

[77] Asmus, T., 1995. "*The Basis of Engine Efficiency*", Presentation by Chrysler Corporation at the China Automotive Technology Conference/Workshop, August 1995

[78] I.Montalto, D.Tavella, F.Decristofaro, A.Casavola, "A new Development Environment for Embedded Control Systems Design: F.I.R.E.",ANIPLA2006

[79] I.Montalto, D.Tavella, F.Decristofaro, A.Casavola, "Realizing Multiple Views of Simulink Models with F.I.R.E. tool",AVEC2006

[80] I.Montalto, D.Tavella, F.Decristofaro, A.Casavola, "Embedded Control Systems Development Environment realized in Simulink", ECC2007

[81] I.Montalto, D.Tavella, F.Decristofaro, A.Casavola, "A new Development Environment for Embedded Control Systems Design: F.I.R.E.",SAE2007